Die regulatorische Funktion des Usher-Syndrom Proteins SANS in Proteinnetzwerken

Dissertation
zur Erlangung des Grades
„Doktor der Naturwissenschaften“
am Fachbereich Biologie
der Johannes Gutenberg-Universität
in Mainz

von Katharina Elisabeth Bauß
geboren am 12.03.1982 in Würzburg
Mainz, November 2013

Tag der mündlichen Prüfung: 10.12.2013

So Long, and Thanks for All the Fish.

4th book of the Hitchhiker's Guide to the Galaxy by Douglas Adams (1952-2001)

Anmerkungen

Die vorliegende Arbeit ist kumulativ gestaltet und besteht im Kern aus den drei Publikationen:
Sorusch *et al*, in Druck: *Usher syndrome protein network functions in the retina and their relation to other retinal ciliopathies* (Publikation I); Bauß *et al*, in Vorbereitung: *"Direct interaction of the Usher syndrome proteins SANS and Ush2a in the retina"* (Publikation II); Bauß *et al*, unter Begutachtung: *"Phosphorylation of the Usher syndrome 1G protein SANS controls Magi2-mediated endocytosis"* (Publikation III).

Bei Publikation I handelt es sich um Kapitel 67 des Buches „Retinal Degenerative Diseases", das im Frühjahr 2014 über den Springer-Verlag im Handel erhältlich sein wird. Publikation II ist noch in Vorbereitung und wurde in Manuskriptform beigefügt. Publikation III wurde bei der Zeitschrift „Journal of Clinical Investigation" eingereicht und ist als Manuskript beigefügt.

Die Ergebnisse der drei Publikationen sind im Abschnitt „Zusammenfassung der Ergebnisse und Diskussion" dargestellt und diskutiert. Alle weiteren Publikationen, zu denen im Rahmen dieser Arbeit Beiträge geleistet werden konnten, sind im Text mit einem Stern (*) hervorgehoben. Eine detaillierte Übersicht der geleisteten Beiträge zu den jeweiligen Publikationen wird im Anhang gegeben.

Veröffentlichungen

Teile der vorliegenden Dissertation wurden auf internationalen Kongressen vorgestellt, befinden sich in Vorbereitung einer Publikation, wurden eingereicht oder wurden in folgenden Zeitschriften publiziert:

Publikationen:

Sorusch N, Wunderlich K, **Bauß K**, Nagel-Wolfrum K, Wolfrum U (in press). Usher syndrome protein network functions in the retina and their relation to other retinal ciliopathies. In: Retinal Degenerative Diseases. Eds: Ash J, Hollyfield JG, La Vail MM, Anderson RE, Grimm C and Rickman CB, Springer.

Bauß K, Knapp B, Jores P, Spitzbarth B, Roepman R, Kremer H, van Wijk E, Maerker T and Wolfrum U (under review). Phosphorylation of the Usher syndrome 1G protein SANS controls Magi2-mediated endocytosis. - eingereicht bei: Journal of Clinical Investigation.

Kersten F, van Wijk E, Hetterschijt L, **Bauß K**, Peters T, Aslanyan M, van der Zwaag B, Wolfrum U, Keunen J, Roepman R and Kremer H (2012). The mitotic spindle protein SPAG5/Astrin connects postmitotically to the Usher protein network. Cilia, 1: 2046-2530.

Overlack N, Kilic D, **Bauß K**, Maerker T, Kremer H, van Wijk E, Wolfrum U (2011). Direct interaction of the Usher syndrome 1G protein SANS and myomegalin in the retina. Biochem. Biophys. Acta, 1813:1883-92.

Schneider E, Maerker T, Daser A, Frey-Mahn G, Beyer V, Farcas R, Schneider-Rätzke B, Kohlschmidt N, Grossmann B, **Bauß K**, Napiontek U, Keilmann A, Bartsch O, Zechner U, Wolfrum U, Haaf T (2009). Homozygous disruption of PDZD7 by reciprocal translocation in a consanguineous family: a new member of the Usher syndrome protein interactome causing congenital hearing impairment. Hum. Mol. Genet., 18:655-66.

Publikationen in Vorbereitung:

Bauß K[#], Sorusch N[#], Wolfrum U (in prep.) Direct interaction of the Usher syndrome proteins SANS and Ush2a (# both authors contributed equally to the work).

Abbildungsverzeichnis

Tabellenverzeichnis

Inhalt

1. Einleitung

In der vorliegenden Arbeit werden die molekularen Grundlagen des humanen Usher-Syndroms (USH) analysiert, der häufigsten Ursache von erblich bedingter Taub-Blindheit (Vernon 1969; Reiners *et al,* 2006). USH-Patienten leiden unter der Beeinträchtigung bis hin zum vollständigen Verlust des Hör- und Sehvermögens, den beiden wichtigsten Sinnen des Menschen (Saihan *et al,* 2009; Wolfrum 2011). In unserer Arbeitsgruppe steht die Netzhaut des Auges im Mittelpunkt der Analysen. Die Aufklärung der zellulären Prozesse, deren Fehlfunktionen im Zusammenhang mit der retinalen Degeneration bei USH stehen, ist das zentrale Thema dieser Dissertation. Dabei stehen das USH1G-Genprodukt SANS und seine Funktion in Abhängigkeit seiner Interaktionspartner im Fokus. Die detaillierte Analyse eines USH-Proteins soll dazu beitragen, die Pathomechanismen aufzuklären, die zur Degeneration der Netzhaut bei USH führen.

1.1 Das Usher-Syndrom des Menschen

USH ist eine autosomal-rezessive Erbkrankheit und wird anhand von Schwere, Einsetzen und Verlauf der Symptome klinisch in drei Typen unterteilt (USH1-3) (Davenport and Omenn 1977). Betroffene Patienten leiden von Geburt an unter fortschreitendem Gehörverlust bzw. vollständiger Taubheit, zum Teil unter Gleichgewichtsstörungen und unter progressiver Verschlechterung des Sehvermögens durch die Degeneration der Netzhaut (*Retinitis pigmentosa*), in manchen Fällen bis hin zur vollständigen Erblindung. Neben der klinischen Variabilität besteht eine genetische Heterogenität (Reiners *et al,* 2006; Saihan *et al,* 2009). Bisher konnten für die zwölf beschriebenen Genloci zehn Gene identifiziert werden.

Obwohl die USH-Subtypen 1-3 einen vergleichbaren Phänotyp hervorbringen, gehören die korrespondierenden Genprodukte zu unterschiedlichen Proteinklassen bzw. -familien. USH1, die schwerwiegendste Form, ist auf Mutationen in den Genen kodierend für den molekularen Motor MyosinVIIa (USH1B), die Gerüstproteine Harmonin (USH1C) und SANS (USH1G), auf das Calciumbindeprotein CIB2 (USH1J) oder die Zell-Zell-Adhäsionsproteine Cadherin23 (USH1D) und Protocadherin15 (USH1F) zurückzuführen (Weil *et al,* 1995; Astuto *et al,* 2000; Bitner-Glindzicz *et al,* 2000; Verpy *et al,* 2000; Ahmed *et al,* 2001; Alagramam *et al,* 2001; Bolz *et al,* 2001; Bork *et al,* 2001; Kikkawa *et al,* 2003; Weil *et al,* 2003; Riazuddin *et al,* 2012). USH2, der häufigste diagnostizierte USH-Typ, entsteht durch Mutationen in den Transmembranproteinen Ush2a (USH2A) und VLGR1/GPR98 (G protein-coupled receptor 98, USH2C) oder dem Gerüstprotein Whirlin (USH2D) (Eudy *et al,* 1998; Bhattacharya *et al,* 2002; van Wijk *et al,* 2004; Weston *et al,*

2004; Yagi *et al,* 2005; van Wijk *et al,* 2006; Ebermann *et al,* 2007). USH3 wird ausgelöst durch Defekte im Transmembranprotein Clarin-1 (USH3A) (Joensuu *et al,* 2001; Adato *et al,* 2002). Die einzelnen klinischen USH-Subtypen, die betroffenen Gene und die kodierten Proteine sind in Tabelle 1 aufgelistet.

Typ	Locus	Gen	Protein	Funktion	Referenz
1B	11q13.5	*MYO7A*	MyosinVIIa	Motorprotein	Weil *et al,* 1995; Astuto *et al,* 2000
1C	11p14-15	*USH1C*	Harmonin	Gerüstprotein	Bitner-Glindizcz *et al,* 2000; Verpy *et al,* 2000
1D	10q21-q22	*CDH23*	Cadherin23	Zell-Zelladhäsion	Bolz *et al,* 2001; Bork *et al,* 2001
1E	21q21	--	--	--	Chaib *et al,* 1997
1F	10q11.2-q21	*PCDH15*	Protocadherin15	Zell-Zelladhäsion	Ahmed *et al,* 2001; Alagramam *et al,* 2001
1G	17q24-25	*SANS*	SANS	Gerüstprotein	Kikkawa *et al,* 2003; Weil *et al,* 2003
1H	15q22-23	--	--	--	Ahmed *et al,* 2009
1J	15q23-q25.1	*CIB2*	CIB2	Calcium-Integrin Bindung	Riazuddin *et al,* 2012
2A	1q41	*USH2A*	Ush2a (Usherin)	Zell-Zelladhäsion, extrazelluläres Matrixprotein	Eudy *et al,* 1998; Bhattacharya *et al,* 2002; van Wijk *et al,* 2004
2C	5q13	*GPR98*	GPR98 (VLGR1b)	Zell-Zelladhäsion, Rezeptor	Weston *et al,* 2004; Yagi *et al,* 2005
2D	9q32-q34	*DFNB31*	Whirlin	Gerüstprotein	van Wijk *et al,* 2006 Ebermann *et al,* 2007
3A	3q25	*CLRN1*	Clarin-1	Zell-Zelladhäsion	Joensuu *et al,* 2001; Adato *et al,* 2002

Tabelle 1: USH-Subtypen, Genloci, betroffene Gene und ihre Genprodukte sowie deren Funktion (Stand: Oktober 2013). --: nicht bekannt.

Genetische Analysen von USH-Patientengruppen haben Mutationen aufgezeigt, die keinem der bisherigen USH-Subtypen zugeordnet werden konnten, daher steht die Identifizierung weiterer USH-Gene aus (Bonnet *et al,* 2011). Zwei dieser USH-Genloci wurden eingegrenzt, entsprechende Gene bzw. Proteine konnten bisher aber nicht identifiziert werden (Chaib *et al,* 1997; Ahmed *et al,* 2009). Des Weiteren gibt es Hinweise auf *genetic modifiers*, die auf die Ausprägung der USH-Subtypen Einfluss nehmen (Bolz *et al,* 2005; Besnard *et al,* 2012). Das Protein PDZD7 (PDZ *d*omain-containing *7*), ein Paralog von Harmonin und Whirlin, wurde zunächst als Kandidatengen für angeborene Taubheit identifiziert, bevor nachgewiesen wurde, dass es über seine Interaktion mit USH-Proteinen und durch parallel-auftretende Mutationen zur genetischen Varianz der USH-Subtypen beiträgt (Schneider *et al,* 2009*; Ebermann *et al,* 2010; Grati *et al,* 2012). USH ist demnach eine genetisch äußerst komplexe Erkrankung, deren molekulare Grundlagen bislang nur unvollständig verstanden sind.

1.2 USH-Proteinnetzwerke

Die biochemischen und biophysikalischen Analysen zu USH durch uns und andere Arbeitsgruppen zeigen, dass die einzelnen USH-Moleküle in ihrer Funktion nicht alleine stehen, sondern in Proteinnetzwerken vorliegen, die von den Gerüstproteinen Harmonin (USH1C), SANS (USH1G) und Whirlin (USH2D) organisiert werden (Adato *et al,* 2005; Reiners *et al,* 2005; Reiners *et al,* 2006; van Wijk *et al,* 2006; Maerker *et al,* 2008). Neuere Arbeiten zeigen, dass das USH1B-Protein MyosinVIIa ebenfalls über seine Interaktionsdomänen Netzwerke aufbaut (Wu *et al,* 2011). Die Gesamtheit dieser Netzwerke, die sich je nach Lokalisation bzw. Funktion in ihrer molekularen Komposition unterscheiden können, wird als USH-Interaktom bezeichnet (Roepman and Wolfrum 2007; Wolfrum 2011). Die Funktion dieser Proteinnetzwerke für die Retina, insbesondere für die Photorezeptorzelle, ist ein zentrales Thema dieser Dissertation. Die bisherigen Analysen deuten darauf hin, dass in das USH-Interaktom weit mehr Moleküle integriert sind, als bisher identifiziert wurden (Abb. 1).

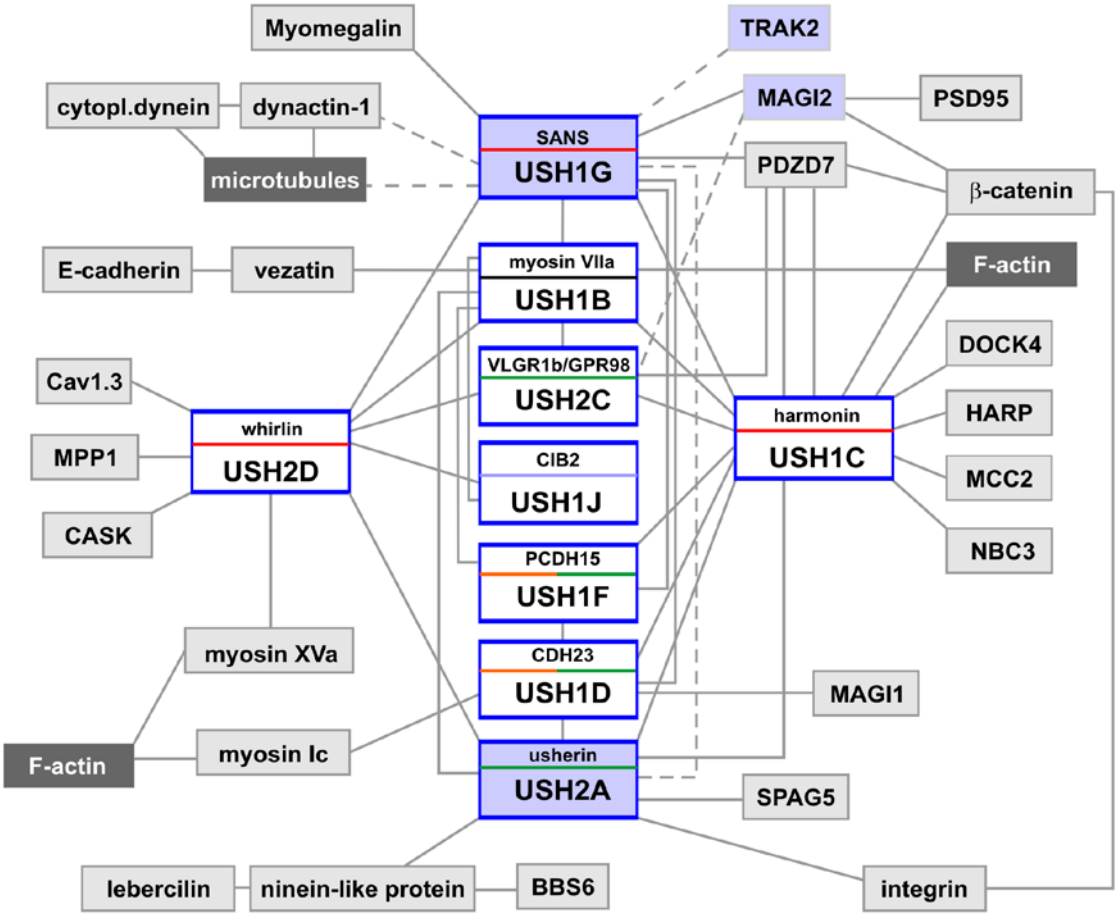

Abbildung 1: Das USH-Interaktom mit einer Auswahl identifizierter Interaktionspartner. USH-Proteine sind blau umrandet und werden je nach Proteinklasse farblich unterschieden: Gerüstproteine rot, Zell-Zell-Adhäsionsproteine orange, Transmembranproteine grün, das Calcium-binde Protein blaugrau und Motorproteine schwarz. Die in dieser Arbeit analysierten Proteine SANS, Ush2a (Usherin), Magi2 und TRAK2 sind farbig hinterlegt, Elemente des Cytoskeletts dunkelgrau (Stand Oktober 2013, modifiziert nach Wolfrum 2011).

Bei USH sind die Haarsinneszellen des Innenohres bereits in ihrer Entwicklung, die Photorezeptorzellen der Retina dagegen durch Degenerationsprozesse nach der vollständigen Entwicklung betroffen. Vorherige Arbeiten haben gezeigt, dass die USH-Proteine in den betroffenen Sinneszellen an funktionell wichtigen *hot spots* lokalisiert sind (Abb. 2; Saihan *et al,* 2009; Wolfrum 2011). Durch die Analysen zu Expression und subzellulärer Lokalisation der USH-Proteine und ihrer Interaktionspartner konnten verschiedene USH-Proteinnetzwerke in diversen subzellulären Kompartimenten nachgewiesen werden (El Amraoui and Petit 2005; Reiners *et al,* 2006; Maerker *et al,* 2008; Yang *et al,* 2010; Overlack *et al,* 2011b*). An den aufgrund ihrer Morphologie *ribbon*-Synapsen genannten Kontaktstellen der Haarsinnes- bzw. der Photorezeptorzellen zu den nachgeschalteten Neuronen sind zum Beispiel alle USH1- und USH2-Proteine lokalisiert (zusammengefasst in: Bonnet and El Amraoui 2012).

Neben synaptischen Netzwerken werden in den Haarsinneszellen des Innenohrs weitere funktionelle Netzwerke von USH-Proteinen aufgebaut (Reiners *et al,* 2006; Caberlotto *et al,* 2011; Grati and Kachar 2011; Wolfrum 2011). Diese Netzwerke sind sowohl für die korrekte Entwicklung als auch für die mechano-elektrische Signaltransduktion (MET) dieser Zellen essentiell (El Amraoui and Petit 2005). Die für die Entwicklung der Haarsinneszellen notwendigen transienten Verbindungen zwischen den Stereocilien werden beispielsweise durch CDH23, PCDH15, Ush2a und GPR89 gebildet (Saihan *et al,* 2009; Lagziel *et al,* 2009; Wolfrum 2011). Die USH1-Proteine CDH23 und PCDH15 bauen außerdem die sogenannten *tip-links* auf, die Verbindungen zwischen den Stereocilien, die für die Reizweiterleitung in den Haarsinneszellen (MET) essentiell sind (Abb. 2A; Kazmierczak *et al,* 2007; Overlack *et al,* 2010). Dagegen interagieren Harmonin, SANS und MyosinVIIa in der sogenannte *upper tip-link density* miteinander, um die schnelle Adaptation schon während des akustischen Signals zu gewährleisten und die Tension der *tip-links* zu kontrollieren (Michalski *et al,* 2009; Grati and Kachar 2011). Auch in Photorezeptorzellen existieren neben den synaptischen weitere USH-Proteinnetzwerke (Abb. 2B; Roepman and Wolfrum 2007; Maerker *et al,* 2008; Overlack *et al,* 2010). Im Fokus der vorliegenden Arbeit stehen die USH-Proteinnetzwerke im periciliären Komplex, die Bezeichnung für ein komplexes Proteinnetzwerk lokalisiert an der Basis des Verbindungsciliums (Papermaster 2002; Maerker *et al,* 2008). In diesem Bereich sind weitere, essentielle Proteinnetzwerke, aufgebaut aus Molekülen des BBSomes und des IFT-Komplexes, lokalisiert (Pazour *et al,* 2002; Nachury *et al,* 2007; Sedmak and Wolfrum 2010).

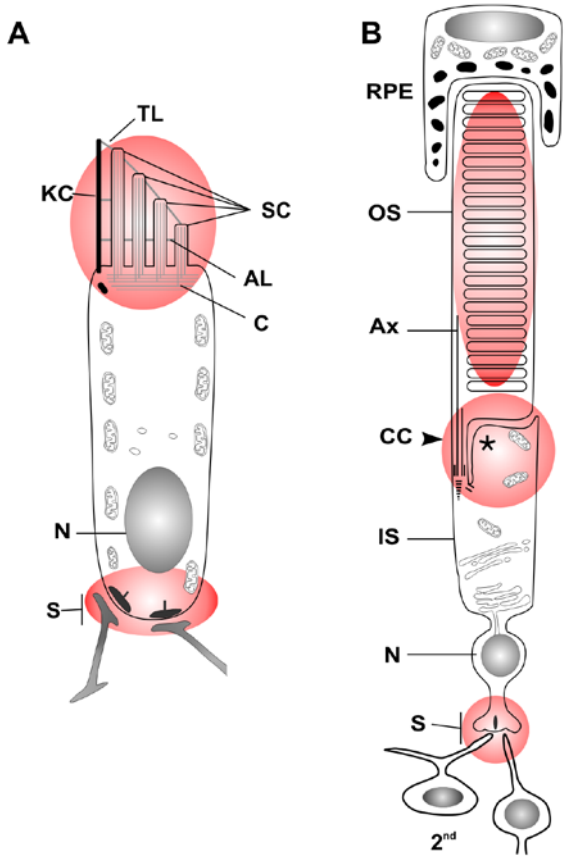

Abbildung 2: Lokalisation der USH-Proteine in den funktionell wichtigen *hot spots* in den sensorischen Zellen von Cochlea und Retina. (A) Die Haarsinneszelle ist in morphologische Untereinheiten gegliedert. Über die Kutikularplatte (C) sind die Stereocilien (SC) verankert und orgelpfeifenartig angeordnet. Die benachbarten SC sind an ihren Spitzen über *tip links* (TL) miteinander verbunden. Während der Entwicklung existieren noch weitere transiente Verbindungen zwischen den SC, hier angedeutet durch die *ankle links* (AL). Ebenfalls nur während der Entwicklung existiert lateral des längsten SC das Kinocilium (KC). **(B)** Die Photorezeptorzelle ist ebenfalls aus verschiedenen subzellulären Kompartimenten aufgebaut. Das lichtsensitive Außensegment (OS), das oben von Zellen des retinalen Pigmentepithels (RPE) umschlossen wird, ist durch das Verbindungscilium (CC) mit dem biosynthetisch aktiven Innensegment (IS) verbunden. Daran schließt sich der Zellkern (N) an. Die *ribbon*-Synapse (S) verbindet die Photorezeptorzelle mit den nachgeschalteten Bipolar- und Horizontalzellen (2nd). Die Lokalisationsschwerpunkte der USH-Proteinnetzwerke sind durch rote Markierungen angedeutet (modifiziert nach Overlack *et al*, 2010).

Die korrekte Lokalisation eines Proteins hängt neben seiner Integration in ein Proteinnetzwerk zunächst von dem gerichteten Transport des Moleküls vom Ort seiner Synthese bis zu seinem Bestimmungsort ab. Vorangegangene Arbeiten zeigen, dass geordnete Transportprozesse innerhalb der Photorezeptorzelle essentiell für deren Entwicklung und die Aufrechterhaltung ihrer Funktion sind (Papermaster 2002; Roepman and Wolfrum 2007). Die hochgradig spezialisierten Photorezeptorzellen sind polarisierte Neuronen, die aus einem licht-sensitiven Außensegment und einem biosynthetisch-aktiven Innensegment aufgebaut sind. Die Membranstapel (Disks) der Außensegmente, in die alle Moleküle der Sehkaskade eingelagert sind, werden kontinuierlich an der Basis des Außensegmentes erneuert, während gealterte Disks an der Spitze des Außensegmentes in den Zellen des retinalen Pigmentepithels

(RPE) phagozytiert werden (Young 1967). Dieser Aufbau erfordert effiziente intrazelluläre Transportprozesse aller Moleküle vom Innensegment über den ciliären Transport bis hin zum Außensegment (Tai *et al,* 1999; Papermaster 2002; Roepman and Wolfrum 2007). Eine wichtige Rolle kommt dabei dem periciliären Komplex zu, dem eine Funktion beim Andocken und Fusionieren von post-Golgi-Vesikeln mit der Membran des apikalen Innensegmentes zugesprochen wird (Zielmembran, siehe Abb. 2B, Sternchen; Deretic 1998; Ghossoub *et al,* 2011). Molekulare Analysen konnten zeigen, dass die USH-Proteine Whirlin und SANS die Organisation des periciliären USH-Proteinnetzwerkes in Photorezeptorzellen übernehmen (Maerker *et al,* 2008; Yang *et al,* 2010; Zou *et al,* 2011). Als direkte Interaktoren können beide Gerüstproteine im Zusammenspiel mit ihren jeweiligen Interaktionspartnern dabei zum einen der Integrität der Zielmembran, zum anderen dem gerichteten Transport von Fracht in Richtung des Außensegmentes von Photorezeptorzellen dienen (Roepman and Wolfrum 2007; Maerker *et al,* 2008; Overlack *et al,* 2011b*).

Die beschriebenen Transportprozesse spielen sowohl für die Entwicklung als auch für die Funktion der Photorezeptorzelle eine wichtige Rolle. Bei der Photorezeptorzelle bzw. ihrem Außensegment handelt es sich um ein sensorisches Primärcilium, das in seiner Struktur und Funktion für die Detektion von Licht modifiziert wurde (Singla and Reiter 2006; Berbari *et al,* 2009). Der Aufbau der Photorezeptorzelle ist demnach vergleichbar mit dem Aufbau des Primärciliums, ein Zellfortsatz, der von jeder Zelle eines Organismus im Laufe seiner Entwicklung gebildet werden kann (Pazour and Witman 2003; Satir and Christensen 2007; Tsang *et al,* 2008). Primärcilien bauen sich aus zwei funktionellen Einheiten auf, dem cytoplasmatisch lokalisierten Basal-Körper eingebettet in der pericentriolaren Matrix (*basal body*) und dem aus der Zelle herausragenden Axonem; sie sind über die *transition zone* miteinander verbunden (D'Angelo and Franco 2009). Mutationen in Genen Cilien-spezifischer Proteine führen zu Multisystemerkrankungen, die unter dem Überbegriff Ciliopathien zusammengefasst werden (Badano and Katsanis 2006; Bisgrove and Yost 2006). Der Vergleich zwischen Primärcilium und Photorezeptorzelle zeigt die Homologien zwischen beiden auf (Abb. 3): Homolog zur *transition zone* des prototypischen Ciliums verknüpft das Verbindungscilium der Photorezeptorzelle das zum Außensegment modifizierte Primärcilium mit dem biosynthetisch aktiven Zellköper, dem Innensegment (Rohlich 1975; Horst *et al*, 1990). Dieser Übergang ist die Engstelle für alle Transportprozesse, die zur Aufrechterhaltung der Funktion sowohl des Primärciliums als auch der Photorezeptorzelle notwendig sind. Der ciliäre Transport wird dabei an der Cilienbasis über exocytotische Prozesse eingeleitet und durch die Proteine des IFT-Komplexes (*intraflagellar transport*)

vermittelt (Rosenbaum *et al,* 1999; Pazour *et al,* 2002; Rosenbaum and Witman 2002; Sedmak and Wolfrum 2010). Für die periciliäre Membran bzw. die Proteine des periciliären Komplexes wird darüber hinaus eine Beteiligung an endocytotischen Prozessen diskutiert (Davenport and Yoder 2005; Nachury *et al,* 2010; Ghossoub *et al,* 2011). In Photorezeptorzellen wird der Spalt zwischen den Membranen des apikalen Innensegmentes und des Verbindungsciliums als Homologie zur *ciliary pocket* des Primärciliums verstanden (rote Linien in Abb. 3). Es handelt sich um eine Einbuchtung der Zellmembran, aus der das Primärcilium hinausragt (zusammengefasst in: Benmerah 2013). Hier wurde für das Primärcilium bereits der Prozess der Endocytose nachgewiesen (Molla-Herman *et al,* 2010; Kaplan *et al,* 2012).

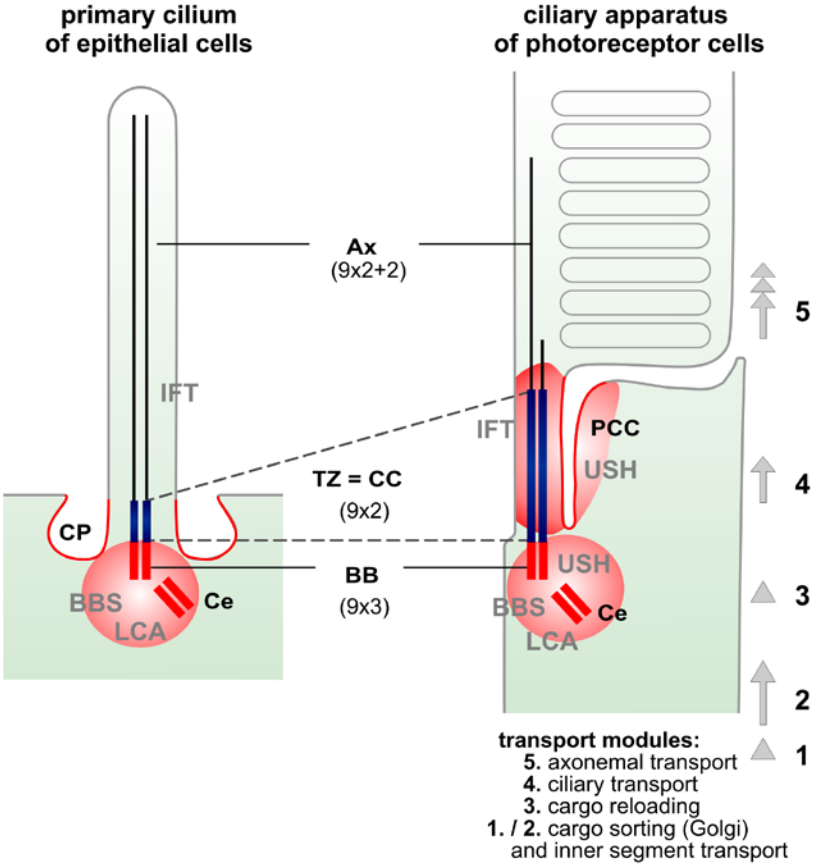

Abbildung 3: Vergleich Primärcilium / Photorezeptorzelle (PRC) sowie die verschiedenen Transportwege innerhalb der PRC. Die *transition zone* (TZ) als Homologie zum Verbindungscilium (CC) entspringt dem Basalkörper (BB), dem das Centriol (Ce) angegliedert ist. Verlängert werden beide Cilien durch das Axonem (Ax). Rot hinterlegt sind die Lokalisationsschwerpunkte der cilien-assoziierten Protein-Komplexe (BBS, LCA, USH) im Bereich von BB und periciliären Komplex (PCC, *periciliary (membrane) complex*). Die rote Membran stellt homolog zur *ciliary pocket* (CP) die Zielmembran für post-Golgi-Vesikel dar. Neben der PRC sind die einzelnen Transportwege innerhalb der Zelle eingezeichnet. Im Innensegment erfolgt der Transport entlang von Mikrotubuli (Modul 1, 2 und 3), das *cargo reloading* wird möglicherweise von USH-Proteinen vermittelt und im Bereich von CC und Ax (Modul 4 und 5) läuft der Transport über Proteine des IFT (*intraflagellar transport*) (verändert nach Sorusch *et al,* 2012* – ARVO Posterpräsentation).

Frühere Analysen deuten darauf hin, dass die USH-Proteinnetzwerke an den genannten intrazellulären und ciliären Transportprozessen beteiligt sind (Reiners *et al,* 2006; Maerker *et al,* 2008; Overlack *et al,* 2011b*). Mutationen in einem der an diesen fein-regulierten Prozessen beteiligten Proteine könnten zu Störungen in der zielgerichteten Verteilung von Molekülen innerhalb der Zelle und damit zur Beeinträchtigung der Funktion der Photorezeptorzelle führen (Roepman and Wolfrum 2007; Kersten *et al,* 2012*). Eine mögliche Folge ist der Zelltod und damit der retinale Phänotyp von USH.

Die Identifizierung und funktionelle Charakterisierung weiterer Interaktionen erlaubt tiefere Einsichten in die Vernetzung des USH-Interaktoms mit Molekülen, die im Zusammenhang mit anderen neurodegenerativen Erkrankungen des Menschen stehen (Wolfrum 2011). Die Kenntnis um diese Proteine ist eine Voraussetzung sowohl für das Verständnis der Funktion individueller USH-Proteine als auch des gesamten Proteinnetzwerkes. In der vorliegenden Arbeit stehen das Gerüstprotein SANS und seine direkten Interaktionspartner Ush2a, Magi2 und TRAK2 im Mittelpunkt.

1.3 Das USH1G-Protein SANS

SANS (scaffold protein containing ankyrin repeats and SAM domain) wird bereits in sehr frühen Stadien in der Entwicklung der Mausretina exprimiert (post natal PN0) (Overlack *et al,* 2008). In der adulten Retina ist SANS im Verbindungscilium und dem damit assoziierten Centriol, im apikalen Innensegment und im Bereich der Synapsen zwischen Photorezeptoren und nachgeschalteten Neuronen lokalisiert, also in den bereits erwähnten funktionellen *hot spots* innerhalb der Photorezeptorzelle (Overlack *et al,* 2008; Overlack *et al,* 2011b*). In den Haarsinneszellen des Innenohres ist SANS mit den Mikrotubuli-reichen Strukturen des MTOC (*microtubule organizing center*) sowie der Kutikularplatte assoziiert und ist ebenfalls im Bereich der Synapsen lokalisiert (Adato *et al,* 2005). Darüber hinaus ist SANS über seine Interaktion mit Harmonin und MyosinVIIa in den *tip-links* der Stereocilien an der mechano-elektrischen Signalweiterleitung (MET) beteiligt (Caberlotto *et al,* 2011).

Seine Domänenstruktur (Publikation II, Abb. 1) klassifiziert SANS als Gerüstprotein, dessen Protein-Binde-Domänen die Interaktion mit sich selbst und mit unterschiedlichen Proteinen zu Multiprotein-Komplexen ermöglicht (Adato *et al,* 2002; Kikkawa *et al,* 2003). Für die N-terminalen Ankyrin-repeats wurden bisher keine Interaktionspartner identifiziert, die zentrale Domäne interagiert mit dem Motorprotein MyosinVIIa (USH1B) und Myomegalin und vermittelt die SANS-Homomerisierung (Adato *et al,* 2005; Overlack *et al,* 2011b*; Wu *et al,* 2011). Der C-Terminus mit SAM-Domäne (*sterile alpha motif*) und dem

PBM (PDZ-*binding motif*) ist mit Harmonin (USH1C) und Whirlin (USH2D) assoziiert (Adato *et al,* 2005; Maerker *et al,* 2008; Yan *et al,* 2010). Weitere Analysen durch uns und andere Arbeitsgruppen weisen zudem auf eine Assoziation von SANS mit dem Mikrotubuli-Cytoskelett hin (Overlack *et al,* 2008; Zallocchi *et al,* 2010). Darüber hinaus zeigen diese Ergebnisse, dass SANS im apikalen Innensegment am Übergang zum Verbindungscilium an der Organisation des periciliären USH-Proteinnetzwerkes beteiligt ist (Maerker *et al,* 2008). In diesem Kompartiment könnte SANS über seine Interaktionspartner den Transport von Membrankomponenten ins Außensegment der Photorezeptorzelle vorbereiten (van Wijk *et al,* 2006; Maerker *et al,* 2008). Für die Beteiligung an Transportprozessen spricht auch die Lokalisation von SANS entlang der Mikrotubuli (Overlack *et al,* 2011b*).

1.4 Zielsetzung der Arbeit

Für das Verständnis der molekularen Grundlagen einer genetisch komplexen Erkrankung ist es unabdingbar, die Funktion der einzelnen Genprodukte zu analysieren und ihre Rolle im zellulären Kontext aufzuklären. Ziel dieser Arbeit ist es, weitere Erkenntnisse zur Funktion von USH-Proteinen, insbesondere für das USH1G-Protein SANS, in der Photorezeptorzelle zu erhalten. Dadurch ergeben sich folgende Zielsetzungen:

1. Die neueren molekular-biologischen und systembiologischen Arbeiten zur Analyse des humanen Usher-Syndroms (USH) deuten darauf hin, dass die Pathomechanismen, die zu USH führen, auf ciliäre Defekte zurückzuführen sind. Bisher ist USH allerdings nicht als Ciliopathie definiert worden. Eine Zielsetzung der vorliegenden Arbeit ist es, in einem Übersichtsartikel die molekularen Verbindungen von USH zu anderen Ciliopathien herauszuarbeiten (Publikation I). Ergänzend soll das USH1G-Protein SANS auf seine Beteiligung an der Ciliogenese überprüft werden (Publikation III).
2. Proteine stehen in ihrer Funktion nicht alleine, sondern bauen funktionelle Module auf, um auf intra- und extrazelluläre Anforderungen reagieren zu können (Hartwell et al, 1999; Spirin and Mirny 2003). Die USH-Proteine bilden solche komplexen Proteinnetzwerke aus, deren Zusammensetzung an ihre Funktion angepasst ist (zusammengefasst in: Roepman and Wolfrum 2007; Wolfrum 2011). Vorangegangene Arbeiten haben gezeigt, dass die bisher identifizierten Interaktionspartner der USH-Proteine in der Photorezeptorzelle verschiedene Proteinnetzwerke aufbauen, deren Fehlfunktionen an den pathophysiologischen Prozessen von USH beteiligt sind. Die Identifizierung und funktionelle Charakterisierung neuer Interaktionspartner soll das Verständnis zur Funktion dieser Netzwerke in Photorezeptorzellen erweitern. Das vorrangige Ziel dieser Arbeit ist es, durch die funktionelle Charakterisierung neuer Interaktionspartner von SANS weitere Erkenntnisse zur Funktion der USH-Proteinen in den funktionellen Modulen zu erarbeiten (Publikation II und III).

3. Die Screens zur Identifizierung neuer Interaktionspartner weisen darauf hin, dass noch weitaus mehr Proteine zur Komplexität des USH-Interaktoms beitragen (Maerker et al, 2008; Overlack et al, 2011b*). Um gerichtet auf zelluläre Anforderungen zu reagieren, können diese vielfältigen Interaktionen nicht simultan stattfinden, die Interaktionen in den verschiedenen Proteinnetzwerken erfordern Regulationsmechanismen. Proteinnetzwerke können durch post-translationale Modifizierung der Netzwerk-Partner reguliert werden, ein weiteres Ziel dieser Arbeit ist deshalb die Überprüfung einer regulatorischen Funktion von SANS in den funktionellen Modulen des USH-Interaktoms (Publikation II und III).

Insgesamt sollen im Rahmen dieser Arbeit neue Erkenntnisse zur Funktion der USH-Proteinnetzwerke in der Photorezeptorzelle gewonnen werden. Dies soll die Kenntnisse der pathophysiologischen Prozesse, die zum retinalen Phänotyp bei USH führen, erweitern. Nur dadurch wird es möglich, fundierte Strategien zur Therapie der retinalen Degeneration von USH-Patienten zu entwickeln (Goldmann *et al,* 2010; Overlack *et al,* 2012).

2. Publikationen

2.1 Sorusch N, Wunderlich K, **Bauß K**, Nagel-Wolfrum K, Wolfrum U. Usher syndrome protein network functions in the retina and their relation to other retinal ciliopathies.

– in Druck

2.2 **Bauß K**[#], Sorusch N[#], Wolfrum U. Direct interaction of the Usher syndrome proteins SANS and Ush2a (# both authors contributed equally to the work).

– in Vorbereitung

2.3 **Bauß K**, Knapp B, Jores P, Spitzbarth B, Kremer H, van Wijk E, Maerker T, Wolfrum U. Phosphorylation of the Usher syndrome protein SANS controls Magi2-mediated endocytosis.

– unter Begutachtung

Publikation I

Sorusch N, Wunderlich K, **Bauß K**, Nagel-Wolfrum K, Wolfrum U (in press). Usher syndrome protein network functions in the retina and their relation to other retinal ciliopathies. In: Retinal Degenerative Diseases. Eds: Ash J, Hollyfield JG, LaVail MM, Anderson RE, Grimm C and Rickman CB, Springer.

Chapter 67

Usher syndrome protein network functions in the retina and their relation to other retinal ciliopathies

Nasrin Sorusch, Kirsten Wunderlich, Katharina Bauss, Kerstin Nagel-Wolfrum, Uwe Wolfrum*

Johannes Gutenberg University Mainz, Institute of Zoology, Dept. Cell & Matrix Biology, Mainz, Germany

*Corresponding author: JGU Mainz, Institute of Zoology, Johannes-von-Mueller-Weg 6, D-55099 Mainz, Germany. Phone: +49 613139-23934. Fax: -23815. Email: wolfrum@uni-mainz.de

Key words: Usher syndrome, deaf-blindness, *Retinitis pigmentosa*, LCA, BBS, ciliopathy, protein networks, interactome, ciliary transport

Abstract

The human Usher syndrome (USH) is the most frequent cause of combined hereditary deaf-blindness. USH is genetically and clinically heterogeneous: 15 chromosomal loci assigned to 3 clinical types, USH1-3. All USH1 and 2 proteins are organized into protein networks by the scaffold proteins harmonin (USH1C), whirlin (USH2D) and SANS (USH1G). This has contributed essentially to our current understanding of the USH protein function in the eye and the ear and explains why defects in proteins of different families cause very similar phenotypes. Ongoing in depth analyses of USH protein networks in the eye indicated cytoskeletal functions as well as roles in molecular transport processes and ciliary cargo delivery in photoreceptor cells. The analysis of USH protein networks revealed molecular links of USH to other ciliopathies, including non-syndromic inner ear defects and isolated retinal dystrophies but also to kidney diseases and syndromes like the Bardet-Biedl syndrome. These findings provide emerging evidence that USH is a ciliopathy molecularly related to other ciliopathies, which opens an avenue for common therapy strategies to treat these diseases.

67.1 Introduction to the human Usher syndrome

The human Usher syndrome (USH), with a prevalence of ~1/6.000, is categorized as rare disease but is also the most frequent cause of combined hereditary deaf-blindness [1, 2]. It is characterized by hearing impairment, vestibular dysfunction and retinal degeneration, *Retinitis pigmentosa* (RP). The 3 clinical subtypes (USH1-3) differ in severity, age of onset, and progression of symptoms. USH is genetically heterogeneous; 10 identified USH genes encode proteins from various families [2, 3]: myosin VIIa (USH1B) is a molecular motor protein; harmonin (USH1C), SANS (scaffold protein containing ankyrin repeats and SAM domain/USH1G), and whirlin (USH2D) are scaffold proteins; cadherin 23 (cdh23/USH1D) and protocadherin 15 (pcdh15/USH1F) are adhesion proteins; the recently identified CIB2 (USH1J) is a calcium- and integrin-binding protein; the G protein-coupled receptor 98 (Gpr98 = VLGR1b, very large G protein coupled receptor/USH2C) is the largest known adhesion GPCR found and like USH2a ("usherin") a transmembrane protein; clarin-1 (USH3A) is a transmembrane protein of the tetraspanin family. Most USH genes are alternatively spliced and exist in several isoforms probably serving in different cellular functions. Moreover, *PDZD7* alleles contribute to digenic USH or act as modifiers of the retinal phenotype [4].

67.2 USH protein networks

The diversity of the affected proteins is surprising, given that the clinical phenotypes of the three USH types are very similar. The successive identification of supramolecular protein networks related to USH provided an explanation to this phenomenon and thereby insights into the complex pathophysiology of USH. In the USH protein interactome all USH1 and USH2 proteins are integrated mainly by direct interactions to the USH scaffold proteins harmonin, SANS, whirlin and the tail of myosin VIIa (Fig. 67.1A) [2, 3, 5, 6]. In addition, the USH3 protein clarin-1 may also associate with the USH1/USH2 protein network [7]. Furthermore, the genetic modifier PDZD7 is part of the USH interactome [4, 8]. Beyond that, direct links of USH protein networks to the actin and the microtubule cytoskeleton are described [5, 9]. Systematic proteomic screens for USH protein network partners revealed direct and indirect interactions of USH proteins with several dozen non-USH proteins including disease related proteins [9, 10]. Interestingly, the set of recently identified interaction partners of USH proteins include proteins related to retinal and syndromic ciliopathies (Fig. 67.1B).

67.3 USH interactome is molecularly linked to other ciliopathies

Ciliopathies are a group of disorders that affect the formation, function and maintenance of cilia (Fig. 67.2A-D). There has been growing evidence that USH, affecting ciliated sensory cells in the inner ear and the retina, displays characteristics of a ciliopathy, and recently discovered molecular links to other ciliopathies support this hypothesis: The USH2 protein whirlin connects USH networks to the RP GTPase regulator (RPGR) [11]. In photoreceptor cells, the splice variant $RPGR^{ORF15}$ is suggested to interact with multiple proteins that are related to cilia function; including the intraflagellar transport (IFT) protein IFT88, the IFT motor KIF3A, and the RPGR interacting protein (RPGRIP1), which is part of the nephrocystin protein network [12, 13]. Mutations in the *RPGRIP1* gene can lead to Leber congenital amaurosis (LCA), probably the most severe form of retinal dystrophy. An additional molecular link between USH and LCA exists through the direct binding of USH2a to the centriolar ninein-like protein (Nlp) isoform B which mediates the molecular bond to the LCA5 protein lebercilin [14]. Lebercilin is a ciliary protein associated with components of the IFT protein complex B in photoreceptor cells [15, 16].

We have recently shown that the USH1G protein SANS binds to the centrosomal protein of 290 kDa (Cep290) (Sorusch et al., in prep.). Cep290 is essential for biogenesis and maintenance of cilia. Mutations in *CEP290* are causative for multiple non-syndromic and syndromic ciliopathies of diverse severity: LCA, nephronophthisis (NPHP), Senior-Loken syndrome (SLS), Joubert syndrome (JBTS), Bardet-Biedl syndrome (BBS), and the lethal Meckel-Gruber syndrome (MKS) [17]. Moreover, Cep290 participates in protein complexes with numerous of other ciliopathy molecules, e.g. RPGR, RPGRIP1, lebercilin, Nlp and BBS6 [17]. The SANS interaction with the comprehensive ciliopathy molecule Cep290 provides additional molecular links of the USH interactome to other ciliopathy networks.

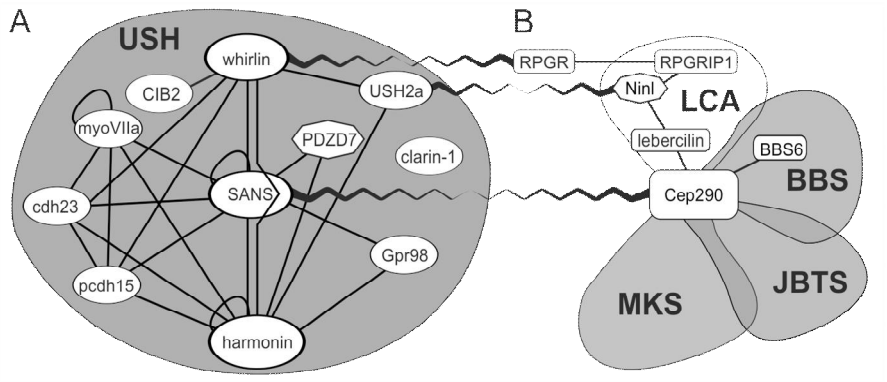

Fig. 67.1: The USH protein interactome (solid lines) **(A) and links to molecules of other ciliopathies** (zig-zag lines) **(B)**.

67.4 USH protein networks in the inner ear and eye.

Mutations in USH genes lead to dysfunction of mechanosensory hair cells in the inner ear and light-sensitive photoreceptor cells as well as the cells of the retinal pigment epithelium (RPE). Intense mouse model analyses revealed that USH proteins and their networks are essential for inter-stereovilli links in the signal perceiving hair bundles [18]. Defects in USH proteins lead to altered stereovilli organization during hair cell differentiation. In addition, USH proteins are present in ribbon synapses of auditory hair cells [2]. There, harmonin scaffolds ion channel complexes regulating electrical and Ca^{2+} signaling in inner hair cell synapses [19].

In RPE cells, myosin VIIa is the only USH protein, essential for melanosome transport into the apical microvillar compartment and for phagocytosis of the outer segment tips (Fig. 67.2) [20]. In photoreceptor cells, most USH proteins seem to be expressed at their ribbon synapses indicating the formation of protein networks [1, 2]. Nevertheless, there is no consistent knowledge on their function in photoreceptor synapses, so far.

However, prominent USH protein networks additionally associate with adhesion complexes in calycal processes and in the periciliary membrane complex (PMC) of photoreceptor cells [2]. Calycal processes are characteristic for vertebrate photoreceptor cells and resemble microvilli-like apical extensions of the inner segment that shield the basolateral region of the outer segment like the calyx of

a flower (Fig. 67.2B). A recent systematic analysis indicated that USH1 proteins are localized in the calycal processes of the photoreceptor inner segments [21]. In contrast, our data revealed the absence of harmonin in the presence of other USH1 and all three USH2 proteins [2]. Anyhow, the USH protein network may serve in adhesion complexes to stabilize the calyx and thereby the fragile area of the *de novo* genesis of outer segment disks. The presence of USH proteins in calycal processes, which are absent in the slender photoreceptor cells of rodents (Fig. 67.2A,B), may explain the incoherency in phenotypes of human patients and USH mouse models.

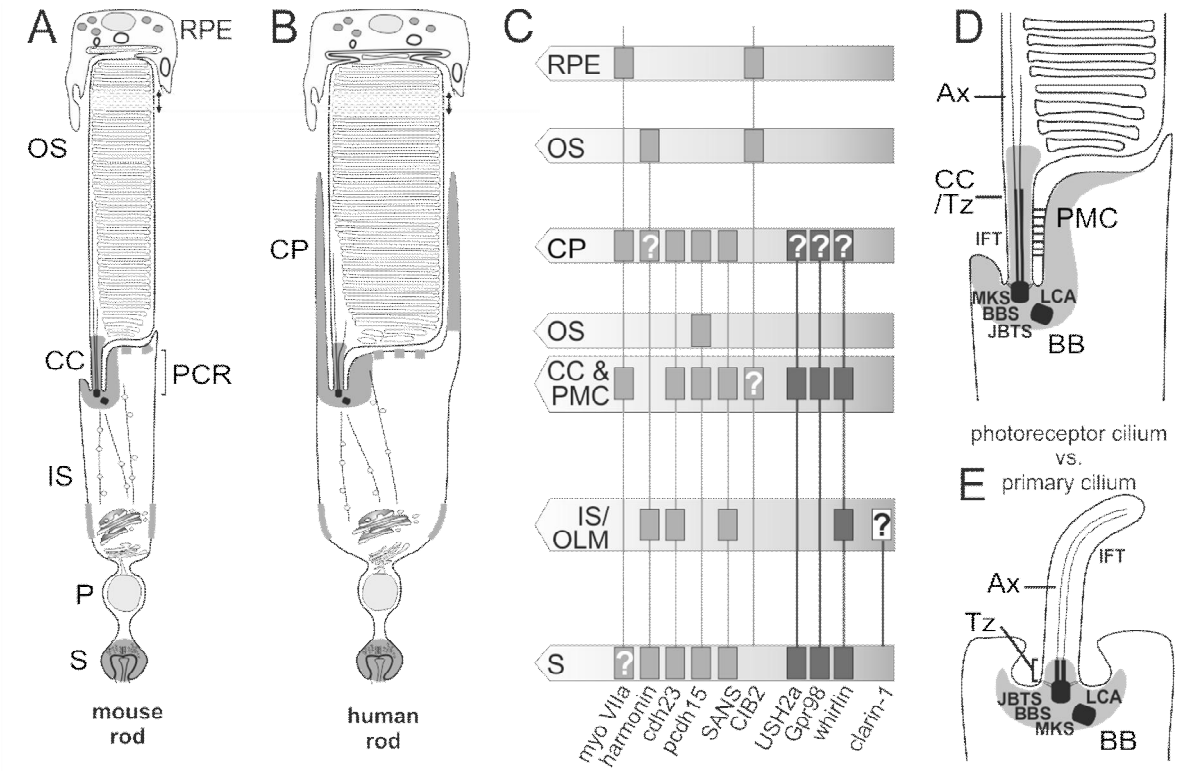

Fig. 67.2: Ciliopathy-related protein localization in photoreceptors and primary cilia.
Rodent **(A)** and human rods **(B)** are composed of the photosensitive outer segment (OS), resembling a modified primary cilium, and the synthetic active inner segment (IS) connected by the connecting cilium (CC). CP, calycal processes; PMC, periciliary membrane complex; P, perikaryon; S, synapses; OLM, outer limiting membrane; RPE, retinal pigment epithelium; *Grey* areas: USH protein networks. **(C)** USH protein localization; question marks: controversial data. **(D, E)** Localization of ciliopathy related protein networks in the photoreceptor cilium (**D**) and in the primary cilium (**E**). *Grey* areas: co-localizations of USH proteins with ciliopathy molecules. Ax, axoneme; BB, basal body; Tz, transition zone.

In the PMC of photoreceptor cells, USH proteins provide the molecular basis for the membrane adhesion between the inner segment and the connecting cilium [6, 10]. Fibrous links of the PMC are homologue to ankle-links in hair cells and composed of extracellular domains of the Gpr98 and USH2a. The transmembrane proteins are anchored via their intracellular tail by whirlin in the periciliary cytoplasm. There is growing evidence that SANS links this complex to the microtubule based transport routes for outer segment cargoes though the cytoplasm of the inner segment [9]. However, USH proteins are also localized in the photoreceptor connecting cilium, the transition zone between the inner and the outer segment. Myosin VIIa is thought to participate in opsin transport across this zone [2, 22].

67.5 USH networks in ciliary transport of photoreceptor cells

The periciliary compartment plays an extraordinary role in the ciliary cargo transport in cilia in general: the transport of cargo through the cytoplasm is specifically targeted to the periciliary region before the cargo import can occur through the transition zone into the ciliary axoneme. Molecules related to ciliopathies, as described above, are essential for these processes [17, 23]. In the periciliary region of photoreceptor cells, the periciliary USH protein network molecularly characterizes the PMC (see above). The inner segment membrane region of the PMC is thought to serve as the target for vesicle transport through the cytoplasm [6, 10]. Current research provides growing evidence that USH proteins work in concert with BBSome components and other ciliopathy proteins in the cargo transfer from the inner segment transport to the ciliary transport module, in which IFT particles and myosin VIIa take over powering the cargo transport to its ciliary destination.

67.6 Conclusions

The protein interactome related to USH is linked with proteins and networks of other ciliopathies. The participation of ciliopathy related proteins in common cellular mechanisms explain the overlap of pathogenic defects in ciliogenesis, cilia maintenance and ciliary transport. Shared molecular features of USH and other ciliopathies may open an avenue for common therapeutic strategies for the treatment of patients affected by these diseases.

Supports: Deutsche Forschungsgemeinschaft (DFG, GRK 1044); European Community FP7/2009/241955 (*SYSCILIA*) and FP7/2009/242013 (*TREATRUSH*); FAUN-Stiftung; Foundation Fighting Blindness (FFB); Forschung contra Blindheit; ProRetina Deutschland.

References:

1. Saihan Z et al. Update on Usher syndrome. Curr Opin Neurol 2009; 22:19-27.

2. Wolfrum U. Protein networks related to the Usher syndrome gain insights in the molecular basis of the disease. In: Ahuja S, ed. Usher Syndrome: Pathogenesis, Diagnosis and Therapy. USA: Nova Science Publishers Inc.; 2011. p. 51-73.

3. Riazuddin S et al. Alterations of the CIB2 calcium- and integrin-binding protein cause Usher syndrome type 1J and nonsyndromic deafness DFNB48. Nat Genet 2012; 44:1265-71.

4. Ebermann I et al. PDZD7 is a modifier of retinal disease and a contributor to digenic Usher syndrome. J Clin Invest 2010; 120:1812-23.

5. Reiners J et al. Molecular basis of human Usher syndrome: deciphering the meshes of the Usher protein network provides insights into the pathomechanisms of the Usher disease. Exp Eye Res 2006; 83:97-119.

6. Yang J. Usher Syndrome: Genes, Proteins, Models, Molecular Mechanisms, and Therapies. In: Naz DS, ed. Hearing Loss: Intech; 2012.

7. Zallocchi M et al. Role for a novel Usher protein complex in hair cell synaptic maturation. PLoS One 2012; 7:e30573.

8. Schneider E et al. Homozygous disruption of PDZD7 by reciprocal translocation in a consanguineous family: a new member of the Usher syndrome protein interactome causing congenital hearing impairment. Hum Mol Genet 2009; 18:655-66.

9. Overlack N et al. Direct interaction of the Usher syndrome 1G protein SANS and myomegalin in the retina. Biochim Biophys Acta 2011; 1813:1883-92.

10. Maerker T et al. A novel Usher protein network at the periciliary reloading point between molecular transport machineries in vertebrate photoreceptor cells. HumMolGenet 2008; 17:71-86.

11. Wright RN et al. RpgrORF15 connects to the usher protein network through direct interactions with multiple whirlin isoforms. Invest Ophthalmol Vis Sci 2012; 53:1519-29.

12. Roepman R, Wolfrum U. Protein networks and complexes in photoreceptor cilia. In: Faupel M, Bertrand E, eds. Subcellular Proteomics - From Cell Deconstruction to System Reconstruction. Vol Subcellular Biochemistry. Dordrecht, The Netherlands: Springer; 2007. p. 209-35.

13. Sang L et al. Mapping the NPHP-JBTS-MKS protein network reveals ciliopathy disease genes and pathways. Cell 2011; 145:513-28.

14. van Wijk E et al. Usher syndrome and Leber congenital amaurosis are molecularly linked via a novel isoform of the centrosomal ninein-like protein. Hum Mol Genet 2009; 18:51-64.

15. den Hollander AI et al. Mutations in LCA5, encoding the ciliary protein lebercilin, cause Leber congenital amaurosis. Nat Genet 2007; 39:889-95.

16. Boldt K et al. Disruption of intraflagellar protein transport in photoreceptor cilia causes Leber congenital amaurosis in humans and mice. J Clin Invest 2011; 121:2169-80.

17. Coppieters F et al. CEP290, a gene with many faces: mutation overview and presentation of CEP290base. Hum Mutat 2010; 31:1097-108.

18. Muller U, Gillespie P. Silencing the cochlear amplifier by immobilizing prestin. Neuron 2008; 58:299-301.

19. Gregory FD et al. Harmonin inhibits presynaptic Cav1.3 Ca(2)(+) channels in mouse inner hair cells. Nat Neurosci 2011; 14:1109-11.

20. Gibbs D et al. Function of MYO7A in the human RPE and the validity of shaker1 mice as a model for Usher syndrome 1B. Invest Ophthalmol Vis Sci 2010; 51:1130-5.

21. Sahly I et al. Localization of Usher 1 proteins to the photoreceptor calyceal processes, which are absent from mice. J Cell Biol 2012; 199:381-99.

22. Wolfrum U, Schmitt A. Rhodopsin transport in the membrane of the connecting cilium of mammalian photoreceptor cells. Cell MotilCytoskeleton 2000; 46:95-107.

23. Zaghloul NA, Katsanis N. Mechanistic insights into Bardet-Biedl syndrome, a model ciliopathy. J Clin Invest 2009; 119:428-37.

Publikation II

Bauß K[#], Sorusch N, Wolfrum U (in preparation). Direct interaction of the Usher syndrome proteins SANS and Ush2a (# both authors contributed equally to the work).

Direct interaction of the Usher syndrome

Proteins SANS and Ush2a

Katharina Bauß[#], Nasrin Sorusch[#] and Uwe Wolfrum*

# both authors contributed equally to the work

*Corresponding Author: Johannes Gutenberg University, Institute of Zoology, Cell and Matrix Biology, Muellerweg 6, D-55099 Mainz, Germany.
Tel.: + 49-6131-39-25148; Fax: 49-6131-39-23815; E-mail: wolfrum@uni-mainz.de

Running title: SANS - Ush2a interaction

Abstract

The human Usher syndrome (USH) is the most common form of hereditary deaf-blindness, mainly affecting the ciliated cells of the inner ear and the retina. USH is a complex ciliopathy with 12 chromosomal loci assigned to 3 clinical subtypes, USH type 1 – 3. We and others have previously demonstrated that all USH1 and USH2 proteins are organized into protein networks. This has contributed essentially to our current understanding of the USH protein function and explains why defects in proteins of diverse families cause very similar phenotypes.

The close molecular association of USH1 and USH2 proteins in the periciliary network decided us to elucidate the binding ability of the USH1G protein SANS (scaffold protein containing ankyrin repeats and SAM domain) to the USH2 protein Ush2a. We affirmed the direct interaction of Ush2a to the central domain of SANS and demonstrated the phosphorylation dependency of this interaction. Furthermore, we confirmed a ternary network of SANS, whirlin and Ush2a.

These data further elucidate the periciliary membrane USH protein complex and support its role in the transport of ciliary cargo. The ternary SANS-Ush2a-whirlin complex may participate in the cargo transfer from inner segment transport carriers to the ciliary delivery system of photoreceptor cells. Furthermore, the direct interaction between the USH1G protein SANS and the USH2 proteins Ush2a and whirlin underlines the close molecular alliance of USH type 1 and type 2.

Introduction

The human Usher syndrome (USH) as ciliopathy affects the ciliated sensory cells of the inner ear and the retina and represents the most frequent cause of combined hereditary deaf-blindness (Reiners *et al.,* 2006; Wolfrum 2011). USH is genetically heterogeneous with at least 12 chromosomal loci involved (Kremer *et al.,* 2006; Dad *et al.,* 2010). Depending on time of onset, progression and severity of symptoms, USH can be divided into 3 clinical subtypes USH type 1 – 3 (Davenport and Omenn 1977). USH1 represents the most severe form, characterized by profound congenital deafness, vestibular dysfunction and pre-pubertal onset of *retinitis pigmentosa,* whereas USH2 is the most prevalent form with moderate hearing impairment without vestibular dysfunction and variable onset of *retinitis pigmentosa* (Reiners *et al.,* 2006; Ben Rebeh *et al.,* 2008; Nakanishi *et al.,* 2010; Vache *et al.,* 2012).

The gene products of the 10 so far identified USH genes belong to diverse protein classes and families, namely molecular motors, cell-cell adhesion molecules, transmembrane receptors and scaffold proteins (Kremer *et al.,* 2006; Reiners *et al.,* 2006; Wolfrum 2011). We and others have previously demonstrated that all USH1 and USH2 proteins are organized into protein networks by direct binding to the PDZ-domain containing scaffold proteins harmonin (USH1C) and whirlin (USH2D) (Reiners *et al.,* 2005; Reiners *et al.,* 2006; Maerker *et al.,* 2008; van Wijk *et al.,* 2009; Yang *et al.,* 2010). More recent work indicated the presence of the USH1G protein SANS (scaffold protein containing ankyrin repeats and SAM domain) and the genetic modifier PDZD7, a direct interaction partner of Ush2a, in these networks (Maerker *et al.,* 2008; Schneider *et al.,* 2009; Ebermann *et al.,* 2010). These studies explain why defects in proteins of diverse families cause very similar USH phenotypes.

For the understanding of the pathophysiology of USH, the elucidation of the functions of protein networks related to USH are important (Wolfrum 2011). In the present study we focused on the USH1G protein SANS. As the name implies SANS is a scaffold protein, which consists of following putative protein binding domains (Figure 1A): three ankyrin repeats at the N-terminus, a less characterized central domain (CENT), a SAM (sterile alpha motif) domain and a class I PBM (PDZ-binding motif) at the C-terminus (Adato *et al.,* 2005). Current research provides growing

evidence that SANS contributes to the intracellular transport through the inner segment to the periciliary region, where SANS is an additional component of the periciliary membrane complex (PCM) (Liu *et al.,* 2007; Maerker *et al.,* 2008; van Wijk *et al.,* 2009; Yang *et al.,* 2010; Overlack *et al.,* 2011).

Although we have characterized several binding partners of SANS in previous investigations (Adato *et al.,* 2005; Maerker *et al.,* 2008), we aspired to identify further interaction proteins to get a more supplemented view of the USH protein networks arranged by SANS in photoreceptor cells. The close proximity of USH1 and USH2 proteins in the periciliary region prompted us to check if SANS interacts with other USH proteins besides whirlin (Maerker *et al.,* 2008).

In the present study, we elucidated the interaction of SANS to Ush2a, whose intracellular domain was identified as directly interacting to SANS. We validated the SANS-Ush2a interaction by independent, complementary assays. Immunolabeling for correlative light and electron microscopy revealed that SANS and Ush2a are localized at the periciliary membrane, the basal body, and the adjacent centriole of the photoreceptor cilium. Furthermore, we demonstrated a the ternary complex composed of the USH1G protein SANS and the two USH2 proteins whirlin and Ush2a which further underlines the close molecular alliance between the USH1 and USH2 protein networks in the USH protein interactome.

Material & Methods

Antibodies and fluorescent dyes

Newly designed polyclonal SANS antibodies were generated against a murine fragment (aa 339-384) and raised in guinea pig. The specificity of antibodies was validated by RNAi approach using specific shRNA against SANS (Bauß *et al.*, under revision). Polyclonal Ush2a antibodies generated against a human fragment (aa 5064-5202) and raised in rabbits, were previously characterized (Maerker *et al.*, 2008; Overlack *et al.*, 2008). Anti-FLAG-tag and anti-RFP-tag antibodies were acquired from Sigma-Aldrich (Sigma-Aldrich Chemie GmbH, Deisenhofen, Germany) or ChromoTek GmbH (Planegg-Martinsried, Germany), respectively. Anti-HA antibodies were from Roche Diagnostics (Mannheim, Germany) and anti-GST from GE Healthcare (Munich, Germany). Monoclonal antibodies against Centrin 2 and 3 as markers for the connecting cilium, the basal body and the adjacent centriole of photoreceptor cells were previously reported (Wolfrum *et al.*, 1998; Trojan *et al.*, 2008). Anti-GFP antibodies were a kind gift of W. Clay Smith (University of Florida, USA) (Peterson *et al.*, 2003). Secondary antibodies conjugated to Alexa 488, 568 or Alexa 647 purchased from Invitrogen (Life Technologies GmbH, Darmstadt, Germany) and biotinylated secondary antibodies (Vector Laboratories Inc., Burlingame, USA) were used. Nuclear DNA was stained with 4′, 6-Diamidin-2′-phenylindoldihydrochlorid (DAPI; 1 µg/ml).

Cell culture

HEK293 (human embryonic kidney cells) or IMCD3 (mouse inner medullary collecting duct cells) cells were used and grown in Dulbecco's modified Eagle's medium (DMEM; HEK293) or Dulbecco's Modified Eagle Medium Nutrient Mixture F-12 (DMEM-F12; IMCD3), containing 10% heat-inactivated foetal calf serum (FCS). Cell lines were chemically transfected with constructs individually or in combination using Lipofectamine™ (LTX) and Plus reagent (Invitrogen™) as transfection reagent.

GST pull-down assays

Parts of the intracellular domain of human Ush2a were subcloned in the pDest15 vector (aa 5064-5202, Ush2a-icd ≡ aa_{1-139}; aa 5064-5196, Ush2a-icdΔPBM ≡ aa_{1-133}; aa 5169-5202, Ush2a-icd ≡ $aa_{106-139}$), expressed in *E. coli* BL21AI and bound to sepharose beads as described in (Gießl *et al.*, 2004). As negative control, GST alone was expressed. Three times FLAG-tagged human SANS full length (aa 2–461; 3xFLAG-SANS) was produced by transfection of HEK293T cells using LTX according to manufacturer's instructions. For the reciprocal assay we subcloned the intracellular domain of Ush2a in the FLAG-expression vector (3xFLAG-Ush2a-icd) and the SANS´ N-terminus (aa 2-126, GST-Nterm), central (aa 125-388, GST-CENT) and SAM-PBM (aa 385-461, GST-SAM-PBM) domain in the GST-expression vector. 24 h post-transfection, cells were washed with PBS and subsequently lysed on ice in lysis buffer (50 mM Tris–HCL pH 7.5, 150 mM NaCl, and 0.5% Triton X-100) containing a protease inhibitor cocktail (PI-mix, Roche Diagnostics GmbH, Risch, Suisse). The cell supernatant was incubated for 3 h at 4°C with equal amounts of beads pre-incubated either with GST

or with GST-fusion proteins. Beads were washed with lysis buffer and precipitated protein complexes were eluted with SDS sample buffer and subjected to SDS-PAGE and Western blot.

Co-(immuno) precipitation assays

GFP-agarose beads (GFP-Trap®_A) were purchased from ChromoTek to perform GFP-Trap® following instructor´s user manual. Briefly, HEK293T cells were co-transfected with GFP-SANS (aa 2-461) and mRFP-Ush2a-icd (aa1-139) or mRFP only as negative control using LTX. 24 h post-transfection, cells were harvested and obtained cell lysates were incubated for 2 h with GFP-Trap®_A. Beads were washed with dilution buffer (10 mM Tris/Cl pH7.5, 150 mM NaCl, 0.5 mM EDTA, PI-mix) and precipitated protein complexes were eluted with SDS sample buffer and subjected to SDS-PAGE and Western blot. To elucidate the influence of posttranslational modifications, transfection media and buffers contain 150 mM DRB (D-ribofuranosyl-benzimidazole) from Biomol GmbH (Hamburg, Germany) or 50 µM of the PP2A inhibitor okadaic acid from AppliChem GmbH (Darmstadt, Germany). For co-IP, 3xFLAG-SANS or FLAG-tagged SANS lacking the PDZ-binding motif (aa 2–450; 3xFLAG-SANSΔPBM) and HA-tagged whirlin (human, pcDNA3-HA-Dest vector, aa 2-907) were singly expressed in HEK293T cells using LTX. Co-IP was performed using ANTI-FLAG® beads from Sigma according to manufacturer's protocol. Briefly, we got cell lysates using TritonX100 lysis buffer containing PI-mix, incubated cell lysates for 2 h at 4°C and then added FLAG-beads for additional 2 h. Samples were eluted with SDS-sample buffer and subjected to SDS-page and Western blot, using antibodies against FLAG-, HA- and GST-tag.

Membrane targeting assay

Human SANS (aa 2-461) was cloned in the MyrPalm-eCFP vector (plasmid 14867, Addgene, Cambridge, MA, USA (Violin *et al.,* 2003)) containing a N-terminal membrane-anchoring peptide. MyrPalm-eCFP-SANS or MyrPalm-eCFP as control were singly or co-transfected with 3xFLAG-Ush2a-icd. 24 h post-transfection cells were prepared for immunocytochemistry. For the phosphorylation approach, cells were incubated in medium containing 150 mM DRB or 50 µM ocadaic acid 6 h after transfection.

Animals and tissue preparation

All experiments described herein conform to the statement by the Association for Research in Vision and Ophthalmology (ARVO) as to care and use of animals in research. Adult C57BL/6J mice were maintained under a 12 h light–dark cycle, with food and water *ad libitum*. After sacrifice of the animals in CO_2 and decapitation, entire eyeballs were dissected prior to further analysis.

Retina cryosectioning and immunofluorescence microscopy analysis

Eyes of adult wild-type mice were cryofixed in melting isopentane and cryosectioned as described elsewhere (Wolfrum 1995). 10 µm cryosections were placed on poly-L-lysine-precoated coverslips and incubated with 0.01% Tween 20 in PBS for 20 min. After several PBS washing steps sections were covered with blocking solution (0.5% cold-water fish gelatin plus 0.1% ovalbumin in PBS) and incubated for a minimum of 30 min followed by an overnight incubation with primary antibodies, diluted in blocking solution at 4°C. Washed cryosections were incubated with appropriate secondary

antibodies (Invitrogen) in PBS with DAPI at room temperature and mounted in Mowiol 4.88 (Carl Roth GmbH & Co. KG, Karlsruhe). Microscopy analyses of immunofluorescence samples were performed with a Leica DM 6000 B microscope (Leica Microsystems GmbH, Wetzlar, Germany), and images were processed with Leica imaging deconvolution software (Leica Mikrosysteme Vertrieb GmbH, Wetzlar, Germany) and/or Adobe Photoshop CS (Adobe Systems Inc., San Jose, CA, USA).

Immunoelectron microscopy

For immunoelectron microscopy, the recently introduced protocol for pre-embedding labeling was applied (Maerker *et al.*, 2008; Sedmak *et al.*, 2009). After washing with PBS, biotinylated secondary antibodies were applied to the sections. Antibody reactions were visualized by a Vectastain ABC-Kit (Vector Laboratories, Inc., Burlingame, CA, USA) and adding 0.01% hydrogen peroxide to 0.05 M diaminobenzidine (DAB) solution. Stained retinas were fixed in 2.5% glutaraldehyde in 0.1 M cacodylate buffer (pH 7.4) and DAB precipitates were silver enhanced followed by post-fixation in cacodylate buffered 0.5% OsO_4 on ice. Dehydrated specimens were flat-mounted between two sheaths of ACLAR®-films (Ted Pella Inc., Redding, USA) in Araldite® resin. Ultrathin sections were analyzed in a transmission electron microscope (Tecnai 12 BioTwin; FEI, Eindhoven, The Netherlands). Images were obtained with a charge-coupled device camera (Surface Imaging Systems SIS Megaview3), acquired by analySIS (Soft Imaging System) and processed with Adobe Photoshop CS.

Results and Discussion

Identification of Ush2a as novel interaction partner of SANS

Loss of SANS´ protein function by mutations in *USH1G* cause USH type 1 leading to inner ear dysfunction and retinal degeneration. Previous data have indicated that SANS is an important component of periciliary USH1-USH2 protein networks in photoreceptor cells (Maerker *et al.*, 2008; Overlack *et al.*, 2011). SANS and whirlin organize the periciliary USH-protein network integrating the USH2 proteins Ush2a and VLGR1 in a USH1-USH2 complex. Ush2a/usherin was original described as an extracellular protein (Bhattacharya *et al.*, 2002). Later, a longer isoform has been described as Ush2a isoform b (van Wijk *et al.*, 2004; van Wijk *et al.*, 2006). Ush2a isoform b contains in addition to the extracellular domains a transmembrane domain and an intracellular domain with a PDZ-binding motif (PBM) at the C-terminus (Figure 1A). Recent expression analyses revealed that Ush2a isoform b is the canonical isoform of the retina (Liu *et al.*, 2007; Yang *et al.*, 2010).

The close molecular association between SANS and Ush2a within the periciliary membrane complex (PMC) (Maerker *et al.*, 2008) prompted us to proof their binding ability. For this, we applied GST-pull down assays using SANS as bait. GST-Ush2a-icd fusion protein or GST alone were immobilized at glutathione sepharose beads and incubated with FLAG-tagged SANS protein. Subsequent Western blot analysis of the recovered proteins with anti-FLAG antibodies showed that Ush2a-icd was able to pull-down SANS, whereas GST alone was not, indicating the direct binding of SANS to the Ush2a isoform b C-terminus *in vitro* (Figure 1B). To pinpoint the interaction domain within the SANS molecule, we performed the reciprocal experiment with FLAG-tagged Ush2a-icd and different GST-tagged SANS domains, namely the N-terminus, the central domain and the SAM-PBM (Figure 1C). The pull downs revealed the central domain of SANS as direct interacting with the Ush2a C-terminus (Figure 1C).

To specify the interacting region within the intracellular domain of Ush2a, we performed immunoprecipitation with FLAG-tagged SANS and analysed the co-precipitation of the GST-tagged intracellular domains of Ush2a (Figure 1D). In contrast to the GST control all three Ush2a-icd constructs were recovered after anti-FLAG pull down. The quantification of recovered polypeptides revealed that in comparison to the entire intracellular domain of Ush2a-icd (100%), in the case of Ush2a-C-terminus lacking the PDZ-binding motif (PBM) ~ 80% and for the small part Ush2a-icd$_{106-139}$

~ 40% of polypeptide were recovered (Figure 1E). Taken together these results indicate that the central domain of SANS directly bind to the intracellular Ush2a domain and that the PBM of Ush2a is not essential for this interaction.

The interaction between SANS and Ush2a is phosphorylation dependent

BLAST analyses predicted several phosphorylation sites in the sequence of the central domain of SANS (http://www.phosphosite.org). This prompted us to test whether the interaction between SANS and Ush2a is regulated by the phosphorylation of central domain of SANS. For this, we co-transfected cells with GFP-tagged SANS and the mRFP-tagged intracellular domain of Ush2a and applied the kinase inhibitor DRB (D-ribofuranosyl-benzimidazole) or ocadaic acid, a potent inhibitor of the protein phosphatase PP2A to the media. Subsequently we performed co-precipitation applying the GFP-Trap® under phosphorylated (ocadaic acid) or de-phosphorylated (DRB) conditions. We observed no interaction between Ush2a and SANS from lysates treated with DRB whereas treatment with ocadaic acid demonstrated co-precipitation of Ush2a with SANS (Figure 2A).

Next, we analysed the phosphorylation dependency of the SANS-Ush2a interaction in a cellular environment. We transfected IMCD3 cells with 3xFLAG-Ush2a-icd and eCFP-SANS N-terminally coupled to a membrane anchoring peptide (MyrPalm-eCFP-SANS) or MyrPalm-eCFP as control. As expected, in cells singly-transfected with MyrPalm-eCFP constructs, eCFP-SANS and eCFP alone were localized to the plasma membrane. In cells singly-transfected with 3xFLAG-Ush2a-icd, FLAG-tagged proteins were localized in the cytoplasm (Figure 2B). In the co-transfection approach the localization of SANS and Ush2a changed due to phosphorylation. Under phosphorylated conditions by adding ocadaic acid the localization of SANS is changed from the plasma membrane to a spot in the cell periphery besides the nucleus, where it co-localized with Ush2a (Fig. 2C, a). Applying DRB neither SANS nor Ush2a changed their spatial distribution in co-transfected cells (Fig. 2D a, b). Co-transfection with MyrPalm-eCFP and Ush2a-icd caused no change of the localization neither in the dephosphorylated approach with DRB nor in the phosphorylated approach with ocadaic acid (Figure 2C and D, b). This assay demonstrated the direct and phosphorylation dependent interaction between SANS and the intracellular part of Ush2a.

Taken together our data showed that the binding of the intracellular domain of Ush2a to the central domain of SANS is regulated by phosphorylation of the central domain of SANS. In this regulation binary binding of both molecules is triggered by phosphorylation and the de-phosphorylation via PP2A abolishes this interaction.

In conclusion, independent assays affirmed the direct interaction of SANS´ central domain with the C-terminal intracellular domain of Ush2a. Further analysis will be necessary to pinpoint the phosphorylation sites in the SANS´ central domain, which mediate this interaction.

Periciliary localization of SANS and Ush2a in retinal photoreceptor cells

A necessary pre-requisite for a cellular interaction between two proteins *in vivo* is their co-expression in the same subcellular compartment. So far, the co-distribution of SANS and Ush2a in the photoreceptor cell was based on labeling of SANS and Ush2a in parallel retinal sections (Maerker *et al.,* 2008). Here, we performed double immunofluorescence staining of retinal sections by introducing a newly generated antibody against SANS and antibodies against Ush2a (Figure 3). Merged images of the double labeled sections revealed the partial co-localization of SANS and Ush2a in the ciliary region of photoreceptor cells, at the cell adhesion complexes of the outer limiting membrane and in the outer plexiform layer of mouse retina (Figure 3B). Furthermore, both interaction partners were localized in the ganglion cell layer. The acquired data confirmed published data to the spatial distribution of the single proteins (Maerker *et al.,* 2008; Overlack *et al.,* 2008; van Wijk *et al.,* 2009; Yang *et al.,* 2010; Overlack *et al.,* 2011; Zou *et al.,* 2011; Bauß *et al.,* under review).

Next we were interested to have a closer look at the ciliary region of photoreceptor cells, where previous studies have demonstrated a periciliary USH protein membrane complex (Maerker *et al.,* 2008; van Wijk *et al.,* 2009; Yang *et al.,* 2010; Zou *et al.,* 2011). To get detailed insights into the ciliary localization of Ush2a and SANS, we performed double labeling experiments of retinal sections with antibodies against Ush2a, SANS and centrin, a molecular marker for the connecting cilium, the basal body and the adjacent centriole (Figure 4). Overlay images double labeled with anti-Ush2a and anti-centrin revealed the localization of Ush2a at the connecting cilium and the basal body as well as between the basal body and adjacent centriole of mouse photoreceptor cells (Figure 4A). In contrast, SANS and centrin double labeling revealed the localization of SANS at the basal body and the

adjacent centriole and between both, but not in the connecting cilium (Figure 4B). The additional double labeling of SANS and Ush2a approved a partial co-localization of both interaction partners at the basal body and the adjacent centriole of mouse photoreceptor cells (Figure 4C).

A more precise subcellular detection was reserved to the high resolution of immunoelectron microscopy analysis. The parallel analysis of ultrathin sections through mouse photoreceptor cells revealed that SANS and Ush2a are localized at and beneath the basal body and adjacent centriole of the connecting cilium. Furthermore, antibody labeling of both interaction partners, SANS and Ush2a, was present at the periciliary membrane of photoreceptor cells (Figure 4D, E).

These data confirmed our results achieved by present immunofluorescence analysis and affirmed previous published data on the localization of SANS and Ush2a in the periciliary region of photoreceptor cells (Liu *et al.,* 2007; Maerker *et al.,* 2008; van Wijk *et al.,* 2009; Yang *et al.,* 2010; Overlack *et al.,* 2011). We provide evidence that SANS is integrated in the periciliary USH1-USH2 protein network not only via binding to whirlin via its C-terminal SAM-PBM domain, but also by direct interaction through its central domain to the intracellular domain of Ush2a. The close molecular relation of the USH1G protein SANS to USH type 2 proteins might also reflect the fact that some human mutations in *USH1G*-cause USH2-like phenotypes and not the more severe USH1 phenotype (Kalay *et al.,* 2005; Bashir, Fatima, and Naz 2010).

SANS and USH2 assembly together with whirlin into a ternary UHS1-USH2 protein complex

Previous data have indicated that the scaffold protein whirlin (USH2D) anchors/organizes the periciliary membrane USH2 protein complex by binding the transmembrane protein VLGR1/GPR98 (USH2C) and USH2A (Maerker *et al.,* 2008; van Wijk *et al.,* 2006; Yang *et al.,* 2010; Wu *et al.,* 2011; Wang *et al.,* 2012), but also USH1G protein SANS (Maerker *et al.,* 2008). These interactions are mediated by the PBMs at C-termini of VLGR1, USH2A and SANS targeting only PDZ1 (VLGR1) or in the case of USH2A and SANS, PDZ1 and PDZ2 of whirlin (Maerker *et al.,* 2008; van Wijk *et al.,* 2006). The binary interaction of SANS and USH2A identified above prompted us to test whether SANS and USH2A can assembly together with whirlin into a ternary protein complex. For this we performed co-immunoprecipitations (co-IP) incubating immobilized full length SANS with and without the C-terminal PBM with the intracellular domain of Ush2A or with whirlin (Figure 5). As

expected from our experiments above, in both immunoprecipiatations Ush2A-icd was recovered indicating that the PBM in SANS is not necessary for Ush2a binding (Figure 5A). In contrast, whirlin binding to SANS was strictly dependent on the presence of SANS-PBM (Figure 5A), which affirmed our previously obtained results (Maerker *et al.,* 2008). Next, we extended our interaction assays and incubated SANS and whirlin with Ush2a (Figure 5A). Adding Ush2a increased the amount of whirlin co-precipitated with SANS. In addition, whirlin was even co-precipitated by SANS lacking the PBM when Ush2a was added. In conclusion, these results indicated that SANS and Ush2a simultaneously bind to whirlin sharing both first PDZ domains as target sites as illustrated in Figure 6A. Data on the subcellular retinal localization of the single components support the facility of an assembly of the ternary complex in the periciliary membrane compartment of photoreceptor cells.

The role of ternary SANS-Ush2a-whirlin network in photoreceptor cell function

There is emerging evidence for a role of SANS in the transport of ciliary cargoes from the trans-Golgi network along microtubules through the inner segment to the periciliary membrane compartment where cargo is handed over to the ciliary transport module for the delivery into the outer segment of photoreceptor cells (Maerker *et al.,* 2008; Overlack *et al.,* 2008; Overlack *et al.,* 2011; Sorusch *et al.,* in press; Bauß *et al.,* under review) (Figure 6). Ush2a and whirlin may either represent cargo for the SANS associated transport through the inner segment to the periciliary membrane complex or the assembly of the ternary complex may participate in the cargo handover module. The consistent data on the co-distribution gathered in the diverse previous studies (Maerker *et al.,* 2008; Overlack *et al.,* 2008; Overlack *et al.,* 2011; van Wijk *et al.,* 2009; Yang *et al.,* 2010; Bauß *et al.,* under review) favors a role of the ternary interplay of the three USH proteins in the periciliary compartment controlling the vesicle cargo transfer to the periciliary membrane of the photoreceptor inner segment (Figure 6B). In our working hypothesis the phosphorylation of SANS may facilitate the release of cargo vesicles from the inner segment transport carrier, phosphorylated SANS may target the vesicles to the periciliary membrane by assembling into the perciliary membrane complex via binding to USH2A and whirlin. The close proximity of the vesicle to the periciliary membrane may promote membrane fusion as known from other cellular modules of exocytosis.

In conclusion, the novel ternary SANS-Ush2a-whirlin interplay certainly emphasizes the close relation of USH1 and USH2 proteins in the interactome related to USH. Moreover, the ternary complex provides a regulatory unit enabling the control of cargo transfer from the inner segment transport carriers to the ciliary transport or intraflageller transport (IFT) machinery that conveys the cargo to its outer segment destination. Mutations in the three USH genes of the ternary complex may certainly deregulate the complex formation and the fine tuning of the ciliary cargo delivery to the outer segment. This deregulation should lead to defective ciliary cargo delivery and subsequent dysfunction of photoreceptor cells inducing retinal degeneration, the retinal phenotype in USH patients.

Disclosure Statement

All authors disclose any actual or potential conflict of interest including any financial, personal or other relationships with other people or organizations within three years of beginning the work submitted that could inappropriately influence their work.

Acknowledgments

We thank Dr. W. Clay Smith for kindly providing the anti-GFP-antibody, Drs. Nora Overlack and Kerstin Nagel-Wolfrum for abundant discussion and Ulrike Maas, Elisabeth Sehn and Gabi Stern-Schneider for excellent technical assistance.

Role of the funding source

This work was supported by the DFG (to UW), BMBF "HOPE2" (01GM1108D, to UW), Forschung contra Blindheit - Initative Usher Syndrom (to UW and NS), Pro Retina Deutschland e. V. (to UW and KB), the FAUN-Stiftung, Nurnberg (to UW), European Community FP7/2009/241955 (SYSCILIA) (to UW, KB and NS) and FP7/2009/242013 (TREATRUSH, to UW). Funding sources did not participate in study design, in the collection, analysis, and interpretation of data; in the writing of the report; and in the decision to submit the paper for publication.

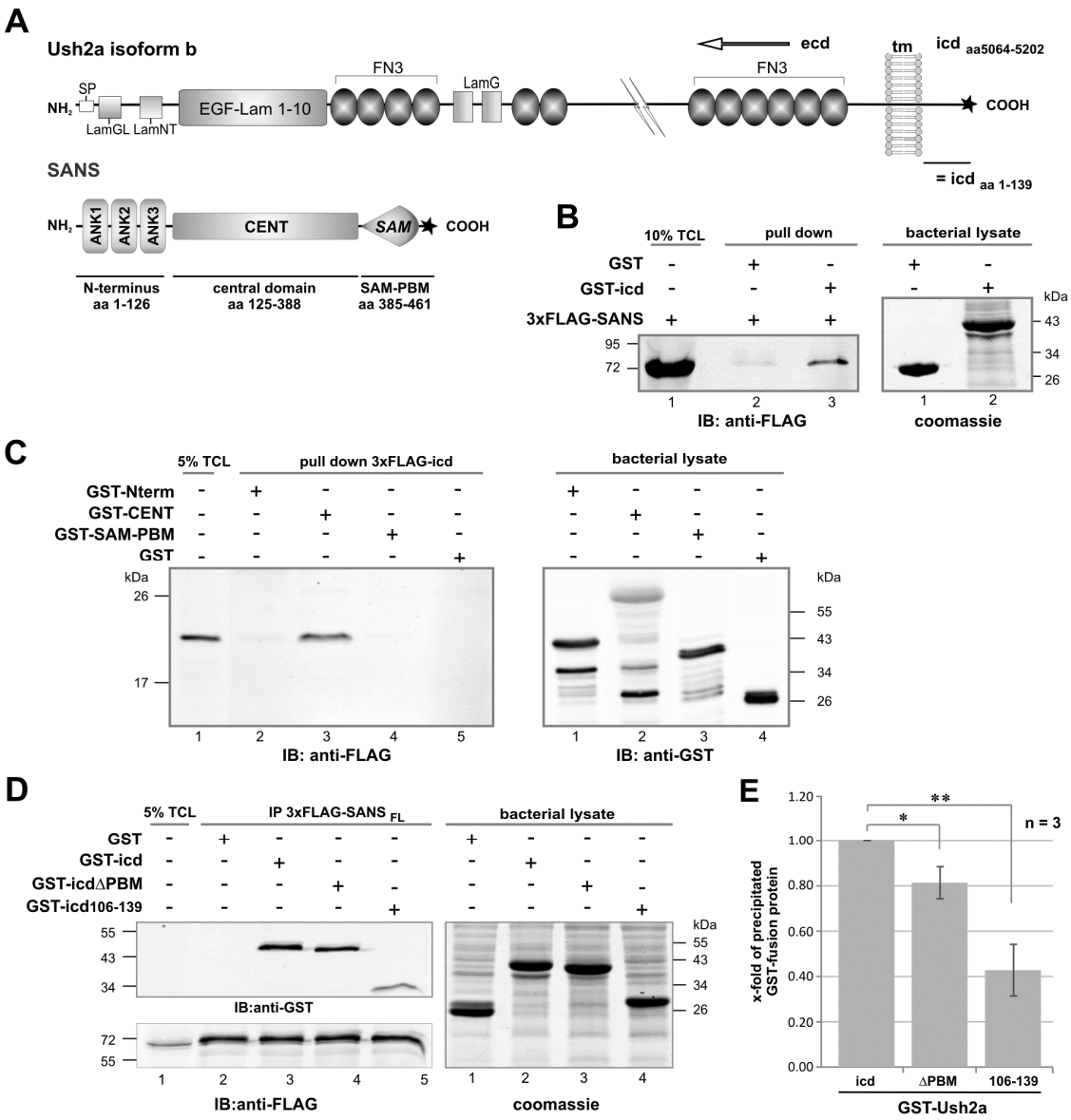

Figure 1: Identification and validation of the direct interaction between Ush2a and SANS. (A) Schematic representation of the binding partners. Ush2a isoform b (600 kDa) composed of the extracellular domain (ecd) with an N-terminal signal peptide (SP), various laminin-like domains (EGF-Lam: laminin-like domain, LamG: Laminin G domain, FN3, LamGL: LamG-like jellyroll fold domain, LamNT: Laminin N-terminal domain (domain VI)) and fibronectin-like domains (FN3) and a transmembrane domain (tm), followed by an intracellular domain (icd) with a PDZ-binding motif (PBM, *asterisk*). SANS domain structure with three ankyrin repeats (ANK) at the N-terminus, a central domain (CENT) and a SAM domain (sterile alpha motif) followed by a PBM (asterisk) at the C-terminus. **(B) GST pull-down** of SANS and Ush2a. Recombinant three times FLAG-tagged SANS full length (3xFLAG-SANS) was incubated with immobilized GST-Ush2a-icd or GST alone. Anti-FLAG Western blot revealed the pull-down of SANS by the Ush2a-icd (~ 68 kDa, lane3) but not by GST alone (lane2). Lane1, and lane1 and 2 in the commassie-stained SDS-gel show 10% input of recombinant proteins. **(C) Reciprocal GST-pull down** with GST-tagged SANS´ domains N-terminus (GST-Nterm), GST-CENT and GST-SAM-PBM and recombinant 3xFLAG-Ush2a-icd. Western blot analysis demonstrated the pull down of Ush2a-icd by the SANS´ CENT but neither by the N-, nor C-terminus or GST alone. GST-contructs were expressed at similar expression levels. **(D) Co-immunoprecipitation** with 3xFLAG-SANS showed the binding of GST-Ush2a-icd and the deletion constructs lacking the PBM (GST-Ush2a-icdΔPBM) as well as the outmost C-terminus (GST-Ush2a-icd$_{106-139}$). **(E) Quantification** of three independent experiments revealed a significant decreased binding to 81% (p-value 0.0225) of GST-Ush2a-icdΔPBM and a significant weak binding of GST-Ush2a-icd$_{106-139}$ of 43% (p-value 0.0065) compared to GST-Ush2a-icd.

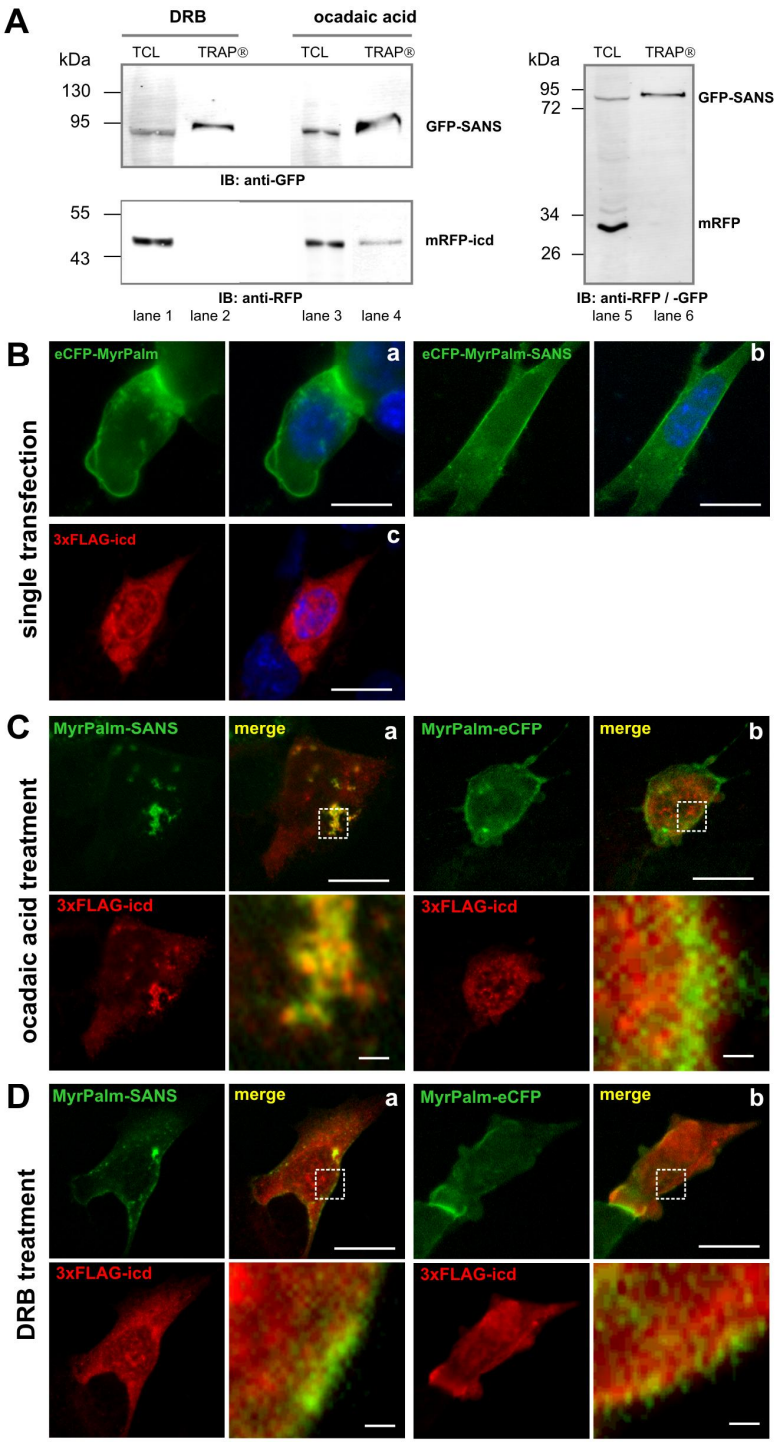

Figure 2: Phosphorylation dependency of the SANS-Ush2a interaction. (A) Co-precipitation by GFP-Trap®: HEK293T cells were co-transfected with GFP-tagged SANS and mRFP-Ush2a-icd or mRFP as negative control. Western blot analyses with anti-GFP and anti-RFP antibodies revealed no co-precipitation of mRFP-Ush2a-icd by GFP-SANS, when the kinase inhibitor DRBwas added but co-precipitation of Ush2a-icd, when the PP2A inhibitor ocadaic acid was added. There was no co-precipitation of mRFP alone (lane 6). Lanes 1, 3 and 5 show 5% input of total cell lysates (TCL). **(B, C) Membrane targeting assay: (B)** Single-transfection of MyrPalm-eCFP-SANS and MyrPalm-eCFP showed the localization at the cell membrane, whereas 3xFLAG-Ush2a-icd showed a cytosolic staining. **(C)** Co-transfection incubated with ocadaic acid demonstrated the recruitment of SANS and Ush2a to a spot in the cell periphery due to phosphorylation, whereas MyrPalm-eCFP did not change the Ush2a-localization. **(D)** Co-transfection incubated with DRB revealed the phosphorylation dependency of the SANS-Ush2a interaction. Neither MyrPalm-eCFP-SANS nor MyrPalm-eCFP were able to recruit Ush2a under de-phosphorylated conditions. Scale bars 5/1 µm.

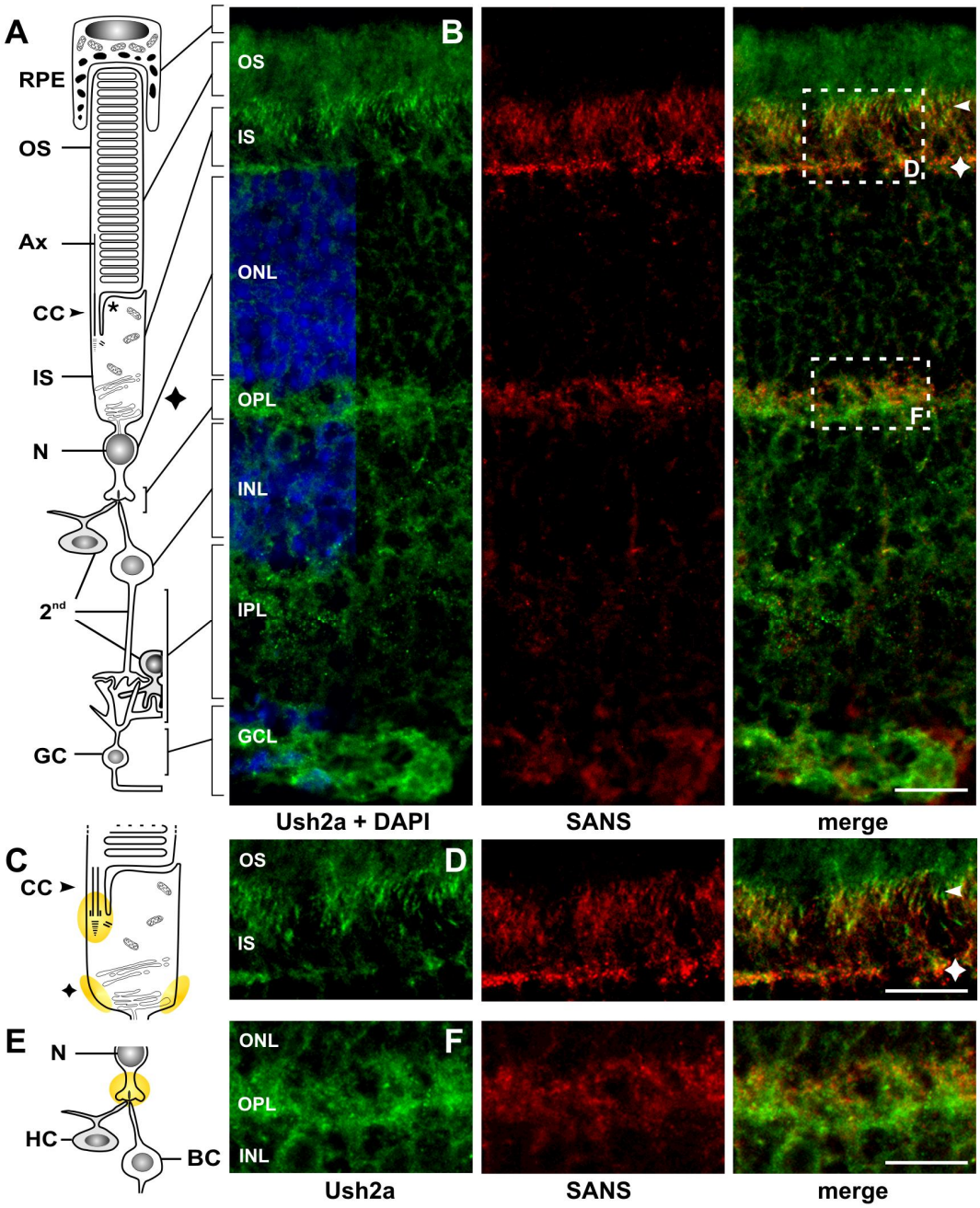

Figure 3: Partial co-localization of Ush2a and SANS in the mouse retina. (A - D) Co-localization study of SANS and Ush2a by indirect immunofluorescence on longitudinal sections through mouse retina. **(A)** Scheme of rod photoreceptor cell with outer segment (OS) enclosed on top by retinal pigment epithelium cell (RPE) and connected to secondary neurons (2^{nd}). **(B)** Ush2a (green) was localized in the apical part of the inner segment (IS), at the *outer limiting membrane* (OLM, *asterisk*) and was also detected in the outer plexiform layer (OPL) and ganglion cell layer (GCL). SANS (red) was localized in the IS, at the OLM and in the synaptic region of the OPL and GCL. Overlay image (merge) showed a partial co-localization of Ush2a and SANS in the region of the connecting cilium (CC, *arrow head*) in the apical IS, at the OLM and in the synaptic region of the OPL. **(C - F) High magnification analyses** of indirect immunofluorescence double labeling of Ush2a and SANS in the IS and OPL of mouse photoreceptor cells. **(C, E) Schemes of the photoreceptor cell compartments** with the regions of partial co-localization of Ush2a and SANS indicated in yellow. **(D)** Overlay image showed partial co-localization of Ush2a and SANS in the periciliary region of photoreceptor cells. **(F)** Overlay image showed partial co-localization of interaction partners in the synaptic region of the OPL. ONL: outer nuclear layer; INL: inner nuclear layer. Nuclei were stained with DAPI. Scale bars: B 10 µm; D/F 5 µm.

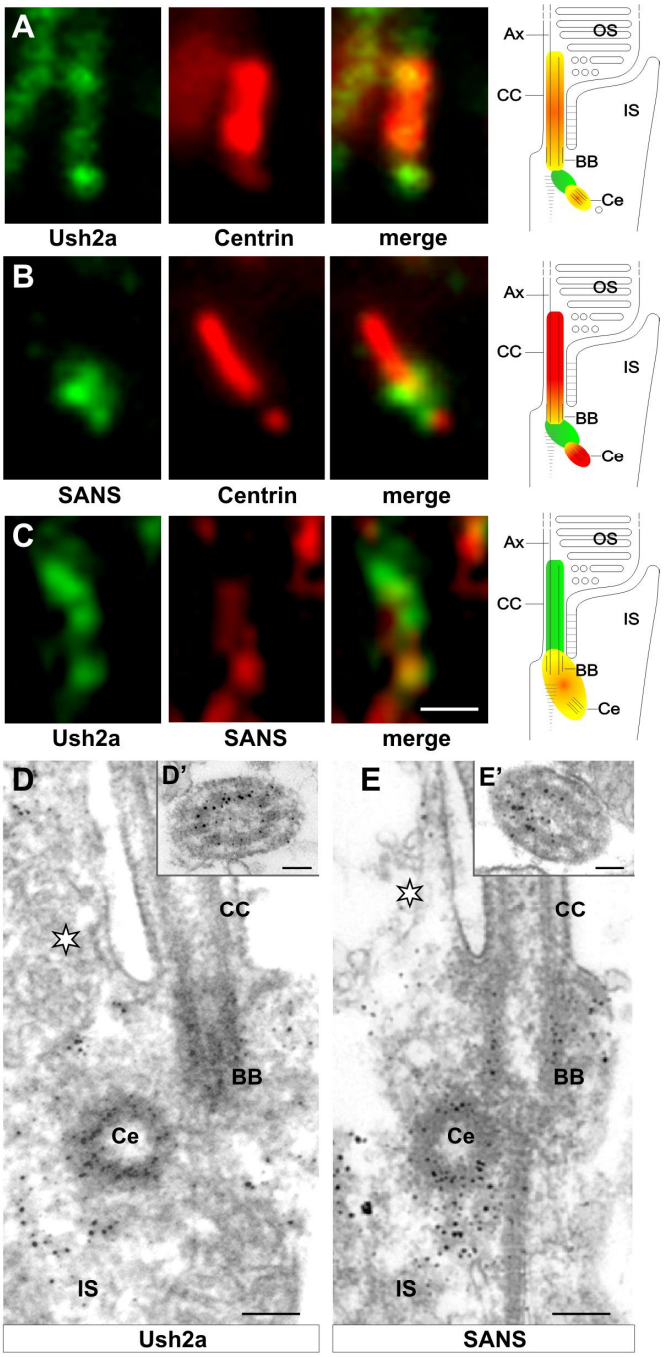

Figure 4: Ciliary localization of SANS and Ush2a in murine photoreceptor cells. (A - C) High magnifications of indirect immunofluorescence double labeling of centrin and Ush2a **(A)** or SANS **(B)** and Ush2a and SANS **(C)** in longitudinal sections of mouse retina. As molecular ciliary marker anti-centrin (red) stained the connecting cilium (CC), the basal body (BB) and the adjacent centriole (Ce). The localization of the molecules was pictured in the schemes of the ciliary-periciliary region of photoreceptor cells. **(A)** High magnification of indirect double immunofluorescence of Ush2a (green) and centrin (red) revealed Ush2a localization in CC, BB and Ce. **(B)** Double labeling of SANS (green) and centrin demonstrated SANS localization at BB and Ce. **(C)** Double labeling of Ush2a (green) and SANS (red) revealed partial co-localization of SANS and Ush2a at the ciliary base, namely the BB and Ce. Ax: axoneme; IS: inner segment; OS: outer segment. **(D, E) Immunoelectron microscopic localization** of SANS and Ush2a in mouse photoreceptor cells. **(D, D´)** Electron micrograph of SANS labeling on longitudinal and cross-sections of mouse photoreceptor cells confirmed the presence of SANS in the periciliary region of the apical IS (*asterisk*), at the BB and the CE, and in the CC. **(E, E´)** Electron micrographs of Ush2a labeling in longitudinal and cross-sections of mouse photoreceptor cells revealed the localization of Ush2a at BB and Ce and in the CC. In the apical IS Ush2a is localized especially at the periciliary membrane. Scale bars: A-C 0.5 µm; D/E 250 nm; D´/E´ 100 nm.

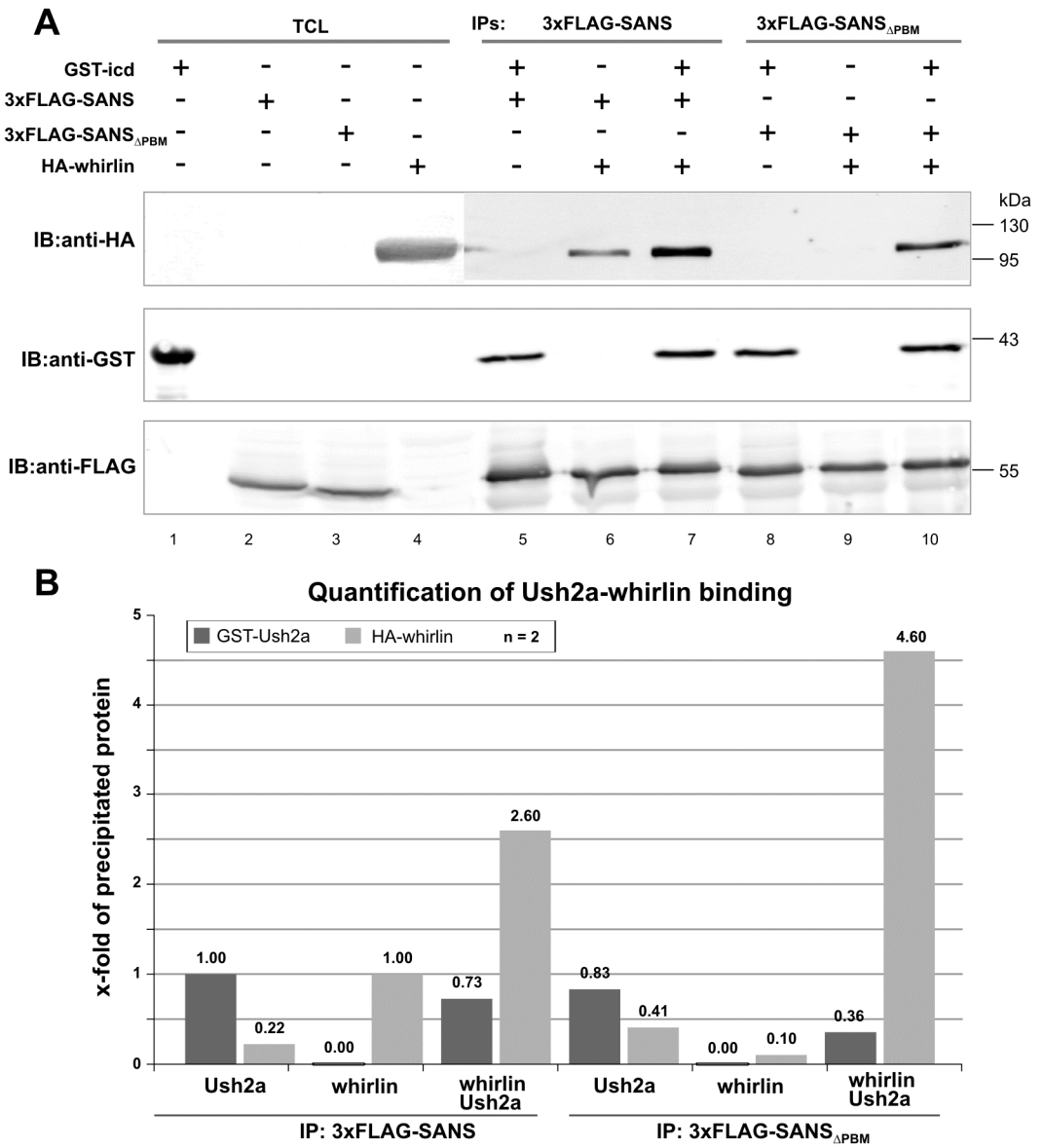

Figure 5: Ternary complex assembly of SANS, Ush2a and whirlin demonstrated by co-immunoprecipitation. (A) Western blot analysis of co-immunoprecipitation using three times FLAG-tagged SANS full length or lacking the PDZ-binding motif (PBM) (3xFLAG-SANS$_{FL}$ / 3xFLAG-SANS$_{\Delta PBM}$) bound to FLAG-beads. FLAG-fusion proteins were incubated with HA-tagged whirlin and GST-tagged intracellular domain of Ush2a (GST-Ush2a$_{icd}$) and precipitates were analyzed using the appropriate antibodies. Western blot analysis with anti-GST revealed the co-precipitation of Ush2a by SANS irrespective of the PBM whereas anti-HA demonstrated the co-precipitation of whirlin by SANS full length but nearly no co-precipitation by SANS lacking the PBM. In the presence of Ush2a, whirlin was precipitated by SANS lacking the PBM (lane10). Lanes 1-4 show 5% of total cell lysates (TCL). **(B) Quantification of precipitated proteins** from two independent experiments revealed the enhanced binding of whirlin by adding Ush2a. When Ush2a is added, 2.6-fold more whirlin is co-precipitated by SANS full length and 4.6-fold more whirlin is co-precipitated by SANS lacking the PBM.

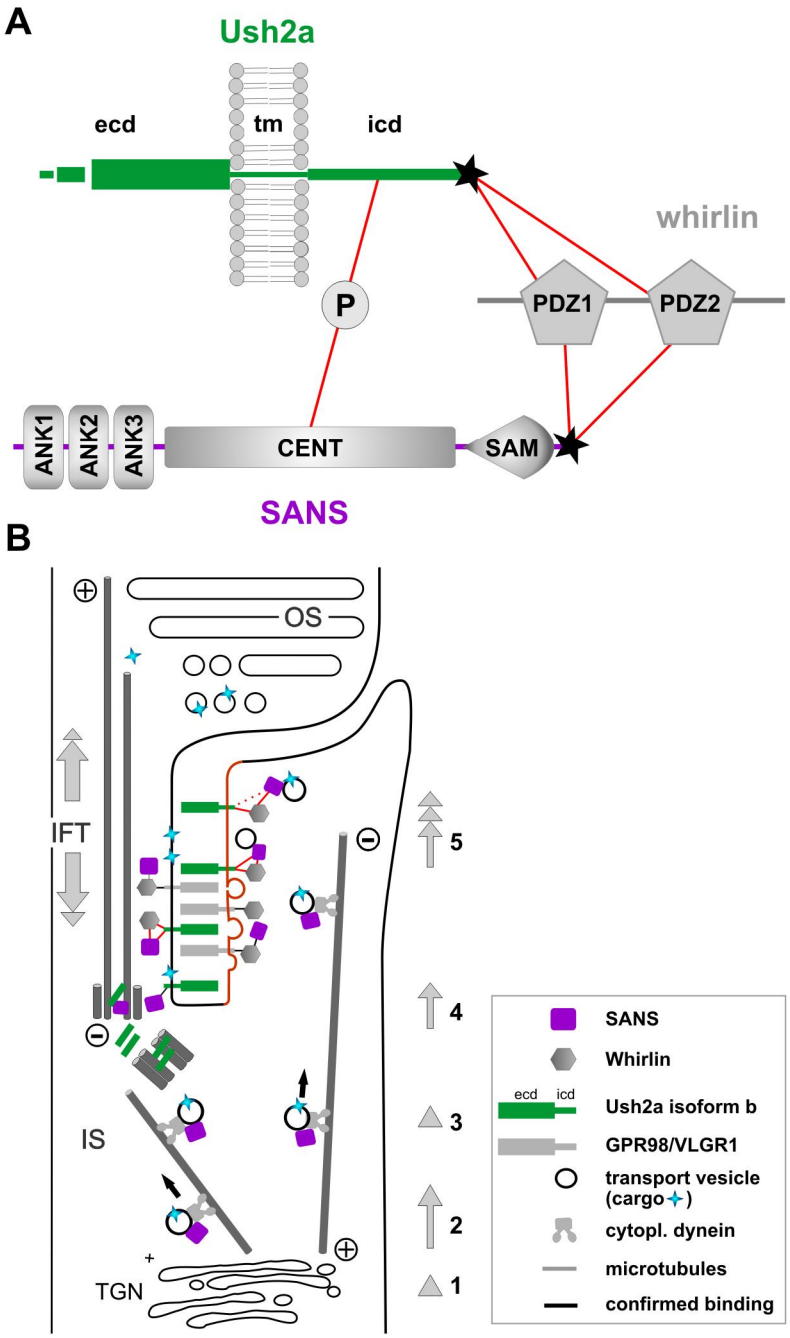

Figure 6: Cartoon of the ternary USH-protein complex and its function in photoreceptor cells. (A) Scheme of the ternary complex between the USH molecules SANS, Ush2a and whirlin. The interactions are indicated by red lines between the single interacting domains. Ush2a interacts via the intracellular domain (icd) in a phosphorylation dependent manner with the central (CENT) domain of SANS (indicated with P) and via the PDZ binding motif (PBM, asterisk) with the PDZ1 and PDZ2 domains of whirlin. SANS interacts also via the PBM with the PDZ domains of whirlin. **(B)** Schematic illustration of the role of SANS-Ush2a-whirlin complex in photoreceptor cell transport modules. Vesicles, carrying ciliary cargos, are transported from the Golgi (1 - cargo sorting) through the inner segment (2 - inner segment transport) to the cargo reloading points (3 - cargo reloading), either the basal body or the periciliary target membrane (red line). SANS is associated with microtubules in the inner segment, where dynein mediates vesicular transport. The SANS-Ush2a-whirlin complex may function in the process of the cargo reloading from the inner segment transport carriers to the ciliary delivery system (4/5 - ciliary transport/axonemal transport). CC: connecting cilium; ecd: extracellular domain; icd: intracellular domain; IFT: intraflagellar transport; IS: inner segment; OS: outer segment; TGN: trans-Golgi network.

6. References

Adato A, Lefevre G, Delprat B, Michel V, Michalski N, Chardenoux S, Weil D, El Amraoui A, Petit C (2005). Usherin, the defective protein in Usher syndrome type IIA, is likely to be a component of interstereocilia ankle links in the inner ear sensory cells. *Hum. Mol. Genet.*, 14: 3921-3932.

Bashir R, Fatima A, Naz S (2010). A frameshift mutation in SANS results in atypical Usher syndrome. *Clin. Genet.*, 78: 601-603.

Ben Rebeh I, Benzina Z, Dhouib H, Hadjamor I, Amyere M, Ayadi L, Turki K, Hammami B, Kmiha N, Kammoun H, Hakim B, Charfedine I, Vikkula M, Ghorbel A, Ayadi H, Masmoudi S (2008). Identification of candidate regions for a novel Usher syndrome type II locus. *Mol. Vis.*, 14: 1719-1726.

Bhattacharya G, Miller C, Kimberling WJ, Jablonski MM, Cosgrove D (2002). Localization and expression of usherin: a novel basement membrane protein defective in people with Usher's syndrome type IIa. *Hear. Res.*, 163: 1-11.

Dad S, Ostergaard E, Thykjaer T, Albrectsen A, Ravn K, Rosenberg T, Moller LB (2010). Identification of a novel locus for a USH3 like syndrome combined with congenital cataract. *Clin. Genet.*, 78: 388-397.

Davenport SLH, Omenn GS. The heterogeneity of Usher syndrome. Vth Int.Conf. Birth Defects, Montreal. 1977.

Ebermann I, Phillips JB, Liebau MC, Koenekoop RK, Schermer B, Lopez I, Schafer E, Roux AF, Dafinger C, Bernd A, Zrenner E, Claustres M, Blanco B, Nurnberg G, Nurnberg P, Ruland R, Westerfield M, Benzing T, Bolz HJ (2010). PDZD7 is a modifier of retinal disease and a contributor to digenic Usher syndrome. *J. Clin. Invest*, 120: 1812-1823.

Gießl A, Trojan P, Pulvermüller A, Wolfrum U (2004). Centrins, potential regulators of transducin translocation in photoreceptor cells. In: Williams DS, ed. *Cell Bilogy and Related Disease of the Outer Retina*. Singapore: World Scientific Publishing Company Pte Ltd, 195-222.

Kalay E, de Brouwer AP, Caylan R, Nabuurs SB, Wollnik B, Karaguzel A, Heister JG, Erdol H, Cremers FP, Cremers CW, Brunner HG, Kremer H (2005). A novel D458V mutation in the SANS PDZ binding motif causes atypical Usher syndrome. *J. Mol. Med.*, 83: 1025-1032.

Kremer H, van Wijk E, Marker T, Wolfrum U, Roepman R (2006). Usher syndrome: molecular links of pathogenesis, proteins and pathways. *Hum. Mol. Genet.*, 15 Spec No 2: R262-R270.

Liu X, Bulgakov OV, Darrow KN, Pawlyk B, Adamian M, Liberman MC, Li T (2007). Usherin is required for maintenance of retinal photoreceptors and normal development of cochlear hair cells. *Proc. Natl. Acad. Sci. U. S. A*, 104: 4413-4418.

Maerker T, van Wijk E, Overlack N, Kersten FF, McGee J, Goldmann T, Sehn E, Roepman R, Walsh EJ, Kremer H, Wolfrum U (2008). A novel Usher protein network at the periciliary reloading point between molecular transport machineries in vertebrate photoreceptor cells. *Hum. Mol. Genet.*, 17: 71-86.

Nakanishi H, Ohtsubo M, Iwasaki S, Hotta Y, Takizawa Y, Hosono K, Mizuta K, Mineta H, Minoshima S (2010). Mutation analysis of the MYO7A and CDH23 genes in Japanese patients with Usher syndrome type 1. *J. Hum. Genet.*, 55: 796-800.

Overlack N, Kilic D, Bauss K, Marker T, Kremer H, van Wijk E, Wolfrum U (2011). Direct interaction of the Usher syndrome 1G protein SANS and myomegalin in the retina. *Biochem. Biophys. Acta*, 1813: 1883-1892.

Overlack N, Maerker T, Latz M, Nagel-Wolfrum K, Wolfrum U (2008). SANS (USH1G) expression in developing and mature mammalian retina. *Vision Res.*, 48: 400-412.

Peterson JJ, Tam BM, Moritz OL, Shelamer CL, Dugger DR, McDowell JH, Hargrave PA, Papermaster DS, Smith WC (2003). Arrestin migrates in photoreceptors in response to light: a study of arrestin localization using an arrestin-GFP fusion protein in transgenic frogs. *Exp. Eye Res.*, 76: 553-563.

Reiners J, Nagel-Wolfrum K, Jürgens K, Märker T, Wolfrum U (2006). Molecular basis of human Usher syndrome: deciphering the meshes of the Usher protein network provides insights into the pathomechanisms of the Usher disease. *Exp. Eye Res.*, 83: 97-119.

Reiners J, van Wijk E, Marker T, Zimmermann U, Jurgens K, te Brinke H, Overlack N, Roepman R, Knipper M, Kremer H, Wolfrum U (2005). Scaffold protein harmonin (USH1C) provides molecular links between Usher syndrome type 1 and type 2. *Hum. Mol. Genet.*, 14: 3933-3943.

Schneider E, Marker T, Daser A, Frey-Mahn G, Beyer V, Farcas R, Schneider-Ratzke B, Kohlschmidt N, Grossmann B, Bauss K, Napiontek U, Keilmann A, Bartsch O, Zechner U, Wolfrum U, Haaf T (2009). Homozygous disruption of PDZD7 by reciprocal translocation in a consanguineous family: a new member of the Usher syndrome protein interactome causing congenital hearing impairment. *Hum. Mol. Genet.*, 18: 655-666.

Sedmak T, Sehn E, Wolfrum U (2009). Immunoelectron microscopy of vesicle transport to the primary cilium of photoreceptor cells. *Methods Cell Biol.*, 94: 259-272.

Trojan P, Krauss N, Choe HW, Giessl A, Pulvermuller A, Wolfrum U (2008). Centrins in retinal photoreceptor cells: Regulators in the connecting cilium. *Prog. Retin. Eye Res.*

Vache C, Besnard T, le Berre P, Garcia-Garcia G, Baux D, Larrieu L, Abadie C, Blanchet C, Bolz HJ, Millan J, Hamel C, Malcolm S, Claustres M, Roux AF (2012). Usher syndrome type 2 caused by activation of an USH2A pseudoexon: implications for diagnosis and therapy. *Hum. Mutat.*, 33: 104-108.

van Wijk E, Kersten FF, Kartono A, Mans DA, Brandwijk K, Letteboer SJ, Peters TA, Marker T, Yan X, Cremers CW, Cremers FP, Wolfrum U, Roepman R, Kremer H (2009). Usher syndrome and Leber congenital amaurosis are molecularly linked via a novel isoform of the centrosomal ninein-like protein. *Hum. Mol. Genet.*, 18: 51-64.

van Wijk E, Pennings RJ, te BH, Claassen A, Yntema HG, Hoefsloot LH, Cremers FP, Cremers CW, Kremer H (2004). Identification of 51 Novel Exons of the Usher Syndrome Type 2A (USH2A) Gene That Encode Multiple Conserved Functional Domains and That Are Mutated in Patients with Usher Syndrome Type II. *Am. J. Hum. Genet.*, 74: 738-744.

van Wijk E, van der Zwaag B, Peters T, Zimmermann U, te Brinke H, Kersten FF, Marker T, Aller E, Hoefsloot LH, Cremers CW, Cremers FP, Wolfrum U, Knipper M, Roepman R, Kremer H (2006). The DFNB31 gene product whirlin connects to the Usher protein network in the cochlea and retina by direct association with USH2A and VLGR1. *Hum. Mol. Genet.*, 15: 751-765.

Violin JD, Zhang J, Tsien RY, Newton AC (2003). A genetically encoded fluorescent reporter reveals oscillatory phosphorylation by protein kinase C. *J. Cell Biol.*, 161: 899-909.

Wang L, Zou J, Shen Z, Song E, Yang J (2012). Whirlin interacts with espin and modulates its actin-regulatory function: an insight into the mechanism of Usher syndrome type II. *Hum. Mol. Genet.*, 21: 692-710.

Wolfrum U (1995). Centrin in the photoreceptor cells of mammalian retinae. *Cell Motil. Cytoskeleton*, 32: 55-64.

Wolfrum U (2011). Protein networks related to the Usher syndrome gain insights in the molecular basis of the disease. In: Satpal A, ed. *Usher Syndrome: Pathogenesis, Diagnosis and Therapy*. Nova Science Publishers, 51-73.

Wolfrum U, Liu X, Schmitt A, Udovichenko IP, Williams DS (1998). Myosin VIIa as a common component of cilia and microvilli. *Cell Motil. Cytoskeleton*, 40: 261-271.

Wu L, Pan L, Wei Z, Zhang M (2011). Structure of MyTH4-FERM domains in myosin VIIa tail bound to cargo. *Science*, 331: 757-760.

Yang J, Liu X, Zhao Y, Adamian M, Pawlyk B, Sun X, McMillan DR, Liberman MC, Li T (2010). Ablation of whirlin long isoform disrupts the USH2 protein complex and causes vision and hearing loss. *PLoS Genet.*, 6: e1000955.

Zou J, Luo L, Shen Z, Chiodo VA, Ambati BK, Hauswirth WW, Yang J (2011). Whirlin replacement restores the formation of the USH2 protein complex in whirlin knockout photoreceptors. *Invest. Ophthalmol. Vis. Sci.*, 52: 2343-2351.

Publikation III

Bauß K, Knapp B, Jores P, Spitzbarth B, Kremer H, van Wijk E, Maerker T, Wolfrum U (under review). Phosphorylation of the Usher syndrome protein SANS controls Magi2-mediated endocytosis.

Phosphorylation of the Usher syndrome protein SANS controls Magi2-mediated endocytosis

Katharina Bauß[1], Barbara Knapp[1], Pia Jores[1], Benjamin Spitzbarth[1], Ronald Roepman[2,3,5], Hannie Kremer[2,4,5,6], Erwin v. Wijk[2,4,5,6], Tina Maerker[1], and Uwe Wolfrum[1]*

[1]Cell and Matrix Biology, Inst. of Zoology, Johannes Gutenberg University of Mainz, Germany; [2]Dept of Human Genetics, [3]Institute for Genetic and Metabolic Disease, [4]Dept of Otorhinolaryngology, Head and Neck Surgery, [5]Nijmegen Centre for Molecular Life Sciences, [6]Donders Institute for Brain, Cognition and Behaviour, Radboud University Nijmegen Medical Centre, Nijmegen, Netherlands

*Corresponding Author: Johannes Gutenberg University, Institute of Zoology, Cell and Matrix Biology, Muellerweg 6, D-55099 Mainz, Germany.

Tel.: +49-6131-39-25148; Fax: +49-6131-39-23815; E-mail: wolfrum@uni-mainz.de

Conflict of interest

All authors disclose any actual or potential conflict of interest including any financial, personal or other relationships with other people or organizations.

Abstract

The human Usher syndrome (USH) is a complex ciliopathy with at least 12 chromosomal loci assigned to 3 clinical subtypes, USH1-3. The heterogeneous USH proteins are organized into protein networks. Here, we identified Magi2 (membrane-associated guanylate kinase inverted-2) as new component of the USH protein interactome, binding to the multifunctional scaffold protein SANS (USH1G). We showed that the Magi2-SANS complex assembly is regulated by the phosphorylation of an internal PBM in the SAM domain of SANS by CK2. We affirmed Magi2´s role in receptor-mediated clathrin-dependent endocytosis and showed that phospho-SANS tightly regulates Magi2-mediated endocytosis. Specific depletions revealed that SANS and Magi2-mediated endocytosis regulated aspects of ciliogenesis. We demonstrated the localization of the complex in the periciliary membrane complex (PCM) facing the ciliary pocket of retinal photoreceptor cells *in situ*. Our data suggest that endocytotic processes may not only contribute to photoreceptor cell homeostasis but also counterbalance the periciliary membrane delivery accompanying the exocytosis processes for the cargo vesicle delivery. In USH1G patients, mutations in *SANS* eliminate Magi2 binding and thereby deregulate endocytosis, lead to defective ciliary transport modules and ultimately disrupt photoreceptor cell function inducing retinal degeneration.

Introduction

The human Usher syndrome (USH) is an autosomal recessive disorder and the most frequent cause of combined deaf-blindness (1-4). Depending on the clinical characteristics, age of onset, severity and progression of symptoms USH is divided into three subtypes USH type 1-3 (5). USH is genetically heterogeneous with at least 12 chromosomal loci described so far (3;6;7). The proteins encoded by the 10 known USH causing genes belong to very different protein families. Nevertheless, previous molecular analyses elucidated the integration of all USH1 and USH2 proteins in functional protein networks organized by the scaffold proteins harmonin, whirlin and SANS (2;3).

Recent data established a protein network organized by the USH proteins whirlin (USH2D) and SANS (USH1G, scaffold protein containing ankyrin repeats and SAM domain) in the periciliary region of vertebrate photoreceptor cells (8-12). This periciliary membrane complex (PMC) is localized at the collar-like extension of the apical inner segment and the connecting cilium, which bridges the biosynthetic active inner segment with the light sensitive outer segment, which resembles a modified primary cilium (13). It has been suggested that the PMC plays an important role connecting the modules of the molecular transport through these two photoreceptor compartments, namely the microtubule-based transport through the inner segment with the intraflagellar transport (IFT) across the connecting cilium and into the outer segment (8;13). Furthermore, this membrane compartment is homologue to the ciliary pocket at the base of prototypic primary cilia, a micro domain, which is a major site for endocytosis and exocytosis regulating ciliary morphogenesis and homeostasis (14;15).

Previous data suggested that SANS participates in microtubule-based transport from the Golgi apparatus through the inner segment to the periciliary compartment and facilitate reloading of ciliary cargo in the PMC of photoreceptor cells (8;11;16). The molecular domain structure of SANS is very efficient for its scaffolding function (17). The N-terminus contains three ankyrin repeats followed by the central domain (CENT), a sterile alpha motif (SAM) and a C-terminal PDZ-binding motif class-I (PBM-I) (Figure 1A). CENT, SAM and PBM-I are all known to mediate protein-protein interactions and their roles have been previously studied (8;17-19). In the present study we searched for novel interacting partners by yeast-2-hybrid screening of a retinal cDNA library to enlighten the precise cellular function of SANS. We identified Magi2 (membrane-associated guanylate kinase inverted-2) as a novel potential binding partner of the SANS´ C-terminus. Magi2, also known as S-SCAM (synaptic scaffolding molecule), belongs to the MAGUK protein family of PDZ domain-containing scaffold proteins. Magi2 plays an essential role in synaptic development and maintenance (20;21). More specifically, Magi2 serves as a scaffold for a variety of proteins assembling synaptic protein complexes (22-24) and there is growing evidence that Magi2 participates in endocytosis as well (20;23;25).

Here we demonstrate that direct binding to the USH1G scaffold protein SANS integrates Magi2 into the USH protein interactome. We show that the assembly of the Magi2-SANS complex is procured by a novel non-canonical internal PBM within the SAM domain of SANS. We show that this

interaction is triggered by CK2-mediated phosphorylation of a serine S422 in the PBM. We provide evidence that Magi2 mediates endocytosis in cultured cells and in the ciliary pocket of photoreceptor primary cilia. Furthermore, we demonstrate that these endocytosis processes are negatively regulated by the binding of phosphorylated SANS to Magi2. Finally, our data suggest that Magi2-mediated endocytosis and its regulation by phosphorylated SANS are essential for the ciliogenesis and maintenance of primary cilia. Since several mutations in the *USH1G* gene affect the Magi2 binding site in the SAM domain of SANS, we hypothesize that the deregulation of the physiological modulation of the SANS-Magi2 complex may underlay the pathophysiological processes leading to neuro-sensory degenerations in human USH patients.

Results

The USH1G protein SANS directly interacts with the MAGUK protein Magi2

To gain further insights into the composition of USH protein networks and thereby into their functions, we searched for novel proteins directly interacting with the USH1G scaffold protein SANS. For this, we performed a yeast-2-hybrid (Y2H) screen on a bovine retinal cDNA library using the C-terminus of human SANS, containing a sterile alpha motif (SAM) and a class I PDZ-binding motif (PBM), as bait (SAM-PBM) (Figure 1A). We identified clones encoding three PDZ domain-containing scaffold proteins as putative interaction partners, namely the USH2D protein whirlin (8), the PDZ-domain-containing RING finger protein 4 (PDZRN4) and the MAGUK protein Magi2 (membrane associated guanylate kinase inverted-2). Here we focus on the analysis of the interaction between SANS and Magi2.

We validated the interaction between SANS and Magi2 in independent complementary assays on different levels, *in vitro*, in cell culture and *in situ*. First, we affirmed the binding of SANS´ SAM-PBM to the PDZ5 domain of Magi2 in Y2H 1:1 assays (Figure 1B). Second, we affirmed the interaction between both proteins *in vitro* by GST-pull down assays using bacterial expressed GST-Magi2-PDZ5, which pulled down FLAG-tagged SANS full-length with and without the PBM from HEK293 cell lysates (Figure 1C). To elucidate, which domains participate in the interaction, we carried out GST-pull downs adopting GST-tagged Magi2-PDZ5 domain and different 3xFLAG-tagged domains of SANS (Figure 1D). We found that GST-PDZ5 pulls down only the SANS-C-terminus with and without the PBM, but neither the N-terminus nor the central domain of SANS. In contrast, we did not recover any SANS domain in GST-pull down assays with GST alone or GST-Magi2-PDZ3 and -PDZ4 (Figure 1E), which were previously identified as binding motifs to other proteins (26). Our GST-pull down results conclusively confirmed that SANS directly binds to Magi2 *in vitro*. This interaction is mediated by the SAM domain in the C-terminus of SANS, whereas the PBM in the C-terminus of SANS is not necessary for the binding to the PDZ5 domain of Magi2. These results go along with the data obtained by bioinformatics' analyses applying POW (PDZ domain-peptide interaction prediction website (http://webservice.baderlab.org/domains/POW/). POW analysis predicted that the Magi2-PDZ5 domain interacts with an internal five amino acid short SDLDL motif (Hs SANS: aa422–426) in the SAM domain with 2.3-fold higher predictor confidence as with the C-terminal PBM affinity of SANS. Alignments of amino acid sequences of SANS´ SAM domains from diverse vertebrate species revealed that the SDLDL motif is conserved in all Eutheria species (Table I). In the marsupial *Monodelphis domestica*, in birds and the lower vertebrate animal models zebrafish and frog, non-polar amino acids are replaced by polar amino acids, which even increase the predictor confidence for Magi2-PDZ5 binding. Furthermore, quantification of the amount of recovered SANS in the GST-pull downs, shown in Figures 1C and D, demonstrated that the recovery was 2.5-fold higher in the case of the SANS full-length lacking the C-terminal PBM compared to the PBM-containing constructs. In experiments adopting constructs of the SANS´ C-terminus without the PBM the

recovery was even 4.7-fold higher. These results suggested that presence of the C-terminal PBM might reduce the affinity of SANS to Magi2.

To analyze this interaction in the cellular environment, we performed co-precipitation assays. For this, we co-transfected HEK293 cells either with 3xFLAG-SANS and mRFP-Magi2-PDZ5 or GFP-SANS and Magi2-HA, respectively and precipitated the mRFP- or GFP-tagged polypeptides applying the Trap® bead system (Figure 1F,G). In these experiments we showed that SANS co-precipitated with the PDZ5 domain and that full length Magi2 co-precipitated with SANS. Next, we performed membrane targeting assays, transfecting murine IMCD3 cells with MyrPalm-eCFP-tagged SANS and/or Magi2-HA (Figure 1H). In singly transfected cells, the N-terminal membrane anchoring MyrPalm-tag attached eCFP-SANS to the plasma membrane (Figure 1H,a), while Magi2-HA was found in the cytoplasm and nucleus (Figure 1H,b). However, in co-transfected cells, Magi2 co-localised with SANS at the plasma membrane (Figure 1H,c), indicating that Magi2 is recruited to the membrane by binding to SANS. This binary interaction between Magi2 and SANS was affirmed by reciprocal experiments utilizing MyrPalm-eCFP-Magi2 and GST-SANS (Supplemental Figure S1). In this case Magi2 recruited the cytoplasmic SANS to the membrane in co-transfected cells, which is not the case in the control with MyrPalm-eCFP alone and GST-SANS.

Mutations in the USH1G gene *SANS* affect complex formation

Next we checked to what extend diseases causing mutations affect SANS-Magi2 complex assembly. So far, mutations in *MAGI2* have not been linked to any disease. Nevertheless, common variants in *MAGI2* were recently found to be associated with increased risk for cognitive impairment in schizophrenic patients (27). In addition, the *MAGI2* protein may be associated with ATXN2 in protein networks. In the *ATXN2* gene expansions of CAG repeats are responsible for spinocerebellar ataxia type 2 (SCA2), which is often associated with *retinitis pigmentosa* (28). *In silico* analyses on the known pathogenic USH disease causing mutations in the USH1G gene *SANS* by screening the database (https://grenada.lumc.nl/LOVD2/Usher_montpellier/home.php?select_db=USH1G) (29) revealed a variety of mutations in *SANS*. With one exception identified mutations lead to truncations of the SANS molecule lacking the SAM domain (Figure 2) (17;30-36). Taken together most disease causing mutations in *SANS* have effects on the predicted Magi2 binding motif and thereby eliminate the SANS-Magi2 complex formation in human USH1G patients.

The interaction of SANS and Magi2 is regulated by phosphorylation

Several previous studies indicated that the binding of molecules to Magi2 is often regulated by phosphorylation (37;38). This prompted us to examine whether the interaction of SANS and Magi2 also depends on phosphorylation. For this, we combined the previously introduced robust membrane targeting assay in IMCD3 cells with the application of D-ribofuranosyl-benzimidazole (DRB), a potent inhibitor of carboxyl-terminal domain kinases. In contrast to DMSO treated controls (Figure 3A), DRB inhibited the recruitment of Magi2-HA to the membrane-bound MyrPalm-eCFP-SANS (Figure 3B) suggesting that phosphorylation regulates the assembly of the SANS-Magi2 complex.

To elucidate which interaction partner needs to be phosphorylated for the SANS-Magi2 interaction, we identified putative phosphorylation sites present in the interacting domains of SANS-SAM (S422) and Magi2-PDZ5 (S1082) by BLAST analyses (http://www.phosphosite.org). Subsequently, we mutated these sites to phospho-mimicking and dephospho-polypeptides. We found that in cells co-transfected with the phospho-mimicking SANS construct (MyrPalm-eCFP-SANS S422E) and HA-tagged full length Magi2 (Magi2-HA), Magi2 was recruited to the cell membrane (Figure 4A). In contrast, in cells co-transfected with the dephospho-construct of SANS (MyrPalm-eCFP-SANS S422A) and Magi2-HA, Magi2 was no longer found at the cell membrane (Figure 4B). In cells co-transfected with wild type full-length SANS and the dephospho-construct of Magi2 (Magi2-HA S1082A), we observed that Magi2 was still recruited to SANS at the cell membrane (Figure 4C). In conclusion, present results demonstrate that the phosphorylation of SANS is essential for the assembly of the SANS-Magi2 complex.

Next, we addressed whether the interaction of the endogenous proteins depends on phosphorylation. Preliminary quantitative real-time PCRs revealed that SANS and Magi2 were expressed in murine IMCD3 cells and knock down experiments validated the specificity of the antibodies for both proteins (Supplemental Figures S2, 3). Indirect immunofluorescence demonstrated that in untreated and DMSO-treated cells both proteins were expressed in the periciliary region of primary cilia (Supplemental Figure S4A, B) or in the pericentriolar region of the centrosome, visualized by antibodies against the pericentriolar marker protein PCM1 (Supplemental Figure S4C). In DRB-treated cells, SANS was no longer concentrated in the pericentriolar matrix, where Magi2 and PCM1 remained, but was found in the nucleus instead (Supplemental Figure S4D). The disappearance of SANS from the pericentriolar region was more evident comparing the intensity profiles of SANS and Magi2 in control and DRB treated cells in the region of interest (ROI, defined by PCM1-staining) as exemplarily shown (Supplemental Figure S4 E, F).

The SAM domain of SANS is phosphorylated by CK2

DRB is widely used as a potent inhibitor for CK2 (casein kinase 2) (39) and BLAST analysis (http://www.phosphosite.org) predicted the serine S422 in the SAM domain of SANS as a putative phosphorylation site for the protein kinase CK2. To experimentally validate whether SANS-SAM is a substrate for CK2 we performed phosphorylation *in vitro* assays by P^{32} incorporation (Figure 5). Quantification of the radioactivity incorporation revealed that the phosphorylation of GST-SAM-PBM was significantly increased about 4-fold in comparison to GST alone (Figure 5B), indicating that CK2 phosphorylates S422 in the SAM domain of SANS.

Magi2-mediated endocytosis is negatively regulated by SANS binding

Previous studies have indicated an important role of Magi2 in endocytotic processes in neurons (23;24;26;28). This prompted us to analyze the role of the Magi2-SANS complex in endocytosis by transferrin uptake assays in IMCD3 cells. Fluorescence microscopy analysis of the time course of Alexa 647-tagged transferrin (Tf647) uptake showed that fluorescent Tf647 vesicles appeared first in

the cytoplasm before they concentrated (30 min) in the perinuclear region of the cell. Immunofluorescent counterstaining of Magi2 revealed the close association of Magi2 with Tf647 vesicles at each time point, which was most prominent after 30 min (Figure 6A, lower panel). To confirm that Tf647 was taken up by endocytotic processes we treated cells with dynasore, which blocks clathrin-mediated endocytosis by inhibiting the dynamin GTPase (40). In dynasore-treated cells Tf647 was no longer found in the cytoplasm, but remained at the cell membrane indicating that the monitored transferrin uptake is based on clathrin-mediated endocytosis (Figure 6B).

Next, we examined whether the formation of the Magi2-SANS complex is related to endocytosis. For this, we measured the transferrin uptake after knock down of Magi2 and SANS, respectively, using specific shRNAs, which we previously validated in IMCD3 cells (Supplemental Figures S2, 3). Knock down of Magi2 significantly reduced the Tf647 uptake by IMCD3 cells to 57% (Figure 7A), while the overexpression of GFP-Magi2 significantly increase the Tf647 uptake by 43% compared to GFP-transfected cells (Supplemental Figure S5). ShRNA-mediated knock down of SANS significantly increased the transferrin uptake by IMCD3 cells by 46% compared to mock transfected cells, while Tf647 uptake in cells transfected with shRNA-empty vectors as control showed a slight increase by 26% (Figure 7B). Furthermore, we analysed whether the observed endocytosis is dependent on the phosphorylation. For this, we treated IMCD3 cells with the kinase inhibitor DRB, which induces dephosphorylation as shown above and measured the uptake of Tf647. Surprisingly we observed a 1.63-fold increase of Tf647 fluorescence in DRB treated cells (Figure 7C). Taken together, these data display that Magi2 mediates endocytosis and that SANS´ phosphorylation negatively affects endocytosis, suggesting a negative regulation of Magi2-mediated endocytosis by phospho-dependent SANS-Magi2 binding.

SANS and Magi2 knock down and inhibition of endocytosis affect ciliogenesis of primary cilia

The co-distribution of SANS and Magi2 in the periciliary region of primary cilia (Supplemental Figure S4) prompted us to test whether the complex partners contribute to ciliogenesis and/or maintenance of primary cilia. For this we knocked down either SANS or Magi2 via the specific shRNAs, which we have validated above, and introduced ciliogenesis in IMCD3 cells by serum starvation. Knock down of SANS resulted in heterogeneous ciliary phenotypes in transfected cells, namely no cilia were found in ~77% of the cells while the cilia of the few ciliated cells were with either shorter (~12%; <1.9 µm) or longer (~4%; >2µm) than control primary cilia or exhibited multiple cilia (~6.8%) (Figure 8). The variable ciliary phenotype may reflect SANS participation in several cellular functional modules related to cilia.

Knock down of Magi2 abolished ciliogenesis in 82% of transfected IMCD3 cells compared to control (Figure 9A, C). In 18% of Magi2 shRNA-transfected cells cilia were present, but reduced in length (<1.5 µm) compared to control (Figure 9B). To examine the link between endocytosis and ciliogenesis we treated IMCD3 cells with the dynamin-inhibitor dynasore during serum starvation. Inhibition of clathrin-dependent endocytosis eliminated primary cilia formation in 70% of dynasore-

treated cells compared to control cells (Figure 9B, D). Analysis of the ciliary shape revealed a reduction in length of the few emerging primary cilia (< 1.7 µm) compared to control (Figure 9Bc, d). Taken together these results indicated that SANS affected ciliogenesis and that Magi2 and clathrin-dependent endocytosis were essential for ciliogenesis of primary cilia in IMDC3 cells.

Subcellular localization of Magi2-USH protein complexes in mouse retina

Next, we were interested to enlighten the role of the Magi2-SANS protein complexes in the mammalian retina. For this, we examined where Magi2 and SANS are co-expressed *in situ*, which is a necessary prerequisite for the interaction of proteins within a functional module *in vivo*. First of all we performed immunofluorescence labelling of Magi2 in longitudinal cryosections through the murine retina. Magi2 was present throughout the retina, except for the nuclear layers and the outer segments (Figure 10B). Most prominent staining was observed in the outer plexiform layer, the outer limiting membrane and the ciliary region.

To determine a more precise localization of Magi2 in the identified compartments of photoreceptor cells, we performed immunofluorescence double labelling with antibodies against Magi2 and molecular markers for these compartments, namely centrin-3 which stains the connecting cilium, the basal body and the adjacent daughter centriole(39), β-catenin, a marker for cell-cell adhesion complexes in the outer limiting membrane, and PSD95, a component of the synaptic terminal of photoreceptor cells (Figure 10C). Merged images of Magi2 and centrin-3 staining revealed that the localization of Magi2 partially overlapped with the centrin-3 staining in the periciliary region of the apical inner segment (Figure 10C, upper panel). In the outer limiting membrane Magi2 partially co-localised with the adhesion complex marker β-catenin (Figure 10C, middle panel). In the synapses of the outer plexiform layer the immunofluorescence of Magi2 and PSD95, predominantly localised in the pre-synaptic terminals of the retinal photoreceptor cells, only slightly overlapped, indicating that Magi2 molecules are predominantly localised in the post-synaptic parts of the bipolar and horizontal cells dendrites.

In a second step, we illuminated the putative co-localization of Magi2 and SANS by double labelling of both interacting proteins in retinal cryosections. Immunofluorescence microscopy analysis revealed substantial co-staining of Magi2 and SANS in the ciliary region of the inner segment of photoreceptor cells, but not at the outer limiting membrane and the synapses of the outer plexiform layer (Figure 10D). As expected from our previous studies (8;9), SANS immunofluorescence was detected predominantly in the pre-synaptic terminals of photoreceptor cells and thereby only little overlap with the Magi2 staining was found. The differential synaptic localization of Magi2 and SANS was affirmed by Western blot analyses of subcellular fractionations adopting differential sucrose centrifugations (Figure 10E). In Western blots of the synaptosomal fraction, in which pre- and postsynaptic parts are still combined, a SANS band and a faint, but detectable Magi2 band was present. In the fraction of the enriched post-synaptic densities Magi2 was most prominent in the absence of any SANS. Thus, it is unlikely that SANS and Magi2 interact at synapses.

Additional triple labeling of both proteins and centrin-2 (39) revealed considerable co-localization of SANS and Magi2 at the base of the photoreceptor connecting cilium (Figure 10F). Furthermore, we demonstrated the assembly of SANS and Magi2 complexes at the ciliary base of photoreceptor cells *in situ*, adopting proximity ligation assays (*in situ* PLA) (Figure 10G).

Next, we examined whether the CK2 kinase and its substrate SANS are also co-distributed in the ciliary region. Previous independent analyses of CK2 and SANS have already demonstrated that both proteins are part of the ciliary machinery of photoreceptor cells (8;39;41). Here, we applied immunofluorescence triple labeling of both proteins and the ciliary apparatus marker centrin-2 in retinal cryosections. High magnification fluorescence microscopy revealed substantial overlap of SANS and CK2 staining at the ciliary base of photoreceptor cells (Supplemental Figure S6A). Furthermore, *in situ* PLA supported the interaction of the SANS-CK2 complex at the ciliary base and at the tip of the connecting cilium of photoreceptor cells (Supplemental Figure S6B). Present data suggested that Magi2, SANS and CK2 interact within the supramolecular module of the periciliary region of retinal photoreceptor cells.

Magi2 is part of an endocytosis module in the periciliary region of photoreceptor cells.

Subsequent, we investigated the precise localization of Magi2 in the ciliary and periciliary region of photoreceptor cells. Adopting immunoelectron microscopy, we have previously shown that SANS is localized in the apical inner segment in the periciliary region, at the centriole-basal body complex, and in lower amounts in the connecting cilium of mouse and human rod photoreceptor cells (8;19). Electron microscopy analysis demonstrated connatural subcellular localization of Magi2 (Figure 11A, B), further supporting our light microscopy results. In addition, we detected Magi2 at dents of the plasma membrane of the ciliary pocket and coated membrane vesicles in the cytoplasm of the apical inner segment (Figure 11B, b). These data suggest that Magi2 associates with membrane vesicles budding from the ciliary pocket into the periciliary region of photoreceptor cells.

To explore further putative components of the endocytosis system in the periciliary compartment of photoreceptor cells, we stained cryosections through the mouse retina for transferrin receptors, which are characteristically associated with receptor-mediated endocytosis. Immunofluorescence microscopy showed that antibodies against the transferrin receptor labeled the apical inner segment of retinal photoreceptor cells (Figure 11C). The high resolution of immunoelectron microscopy revealed that antibodies against the extracellular parts of the transferrin receptor decorated predominantly the extracellular face of the plasma membrane of the ciliary pocket of photoreceptor cells (Figure 11D, E). Additional less intense labeling of transferrin receptors was present along other parts of the membrane of the apical inner segment. Taken together, present data suggest that transferrin receptor-mediated endocytosis takes place at the ciliary pocket of photoreceptor cells.

Discussion

In this study, we showed by complementary interaction assays and *in situ* localization that the USH1G protein SANS directly interacts with the MAGUK protein Magi2. Our data revealed that SANS binds via its SAM domain to the PDZ5 domain of Magi2 displaying a novel non-canonical targeting mode for PDZ domain interactions. PDZ domains mediate protein-protein interactions via targeting PDZ-binding motifs (PBMs) at the C-terminus (42), but less frequently also recognize internal peptide sequences of ligand proteins (43). We have previously described a canonical PDZ/target interaction between SANS' C-terminal PBM and the PDZ1 and PDZ2 domains of the USH2D protein whirlin (8). In the latter study, we showed that deletion of SANS´ PBM completely abolishes the binding of SANS to both PDZ domains indicating that SANS´ SAM domain does not contribute to this interaction. However, an unexpected interaction mode for PDZ and SAM domains has been recently described for the USH1C protein harmonin and SANS (7). Yan and co-workers demonstrated a highly stable complex of harmonin and SANS by synergistic interaction of PDZ1 domain of harmonin with the C-terminal PBM-I SANS and N-terminus of harmonin with the SAM domain of SANS. Here, we showed that the SAM domain of SANS also takes part in direct targeting the PDZ5 domain of Magi2. Bioinformatics predicted five highly conserved amino acids in the central part of the SAM domain as the internal PBM. In contrast to the assembly of the SANS/harmonin complex, the C-terminal PBM of SANS does not contribute to the SANS/Magi2 interaction, but seems to reduce the affinity of SANS to Magi2. Although SAM domains are among the most common protein domains in eukaryotic genomes (44), to our knowledge the present binding module is the first between a SAM and a PDZ domain.

The depicted interaction mode between SANS and Magi2 via the SAM domain provides SANS an expanded degree of freedom in its scaffold function, enabling SANS to bind with its C-terminal PBM-I to a second PDZ domain-containing protein. Accordingly, in the periciliary region of photoreceptor cells, SANS can simultaneously interact with the PDZ-domains of whirlin (8) and with the PDZ5 of Magi2 via SAM.

Although it is well accepted that interactions mediated by PDZ domains are not static, it is known only for a few molecular examples, how the plasticity of PDZ domains in ligand binding is regulated (43;45). Here, we demonstrate that the phosphorylation of the ligand SANS regulates its binding to a PDZ domain of Magi2. Our data conclusively show that the assembly of the SANS-Magi2 complex is strictly dependent on the phosphorylation of serine S422 in the SAM domain of SANS by protein kinase CK2. S422 is the first of the five amino acids predicted as internal PDZ binding site for the PDZ5 of Magi2. From this it is apparent that the S422 phosphorylation introduces the conformational change that facilitates binding of SANS to Magi2. The differential regulation of molecular targeting to the scaffold molecule SANS by reversible phosphorylation provides the plasticity to participate in different functional cellular modules, which we and others have described for SANS in the protein interactome related to USH (8;19;46). It is the first regulation mechanism identified in the entire USH protein interactome so far, and in the future it will be interesting to

address whether the phosphorylation by CK2 or other kinases only regulates the assembly of the SANS-Magi2 complex or also controls the interaction between other interactome partners, which have been previously identified (8;11;18;19). It is certainly possible that the scaffold function of SANS is modulated by phosphorylation in general.

There is emerging evidence that Magi2 plays important roles in the development and function of synapses, participating in receptor endocytosis and post-endocytotic trafficking (20;23); Yamagata2010}. Our findings coherently affirm that Magi2 participates in receptor-mediated endocytosis. The localization of Magi2 at post-synapses of inner and outer plexiform layer synapses suggests that Magi2 also supports endocytosis in retinal neurons. However, our present data revealed Magi2 as component of the periciliary membrane complex (PMC) in the apical photoreceptor inner segment, facing the ciliary pocket. In diverse cell lines the ciliary pocket of primary cilia has been recently demonstrated as a hot spot for frequent endocytosis (14;15;47;48). Here we showed that knock down of Magi2 is essential for ciliogenesis and/or maintenance of primary cilia in IMDC3 cells. Furthermore, we demonstrated that the inhibition of endocytosis also drastically reduced the formation of primary cilia indicating that endocytosis is required for cilia morphogenesis. Our data support previous findings on endocytotic processes at the ciliary base for controlling ciliary and periciliary membrane homeostasis (49). Interestingly, endocytosis inhibition phenocopies the ciliary phenotype induced by Magi2 depletion suggesting that Magi2-mediated endocytosis is essential for ciliogenesis and/or maintenance of primary cilia.

The association of Magi2 with putative endocytotic vesicles in the periciliary compartment suggests that Magi2 also mediates endocytosis in photoreceptor cells. This hypothesis is further supported by the clustering of transferrin receptors, a hallmark for receptor-mediated endocytosis (50), at the ciliary pocket membrane of photoreceptor cells. In addition, the abundance of transferrin receptors suggests that their ligand transferrin is taken up in the ciliary pocket of photoreceptor cells(51). Transferrin is mainly synthesised in the retinal pigment epithelial cells and assists in shuttling iron to photoreceptor cells (52). Since iron is an important cofactor of various enzymes but can also generate harmful free radicals (53), the control of its endocytosis is essential for the cellular homeostasis (54). In the retina, unbalanced iron homeostasis leads to photoreceptor pathology (55), and previous studies have monitored death of photoreceptor cells caused by either a lack or an excess of iron (56;57).

In primary cilia, it has been previously hypothesized that membrane cargo cross the periciliary diffusion barrier by endocytosis to enable ciliary import (58;59). Our present findings support this hypothesis indicating that Magi2 expression and the maintenance of the endocytosis machinery are essential for ciliogenesis and/or retention of primary cilia. It is worth to speculate that Magi2-related endocytosis participates in the tight control of ciliary membrane cargo delivery and membrane retrieval via endocytosis at the base of primary cilia in general and the periciliary membrane complex (PMC) of photoreceptor cells in particular.

There is growing evidence that the scaffold protein SANS integrates in distinct protein complexes associated with the microtubule cytoskeleton, namely microtubule-based transport and centriolar function (8;9;19; Sorusch *et al*, in press). The present SANS knock down resulted in diverse ciliary phenotypes, namely deprivation, but also facilitation of cilia growth as well as multiple ciliation suggesting that SANS participates in the regulation of different aspects of ciliogenesis and/or maintenance. As known from other centrosome components the formation of multiple cilia may be based on a role of SANS in the regulation of centriole duplication (60). Failure of centriole duplication control leads to an increase of centrioles and basal bodies nucleating primary cilia growth as found in SANS-depleted cells. The directly opposed phenotype in ciliary length may reflect on the one hand a ciliary transport defect in cells with either no or short cilia and on the other hand an amplified ciliary growth in cells with long cilia, respectively.

The next important question is how SANS is enrolled in the endocytosis module of the ciliary pocket of the primary cilia of photoreceptor cells. Our previous work suggested that SANS is part of a protein complex in the intercellular transport module for cargo transport through the inner segment and of vesicle cargo targeting to the PMC of photoreceptor cells (8;19). Here, we demonstrated that SANS and Magi2 are co-expressed and can assemble into a protein complex in the periciliary region of photoreceptor cells. These data suggest that the interaction between SANS and Magi2 may participate in targeting cargo vesicles to periciliary membranes, which is followed by subsequent vesicle docking and fusion. However, this vesicle membrane delivery resembles an exocytosis process, but not endocytosis mediated by Magi2 as discussed above. Interestingly, we showed that the Magi2-mediated endocytosis is negatively regulated by binding of phosphorylated SANS. One possible model for the SANS-Magi2 function in the periciliary region of photoreceptor cells is that, upon approaching of the SANS transport complex at the periciliary region compartment, SANS is phosphorylated by the periciliary resident CK2 (39) (Figure 12B). Thereby, the affinity of the phospho-SANS for Magi2 increases and the phospho-SANS-Magi2 complex assembles, which in turn shuts down endocytosis and facilitates the exocytosis process for the cargo vesicle delivery into the periciliary membrane for further translocation into the outer segment (Figure 12A).

In conclusion, our study uncovers a novel mechanism, by which SANS controls Magi2-mediated endocytosis conjoining the down-regulation of endocytotic processes with the facilitation of vesicular cargo transport and delivery modules in ciliated photoreceptor cells and cilia in general. Most disease causing mutations in *SANS* eliminate the SANS-Magi2 complex formation. These defects may unbalance the regulation of these processes, ultimately leading to ciliary pathogenesis observed in human USH1G patients.

Methods

Antibodies and fluorescent dyes

Following antibodies were used: anti-transferrin receptor (TfR, sc-65877), anti-Magi2 (sc-25664) and anti-ß-catenin (sc-7963) from Santa Cruz Inc., Santa Cruz, USA); anti-tubulin, anti-FLAG, anti-Magi2 (SAB1404762) and anti-PSD95 (7E3-1B8) from Sigma-Aldrich (Hamburg, Germany); anti-HA from Roche Diagnostics (Mannheim, Germany), anti-RFP from ChromoTek (Planegg-Martinsried, Germany), anti-actin from Millipore GmbH (Schwalbach, Germany) and anti-GST from GE Healthcare (Munich, Germany). Novel SANS-CENT antibodies (aa339-384) were generated in guinea pig and validated by specific antigen-recognition, shRNA knock downs and quantitative real-time PCR (Supplemental Fig. S2). Different centrin antibodies (61) were used as ciliary markers. Anti-GFP antibodies were a gift from W. Clay Smith (Gainesville, USA) (62). Alexa647® transferrin and secondary antibodies (Alexa488®, Alexa568® or Alexa647®) were purchased from Molecular Probes® (Life Technologies, Darmstadt, Germany) or from Rockland Inc. (Gilbertsville, USA). Biotinylated secondary antibodies (Vector Laboratories, Burlingame, USA) were used for pre-embedding electron microscopy. Nuclear DNA was stained with 4′, 6-Diamidin-2′-phenylindoldihydrochlorid (DAPI, 1 µg/ml) (Sigma-Aldrich).

Yeast-2-Hybrid screen

Yeast two-hybrid (Y2H) screen of retinal cDNA libraries was performed as previously described (63). Briefly, SAM-PBM domain of human SANS (NCBI:NM_173477.3; aa385-461) fused to DNA-binding domain (BD) of GAL4 transcription factor was used as bait to screen a bovine oligo-dT primed retinal cDNA library, fused to DNA-activation domain (AD) of GAL4. Interactions were identified and analysed by assessment of the HIS1, ADE3, LacZ and MEL1 reporter genes. To confirm interactions, bait and prey were co-transformed in the yeast strain *PJ694α* and analysed as described above.

GST-Pull down

PDZ3 (aa622-698), PDZ4 (aa765-864) and PDZ5 (aa1039-1112) domains of murine Magi2 (NCBI:BC059005) were subcloned in the pDEST™15 vector (Gateway®, Invitrogen™), expressed in *E. coli* and bound to glutathione-sepharose beads (GE Healthcare) as described in (61). 3xFLAG-tagged recombinant polypeptides were generated in HEK293 cells transfected with the appropriate expression plasmids. 24 h post-transfection cells were washed with PBS (140 mM NaCl, 2.7 mM KCl, 10 mM $Na_2HPO_4x2H_2O$, 1.8 mM KH_2PO_4, pH 7.4) and lysed in lysis buffer (50 mM Tris–HCL pH 7.5, 150 mM NaCl, 0.5% Triton-X-100) containing protease inhibitor cocktail (PI-mix; Roche Diagnostics). Cell lysates were incubated for 2 h with GST-fusion proteins bound to glutathione-sepharose beads at 4ºC under constant shaking. Samples were washed with lysis buffer, precipitated proteins were eluted with SDS sample buffer and subjected to SDS-PAGE and Western blot employing the Odyssey InfraRed imaging system (LI-COR Biosciences, Lincoln, USA) for detection.

De-/Phosphorylation assays

Recombinant GST-SAM-PBM was bound to beads as described above. Briefly, samples were divided in equal aliquots and incubated with 2 µCi [γ-^{32}P]-ATP (PerkinElmer, Rodgau, Germany) in 500 ml kinase buffer (20 mM Tris-HCl, pH 7.5, 50 mM KCl, 10 mM $MgCl_2$, 1 mM EGTA, PI-mix) including 62.5 units CK2 (Calbiochem, EMD Millipore) or buffer alone as control for 1h at 30°C. Reactions were stopped by washing. Samples were subjected to SDS-PAGE (input/size control by coomassie staining) and analysed by measuring the incorporated, residual radioactivity using a 2200CA Tri-Carb® Liquid Scintillation Analyzer (Canberra Packard, Frankfurt, Germany) or autoradiography. Imaging was done by exposition of X-ray films.

GFP-/RFP-Trap®

GFP- or RFP-fused polypeptides were immobilized at Trap® agarose beads (ChromoTek) and used for co-precipitation assays according to the manufacturer´s protocol. Briefly, cell lysates from co-transfected HEK293 cells (mRFP-tagged PDZ5 domain of Magi2 or mRFP alone together with 3xFLAG-SANS, or GFP-SANS and Magi2-HA) were suspended in lysis buffer (10 mM Tris/Cl pH 7.5, 150 mM NaCl, 0.5 mM EDTA, 0.5% NP-40), spun and the supernatant was diluted to 500µl in dilution buffer (10 mM Tris/Cl pH 7.5, 150 mM NaCl, 0.5 mM EDTA). 50 µl were separated as input (total cell lysate, TCL) and samples were added to equilibrated beads for 2 h at 4°C under constant shaking. After washing, precipitated protein complexes were eluted with SDS-sample buffer and subjected to SDS-PAGE and Western blots.

Cell culture

We cultured HEK293 (human embryonic kidney cells) in Dulbecco's modified Eagle's medium (DMEM) for high expression levels and IMCD3 (mouse inner medullary collecting duct cells) cells in DMEM-F12 for intrinsic protein analyses containing 10% heat-inactivated foetal calf serum (FCS). Cells were transfected with plasmids using Lipofectamine® LTX and Plus Reagent (Invitrogen™, Karlsruhe, Germany) according to manufacturer's instructions. To induce ciliogenesis, IMCD3 cells were starved 24 h after seeding or transfection in low serum medium containing 0.5% FCS for additional 48 h.

Membrane targeting assay

Human SANS (aa2-461) and murine Magi2 (aa2-1112) were subcloned in the MyrPalm-eCFP vector (plasmid 14867, Addgene, Cambridge, USA (64)) containing a N-terminal membrane-anchoring peptide and eCFP. MyrPalm-eCFP-SANS was single- or co-transfected with murine Magi2 (aa2-1112) C-terminally tagged with HA (Magi2-HA). 24 h post-transfection cells were subjected to immunocytochemistry. For kinase inhibition assays transfected cells were incubated in medium containing 150mM DRB (D-ribofuranosyl-benzimidazole, BIOMOL, Hamburg, Germany) or DMSO (dimethyl sulfoxide) as control.

Mutagenesis

Expression plasmids containing SANS or Magi2 were used for mutagenesis to generate de- / phospho-mimicking constructs. Primers were designed on Agilent homepage (http://www.genomics.agilent.com) and mutagenesis PCR was performed according to the manufacturer's instructions (Agilent Technologies, Waldbronn, Germany). Used primers see Supplemental Table SI.

Immunocytochemistry

Cells were fixed with methanol containing 0.05% EGTA, air-dried and subsequently washed with PBS and incubated with 0.01% Tween20 for 10 min. shRNA-transfected cells or cells in transferrin uptake-assays were fixed with 3% PFA for 15 min at 4°C, washed with PBS and incubated with NH_4Cl and 0.01% Tween20 for 10 min each. Subsequently, cells were incubated in blocking solution (0.5% cold-water fish gelatine, 0.1% ovalbumin in PBS) for 30 min before primary antibodies were incubated overnight at 4°C. After washing, samples were incubated with secondary antibodies and DAPI for 1.5 h at room temperature. After washing cover slips were mounted in Mowiol (Roth, Karlsruhe, Germany). Samples were analysed with a Leica DM6000B microscope (Leica, Bensheim, Germany) and images were processed with Adobe Photoshop CS for reducing grey scales, merge images, changing colours, changing image size and higher magnifications (Adobe Systems, San Jose, USA).

Short hairpin RNA (shRNA) against Magi2 and SANS

shRNAs against SANS were purchased from OriGene (Rockville, USA). 12 h after transfection, IMCD3 cells were treated with puromycin (Roth) for selection of transfected cells. For Magi2 knock down double-stranded 21-nucleotide oligos were annealed overnight and cloned with the restriction sites for HpaI and HindIII into the shRNA vector (pAAV2.1-sc-shRNA-CMV-eGFP). Magi2 gene-specific inserts named Oligo 1-3 were 21-nucleotide sequence separated by AAGTTCTCT non-complementary spacers from the reverse complement of the same 21-nucleotide sequence. Used oligos see Supplementary Table I. shRNA were transfected into IMCD3 cells with 50% confluence using LTX. Knock down efficiency was validated 72 h post-transfection by anti-SANS or anti-Magi2 Western blots and by quantitative real-time PCR (qPCR). shRNA03/Oligo3 showed strongest knock down efficiency compared to empty vector and normalized to actin or to tubulin, respectively. 72 h post-transfection cells were prepared for uptake-assays and/or immunocytochemistry.

Reverse transcription and quantitative real-time PCR

Total RNA was isolated from cells by RNA isolation kit from Macherey-Nagel (Düren, Germany). Reverse transcription (RT) was performed with 1 µg of total RNA with the SuperScript III First Strand synthesis kit (Invitrogen) following manufacturer's instructions with a mixture of random hexamers and oligo-dT primers. qPCR was performed on CFX96 real-time system (Bio-Rad, Munich, Germany) using the SYBRGreen iTAQ according to manufacturer´s instructions. In a total volume of 20 µl, diluted cDNA (1:5) and 4 nM of each primer/reaction were used. Cycling conditions were 95°C for 30 sec, 45 cycles at 95°C for 5 sec, 60°C for 30 sec followed by plate read, and melt curve analysis for 65°C to 95°C using primers, specific for murine Magi2/SANS (Supplemental table SI.) Quantification was done with three independent experiments.

Transferrin uptake assay

At 75% confluence IMCD3 cells were incubated in serum-free media for 2h at 37°C to remove endogenous iron. Alexa-647 labelled transferrin (Tf647®) was diluted in serum-free media (10µg/ml) and incubated for 30 min at 4°C. After washing with pre-warmed, serum containing medium, cells were incubated for additional 5 to 30 min at 37°C in serum-containing medium. Washing with PBS containing 0.5 % acidic acid to remove surface-bound transferrin was followed by fixation with 3% PFA. Quantification of non-processed images was performed with CellProfiler 2.0 (r11710) cell image analysis software (Broad Institute, Cambridge, USA). All experiments were done 3-5 times; at least 5 images from each sample were used for quantification. In overexpression experiments, cells were transfected 24 h before uptake assay with GFP or GFP-Magi2 (aa2-1112) using LTX®. In dephosphorylation experiments, cells were grown overnight in DRB-medium and DRB was added to all media used during uptake assay. To inhibit endocytosis, IMCD3 cells were treated with 80 µM dynasore (Dynasore hydrate D7693, Sigma-Aldrich) solved in DMSO.

Synaptic fractionation

Synapses were fractionated via differential sucrose gradient centrifugation as previously described (65) using an ultracentrifuge Optima-Max with rotor MLS50 (Beckman Coulter, Krefeld, Germany). Briefly, bovine retinae were homogenized in 10 ml/g buffer A (320 mM sucrose, 5 mM HEPES, pH 7.4, PI-mix) and cell debris/nuclei were removed by centrifugation for 10 min at 1,000 g. 0.5% of homogenate was separated (total retina lysate, TRL), supernatant was centrifuged for 20 min at 12,000 g to separate crude membranes (P2) and soluble cytoplasmic components (S2). P2 was suspended in 1.5 ml/g buffer B (A with 5 mM Tris/HCl, pH 8.1), loaded on a discontinuous sucrose gradient (1.2, 1, and 0.85 M) and centrifuged for 2 h at 80,000g. Synaptosomes were collected at interphase of 1.2 and 1 M sucrose, mixed with 5x vol. of hypo-osmotic solution (1 mM Tris/HCl, pH 8.1) and stirred for 30 min on ice. Solution was centrifuged for 30 min at 33,000 g and pellet was suspended in

1.5 ml/g of 5 mM Tris/HCl pH 8.1, loaded on top of a sucrose gradient and centrifuged for 2 h at 80,000g. Synaptic junction complexes were collected at the interphase of 1.2 and 1 M sucrose, added to a 1:1 solution of buffer B and C (B + 0.5% Triton X-100) and stirred for 15 min on ice to separate pre- and post-synaptic membranes. Solution was centrifuged 30 min at 33,000 g to pellet the PSD fraction. For microsomes, S2 was pelleted 2 h at 100,000 g. Protein content was determined by coomassie staining, TRL and fractions were subjected to SDS-PAGE and Western blots.

Immunohistochemistry

Eyes of mice were cryofixed in melting isopentane and cryosectioned as described elsewhere (66). Cryosections were placed on poly-L-lysine-precoated coverslips, incubated with 0.01% Tween20-PBS, washed several times, covered with blocking solution and incubated in blocking for 30 min followed by overnight incubation at 4°C with primary antibodies. Washed cryosections were incubated with secondary antibodies in blocking solution containing DAPI (Sigma) for 1.5 h at room temperature. After washing, sections were mounted in Mowiol (Roth). Specimen were analysed on a Leica DM6000B microscope, images were processed with Leica imaging software and Adobe Photoshop CS. Images in Figures 8, 9, 10 F/G, 11 C, S4A,B and S6 were 3D-deconvoluted with Leica software.

Proximity ligation assay (PLA)

In situ proximity ligation assay (PLA) was developed to support the interaction of two co-localised proteins by visualizing protein-protein interactions with a single-molecule resolution (67). Following PLA probes were purchased from Olink Bioscience (Uppsala, Sweden): Duolink PLA probe anti-rabbit PLUS, anti-mouse PLUS, anti-guinea pig MINUS and Duolink *in situ* Detection Reagent Red. PLAs were performed according to manufacturer´s protocol adapted to our immunohistochemistry protocol, applied on unfixed cryosections of murine retina. Briefly, cryosections were incubated overnight at 4°C with primary antibodies, subsequently counterstained with anti-centrin-2 for 2 h before fixation with 2% PFA in PBS. Next, PLA probes were added to sections for 2 h at room temperature. Ligation was performed for 30 min at 37°C and amplified for 100 min.

Immunoelectron microscopy

For immunoelectron microscopy we applied the pre-embedding labelling protocol described by (68). Ultrathin sections were analysed in a transmission electron microscope (Tecnai 12 BioTwin; FEI, Eindhoven, The Netherlands). Images were obtained with a charge-coupled device camera (SIS Megaview3; Surface Imaging Systems), acquired by analySIS (Soft Imaging System) and processed with Adobe Photoshop CS.

Animals and tissue dissection

All experiments described herein are conforming to the statement by the Association for Research in Vision and Ophthalmology (ARVO) as to care and use of animals in research. C57BL/6J mice were maintained under a 12 h light–dark cycle, with food and water *ad libitum*. After sacrifice of the animals in CO_2 and decapitation, subsequently appropriate tissues were dissected. Bovine retinas were dissected from eye balls obtained from a local slaughter house.

Statistical analyses

All values represent means ± SD (standard deviation). To probe for significance of observed differences, the Student's t test was performed (unpaired, two tailed, assuming equal variance) with individual data-points from minimum three independent experiments. P-value > 0.05 was considered to be significant.

Acknowledgments

Authors thank Ulrike Maas, Elisabeth Sehn and Gabi Stern-Schneider for excellent technical assistance. Authors thank Dr. W. Clay Smith for providing the anti-GFP antibodies. Authors thank Dr. Stylianos Michalakis for providing the shRNA AAV-vector. Authors thank Anna Valeria Etz for testing the usability of the software CellProfiler. Authors thank Dr. Kerstin Nagel-Wolfrum for abundant discussion. This work was supported by the BMBF “HOPE2” (01GM1108D to UW), DFG (GRK 1044 to UW), Forschung contra Blindheit-Initative Usher Syndrom (to HK, UW), ProRetina Deutschland eV (to UW, KB), the FAUN-Stiftung, Nurnberg (to UW), European Community FP7/2009/241955 (SYSCILIA) (to HK, RR, UW) and FP7/2009/242013 (TREATRUSH) (to UW), the LSBS and The Foundation Fighting Blindness C-CMM-0811-0547-RAD03 (to HK).

References

1. Petit C 2001. Usher syndrome: from genetics to pathogenesis. *Annu.Rev.Genomics Hum.Genet.* 2:271-297.
2. Kremer H, van Wijk E, Maerker T, Wolfrum U, Roepman R 2006. Usher syndrome: molecular links of pathogenesis, proteins and pathways. *Hum.Mol.Genet.* 15SpecNo2:R262-R270.
3. Reiners J, Nagel-Wolfrum K, Juergens K, Maerker T, Wolfrum U 2006. Molecular basis of human Usher syndrome: deciphering the meshes of the Usher protein network provides insights into the pathomechanisms of the Usher disease. *Exp.Eye Res.* 83:97-119.
4. Wolfrum U 2011. Protein networks related to the Usher syndrome gain insights in the molecular basis of the disease. In: Satpal A, ed. *Usher Syndrome: Pathogenesis, Diagnosis and Therapy*. Nova Science Publishers, 51-73.
5. Davenport SLH and Omenn GS. The heterogeneity of Usher syndrome. Vth Int.Conf. *Birth Defects*, Montreal. 1977.
6. Saihan Z, Webster AR, Luxon L, Bitner-Glindzicz M 2009. Update on Usher syndrome. *Curr.Opin.Neurol.* 22:19-27.
7. Yan J, Pan L, Chen X, Wu L, Zhang, M 2010. The structure of the harmonin/sans complex reveals an unexpected interaction mode of the two Usher syndrome proteins. *Proc.Natl.Acad.Sci.U.S.A* 107:4040-4045.
8. Maerker T, van Wijk E, Overlack N, Kersten FF, McGee J, Goldmann T, Sehn E, Roepman R, Walsh EJ, Kremer H et al. 2008. A novel Usher protein network at the periciliary reloading point between molecular transport machineries in vertebrate photoreceptor cells. *Hum.Mol.Genet.* 17:71-86.
9. Overlack N, Maerker T, Latz M, Nagel-Wolfrum K, Wolfrum U 2008. SANS (USH1G) expression in developing and mature mammalian retina. *Vision Res.* 48:400-412.
10. van Wijk E, Kersten FF, Kartono A, Mans DA, Brandwijk K, Letteboer SJ, Peters TA, Maerker T, Yan X, Cremers CW et al. 2009. Usher syndrome and Leber congenital amaurosis are molecularly linked via a novel isoform of the centrosomal ninein-like protein. *Hum.Mol.Genet.* 18:51-64.
11. Yang J, Liu X, Zhao Y, Adamian M, Pawlyk B, Sun X, McMillan DR, Liberman MC, Li T 2010. Ablation of whirlin long isoform disrupts the USH2 protein complex and causes vision and hearing loss. *PLoS.Genet.* 6:e1000955.
12. Zou J, Luo L, Shen Z, Chiodo VA, Ambati BK, Hauswirth WW, Yang J 2011. Whirlin replacement restores the formation of the USH2 protein complex in whirlin knockout photoreceptors. *Invest.Ophthalmol.Vis.Sci.* 52:2343-2351.
13. Roepman R and Wolfrum U 2007. Protein networks and complexes in photoreceptor cilia. *Subcell.Biochem.* 43:209-235.
14. Molla-Herman A, Ghossoub R, Blisnick T, Meunier A, Serres C, Silbermann F, Emmerson C, Romeo K, Bourdoncle P, Schmitt A et al. 2010. The ciliary pocket: an endocytic membrane domain at the base of primary and motile cilia. *J.Cell Sci.* 123:1785-1795.
15. Ghossoub R, Molla-Herman A, Bastin P, and Benmerah A 2011. The ciliary pocket: a once-forgotten membrane domain at the base of cilia. *Biol.Cell* 103:131-144.
16. van Wijk E, van der Zwaag B, Peters T, Zimmermann U, te Brinke H, Kersten FF, Maerker T, Aller E, Hoefsloot LH, Cremers CW et al. 2006. The DFNB31 gene product whirlin connects to the Usher protein network in the cochlea and retina by direct association with USH2A and VLGR1. *Hum.Mol.Genet.* 15:751-765.
17. Weil D, El Amraoui A, Masmoudi S, Mustapha M, Kikkawa Y, Laine S, Delmaghani S, Adato A, Nadifi S, Zina ZB et al. 2003. Usher syndrome type I G (USH1G) is caused by mutations in the gene encoding SANS, a protein that associates with the USH1C protein, harmonin. *Hum.Mol.Genet.* 12:463-471.
18. Adato A, Lefevre G, Delprat B, Michel V, Michalski N, Chardenoux S, Weil D, El Amraoui A, Petit C 2005. Usherin, the defective protein in Usher syndrome type IIA, is likely to be a component of interstereocilia ankle links in the inner ear sensory cells. *Hum.Mol.Genet.* 14:3921-3932.
19. Overlack N, Kilic D, Bauss K, Maerker T, Kremer H, van Wijk E, Wolfrum, U 2011. Direct interaction of the Usher syndrome 1G protein SANS and myomegalin in the retina. Biochim.Biophys.Acta 1813:1883-1892.

20. Kawata A, Iida J, Ikeda M, Sato Y, Mori H, Kansaku A, Sumita K, Fujiwara N, Rokukawa C, Hamano M et al. 2006. CIN85 is localized at synapses and forms a complex with S-SCAM via dendrin. *J.Biochem.* 139:931-939.
21. Yamagata M and Sanes JR 2010. Synaptic localization and function of Sidekick recognition molecules require MAGI scaffolding proteins. *J.Neurosci.* 30:3579-3588.
22. Hirao K, Hata Y, Ide N, Takeuchi M, Irie M, Yao I, Deguchi M, Toyoda A, Sudhof TC, Takai Y 1998. A novel multiple PDZ domain-containing molecule interacting with N-methyl-D-aspartate receptors and neuronal cell adhesion proteins. *J.Biol.Chem.* 273:21105-21110.
23. Xu J, Paquet M, Lau AG, Wood JD, Ross CA, Hall RA 2001. beta 1-adrenergic receptor association with the synaptic scaffolding protein membrane-associated guanylate kinase inverted-2 (MAGI-2). Differential regulation of receptor internalization by MAGI-2 and PSD-95. *J.Biol.Chem.* 276:41310-41317.
24. Yap CC, Muto Y, Kishida H, Hashikawa T, Yano R 2003. PKC regulates the delta2 glutamate receptor interaction with S-SCAM/MAGI-2 protein. *Biochem.Biophys.Res.Commun.* 301:1122-1128.
25. Danielson E, Zhang N, Metallo J, Kaleka K, Shin SM, Gerges N, Lee, SH 2012. S-SCAM/MAGI-2 is an essential synaptic scaffolding molecule for the GluA2-containing maintenance pool of AMPA receptors. *J.Neurosci.* 32:6967-6980.
26. Deng F, Price MG, Davis CF, Mori M, Burgess, DL 2006. Stargazin and other transmembrane AMPA receptor regulating proteins interact with synaptic scaffolding protein MAGI-2 in brain. *J.Neurosci.* 26:7875-7884.
27. Koide T, Banno M, Aleksic B, Yamashita S, Kikuchi T, Kohmura K, Adachi Y, Kawano N, Kushima I, Nakamura Y et al. 2012. Common variants in MAGI2 gene are associated with increased risk for cognitive impairment in schizophrenic patients. *PLoS.One* 7:e36836.
28. Paciorkowski AR, Shafrir Y, Hrivnak J, Patterson MC, Tennison MB, Clark HB, Gomez CM 2011. Massive expansion of SCA2 with autonomic dysfunction, retinitis pigmentosa, and infantile spasms. *Neurology* 77:1055-1060.
29. Roux AF, Faugere V, Vache C, Baux D, Besnard T, Leonard S, Blanchet C, Hamel C, Mondain M, Gilbert-Dussardier B et al. 2011. Four-year follow-up of diagnostic service in USH1 patients. *Invest.Ophthalmol.Vis.Sci.* 52:4063-4071.
30. Mustapha M, Chouery E, Torchard-Pagnez D, Nouaille S, Khrais A, Sayegh FN, Megarbane A, Loiselet J, Lathrop M, Petit C et al. 2002. A novel locus for Usher syndrome type I, USH1G, maps to chromosome 17q24-25. *Hum.Genet.* 110:348-350.
31. Kalay E, de Brouwer AP, Caylan R, Nabuurs SB, Wollnik B, Karaguzel A, Heister JG, Erdol H, Cremers FP, Cremers CW et al. 2005. A novel D458V mutation in the SANS PDZ binding motif causes atypical Usher syndrome. *J.Mol.Med.* 83:1025-1032.
32. Ouyang XM, Yan D, Du LL, Hejtmancik JF, Jacobson SG, Nance WE, Li AR, Angeli S, Kaiser M, Newton V et al. 2005. Characterization of Usher syndrome type I gene mutations in an Usher syndrome patient population. *Hum.Genet.* 116:292-299.
33. Bashir R, Fatima A, Naz, S 2010. A frameshift mutation in SANS results in atypical Usher syndrome. *Clin.Genet.* 78:601-603.
34. Bonnet C, Grati M, Marlin S, Levilliers J, Hardelin JP, Parodi M, Niasme-Grare M, Zelenika D, Delepine M, Feldmann D et al. 2011. Complete exon sequencing of all known Usher syndrome genes greatly improves molecular diagnosis. *Orphanet.J.Rare Dis.* 6:21.
35. Rizel L, Safieh C, Shalev SA, Mezer E, Jabaly-Habib H, Ben Neriah Z, Chervinsky E, Briscoe D, Ben Yosef, T 2011. Novel mutations of MYO7A and USH1G in Israeli Arab families with Usher syndrome type 1. *Mol.Vis.* 17:3548-3555.
36. Imtiaz F, Taibah K, Bin-Khamis G, Kennedy S, Hemidan A, Al Qahtani F, Tabbara K, Al Mubarak B, Ramzan K, Meyer BF et al. 2012. USH1G with unique retinal findings caused by a novel truncating mutation identified by genome-wide linkage analysis. *Mol.Vis.* 18:1885-1894.
37. Hirabayashi S, Nishimura W, Iida J, Kansaku A, Kishida S, Kikuchi A, Tanaka N, Hata Y 2004. Synaptic scaffolding molecule interacts with axin. *J.Neurochem.* 90:332-339.
38. Min W, Lin Y, Tang S, Yu L, Zhang H, Wan T, Luhn T, Fu H, Chen H 2008. AIP1 recruits phosphatase PP2A to ASK1 in tumor necrosis factor-induced ASK1-JNK activation. *Circ.Res.* 102:840-848.

39. Trojan P, Rausch S, Giessl A, Klemm C, Krause E, Pulvermuller A, Wolfrum U 2008. Light-dependent CK2-mediated phosphorylation of centrins regulates complex formation with visual G-protein. *Biochim.Biophys.Acta* 1783:1248-1260.
40. Kirchhausen T, Macia E, Pelish HE 2008. Use of dynasore, the small molecule inhibitor of dynamin, in the regulation of endocytosis. *Methods Enzymol.* 438:77-93.
41. Hollander BA, Liang M-Y, Besharse JC 1999. Linkage of a nucleolin-related protein and casein kinase II with the detergent-stable photoreceptor cytoskeleton. *Cell Motil.Cytoskel.* 43:114-127.
42. Chimura T, Launey T, Ito M 2011. Evolutionarily conserved bias of amino-acid usage refines the definition of PDZ-binding motif. *BMC Genomics* 12:300.
43. Ivarsson Y 2012. Plasticity of PDZ domains in ligand recognition and signaling. *FEBS Lett.* 586:2638-2647.
44. Qiao F and Bowie JU 2005. The many faces of SAM. *Sci.STKE.* 286:re7.
45. Lee HJ and Zheng JJ 2010. PDZ domains and their binding partners: structure, specificity, and modification. *Cell Commun.Signal.* 8:8.
46. Caberlotto E, Michel V, Foucher I, Bahloul A, Goodyear RJ, Pepermans E, Michalski N, Perfettini I, Alegria-Prevot O, Chardenoux S et al. 2011. Usher type 1G protein sans is a critical component of the tip-link complex, a structure controlling actin polymerization in stereocilia. *Proc.Natl.Acad.Sci.USA* 108:5825-5830.
47. Clement CA, Ajbro KD, Koefoed K, Vestergaard ML, Veland IR, Henriques de Jesus MP, Pedersen LB, Benmerah A, Andersen CY, Larsen LA et al. 2013. TGF-beta signaling is associated with endocytosis at the pocket region of the primary cilium. *Cell Rep.* 3:1806-1814.
48. Ghossoub R, Hu Q, Failler M, Rouyez MC, Spitzbarth B, Mostowy S, Wolfrum U, Saunier S, Cossart P, Jamesnelson W et al. 2013. Septins 2, 7 and 9 and MAP4 colocalize along the axoneme in the primary cilium and control ciliary length. *J.Cell Sci.* 126:2583-2594.
49. Kaplan OI, Doroquez DB, Cevik S, Bowie RV, Clarke L, Sanders AA, Kida K, Rappoport JZ, Sengupta P, Blacque OE 2012. Endocytosis genes facilitate protein and membrane transport in C. elegans sensory cilia. *Curr.Biol.* 22:451-460.
50. Liu AP, Aguet F, Danuser G, Schmid SL 2010. Local clustering of transferrin receptors promotes clathrin-coated pit initiation. *J.Cell Biol.* 191:1381-1393.
51. Hinrichsen L, Harborth J, Andrees L, Weber K, Ungewickell EJ 2003. Effect of clathrin heavy chain- and alpha-adaptin-specific small inhibitory RNAs on endocytic accessory proteins and receptor trafficking in HeLa cells. *J.Biol.Chem.* 278:45160-45170.
52. Davis AA and Hunt RC 1993. Transferrin is made and bound by photoreceptor cells. *J.Cell Physiol.* 156:280-285.
53. Ponka, P 1999. Cellular iron metabolism. *Kidney Int.Suppl.* 69:S2-11.
54. Yefimova MG, Jeanny JC, Keller N, Sergeant C, Guillonneau X, Beaumont C, Courtois Y 2002. Impaired retinal iron homeostasis associated with defective phagocytosis in Royal College of Surgeons rats. *Invest.Ophthalmol.Vis.Sci.* 43:537-545.
55. He X, Hahn P, Iacovelli J, Wong R, King C, Bhisitkul R, Massaro-Giordano M, Dunaief JL 2007. Iron homeostasis and toxicity in retinal degeneration. Prog.Retin.Eye Res. 26:649-673.
56. Wang ZJ, Lam KW, Lam TT, Tso MO 1998. Iron-induced apoptosis in the photoreceptor cells of rats. *Invest.Ophthalmol.Vis.Sci.* 39:631-633.
57. Picard E, Ranchon-Cole I, Jonet L, Beaumont C, Behar-Cohen F, Courtois Y, Jeanny JC 2011. Light-induced retinal degeneration correlates with changes in iron metabolism gene expression, ferritin level, and aging. *Invest.Ophthalmol.Vis.Sci.* 52:1261-1274.
58. Jin H, White SR, Shida T, Schulz S, Aguiar M, Gygi SP, Bazan JF, Nachury MV 2010. The conserved Bardet-Biedl syndrome proteins assemble a coat that traffics membrane proteins to cilia. *Cell* 141:1208-1219.
59. Nachury MV, Seeley ES, Jin H 2010. Trafficking to the ciliary membrane: how to get across the periciliary diffusion barrier? *Annu.Rev.Cell Dev.Biol.* 26:59-87.
60. Tsang WY and Dynlacht BD 2013. CP110 and its network of partners coordinately regulate cilia assembly. *Cilia* 2:9.

61. Giessl A, Trojan P, Pulvermüller A, Wolfrum U 2004. Centrins, potential regulators of transducin translocation in photoreceptor cells. In: Williams DS, ed., *Cell Biology and Related Disease of the Outer Retina.* World Scientific Publishing Company Pte Ltd, Singapore. 195-222.
62. Peterson JJ, Tam BM, Moritz OL, Shelamer CL, Dugger DR, McDowell JH, Hargrave PA, Papermaster DS, Smith WC 2003. Arrestin migrates in photoreceptors in response to light: a study of arrestin localization using an arrestin-GFP fusion protein in transgenic frogs. *Exp.Eye Res.* 76:553-563.
63. Letteboer SJ and Roepman R 2008. Versatile screening for binary protein-protein interactions by yeast two-hybrid mating. *Methods Mol.Biol.* 484:145-159.
64. Violin JD, Zhang J, Tsien RY, Newton AC 2003. A genetically encoded fluorescent reporter reveals oscillatory phosphorylation by protein kinase C. *J.Cell Biol.* 161:899-909.
65. Li JB, Gerdes JM, Haycraft CJ, Fan Y, Teslovich TM, May-Simera H, Li H, Blacque OE, Li L, Leitch CC et al. 2004. Comparative genomics identifies a flagellar and basal body proteome that includes the BBS5 human disease gene. *Cell* 117:541-552.
66. Wolfrum U 1991. Centrin- and a-actinin-like immunoreactivity in the ciliary rootlets of insect sensilla. *Cell Tissue Res.* 266:231-238.
67. Weibrecht I, Leuchowius KJ, Clausson CM, Conze T, Jarvius M, Howell WM, Kamali-Moghaddam M, Soderberg O 2010. Proximity ligation assays: a recent addition to the proteomics toolbox. *Expert.Rev.Proteomics.* 7:401-409.
68. Sedmak T, Sehn E, Wolfrum U 2009. Immunoelectron microscopy of vesicle transport to the primary cilium of photoreceptor cells. *Methods Cell Biol.* 94:259-272.

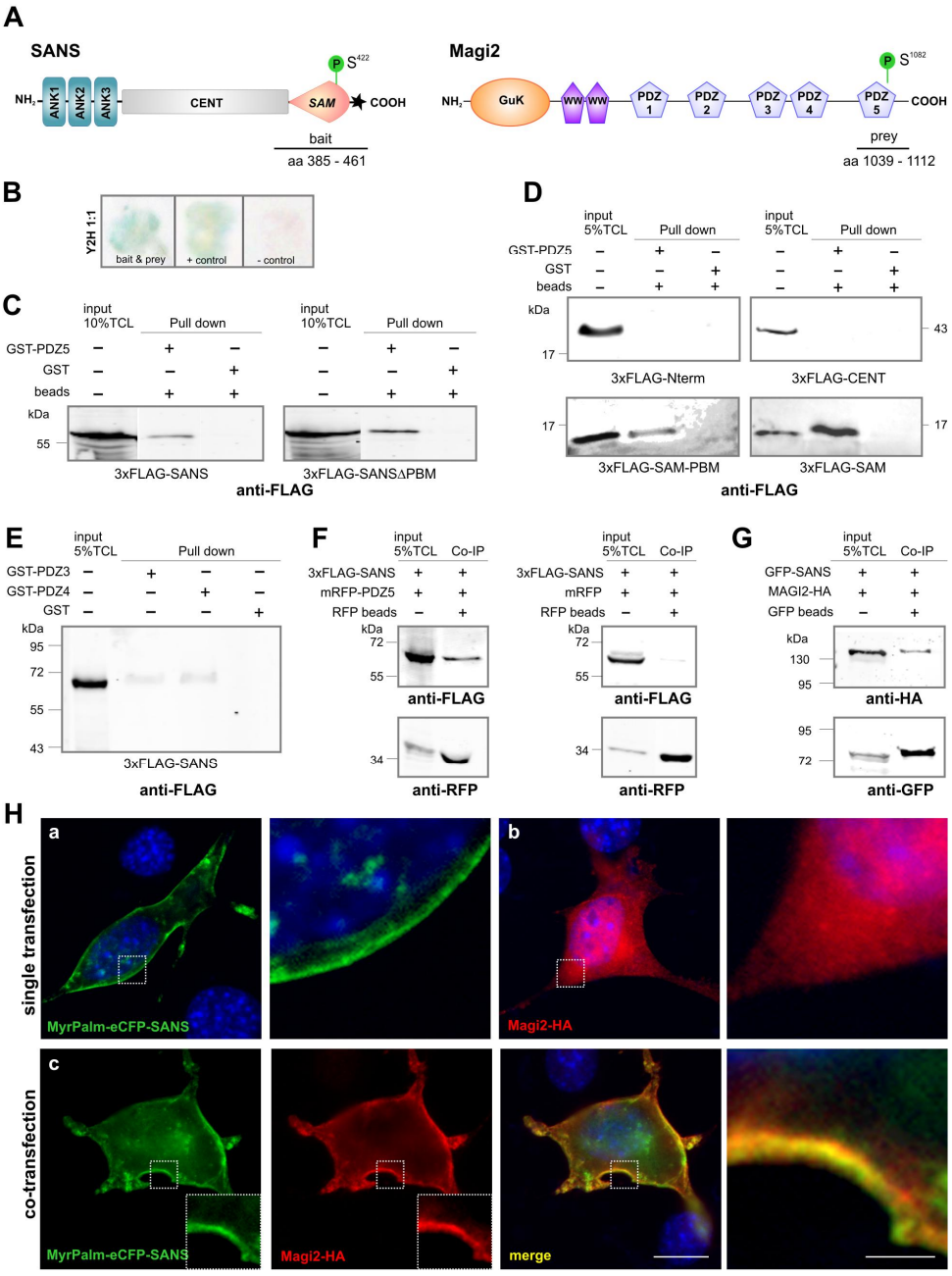

Figure 1 Validation of the direct interaction between SANS and Magi2: (A) Domain structure schemes SANS is composed of ANK (ankyrin-repeats), CENT (central domain), SAM (sterile alpha motif) and a C-terminal PBM (PDZ-binding motif, *asterisk*). Magi2 is characterized by GuK (guanylate kinase), PDZ1-5 domains and WW (tryptophan) repeats. P: predicted phosphorylation sites (SANS S^{422}, Magi S^{1082}). **(B) Yeast-2-hybrid:** lines indicate bait and identified prey. **(C-E) GST-Pull downs: (C)** FLAG-tagged SANS full length with (3xFLAG-SANS) and without PBM (3xFLAG-SANSΔPBM) were assayed with immobilized GST-PDZ5 or GST alone. Western blots revealed recovery of SANS irrespective of the PBM. **(D)** SANS´ N-terminus (3xFLAG-Nterm), central domain (3xFLAG-CENT), and C-terminus with/without PBM (3xFLAG-SAM-PBM/3xFLAG-SAM) were assayed. Recovery was restricted to SANS C-terminus irrespective of PBM. **(E)** Recovery of FLAG-tagged SANS full length assayed with GST-PDZ3 and 4 of Magi2 failed. **(F, G) Trap® assays: (F)** 3xFLAG-SANS was assayed with immobilized mRFP-PDZ5. SANS was co-precipitated with Magi2-PDZ5. **(G)** Magi2-HA was assayed with immobilized GFP-SANS. Magi2 was co-precipitated with SANS. **(H) Membrane targeting assay:** IMCD3 cells were singly **(a; b)** or co-transfected **(c)** with eCFP-tagged SANS N-terminally fused to a membrane-anchoring signal (MyrPalm-eCFP-SANS) or/and Magi2 C-terminally HA-tagged (Magi2-HA). **(a)** IMCD3 cells singly-transfected with MyrPalm-eCFP-SANS (green) showed SANS enriched at the plasma membrane. **(b)** Cells single-transfected with Magi2-HA (red) showed a perinuclear, cytoplasmic staining. **(c)** In co-transfected cells Magi2 co-localised with SANS (yellow). Nuclei were stained with DAPI. Scale bars, 10/2.5 µm. TCL: total cell lysate.

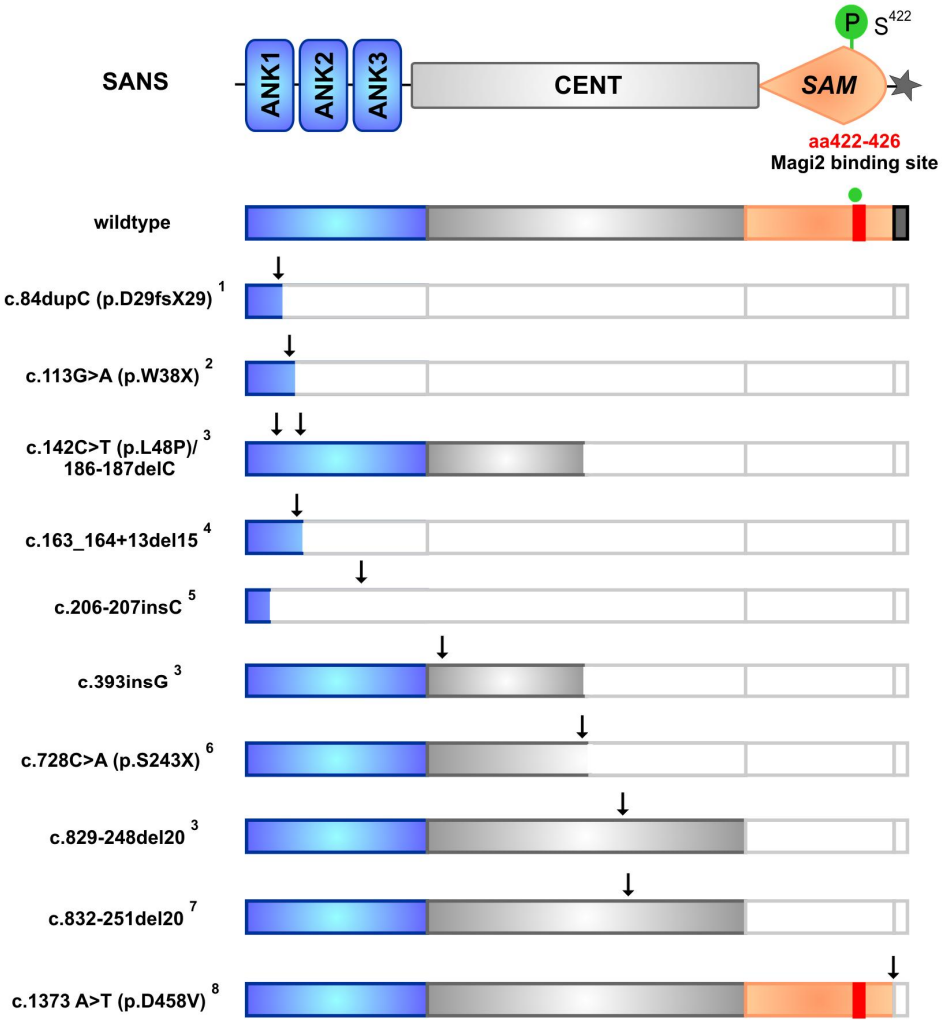

Figure 2: Schematic representation of the pathogenic mutations identified in the USH1G gene *SANS*: SANS domain structure: blue, ankyrin repeats (ANK1-3); grey, central domain (CENT); orange, SAM domain; C-terminal PBM, asterisk. Magi2 binding site and are indicated in red or green, respectively. Identified variations are designated with an arrow and displaying the resulted change in the SANS molecules. References: 1=(34); 2=(32); 3=(17); 4=(33); 5=(35); 6=(36); 7=(30); 8=(31).

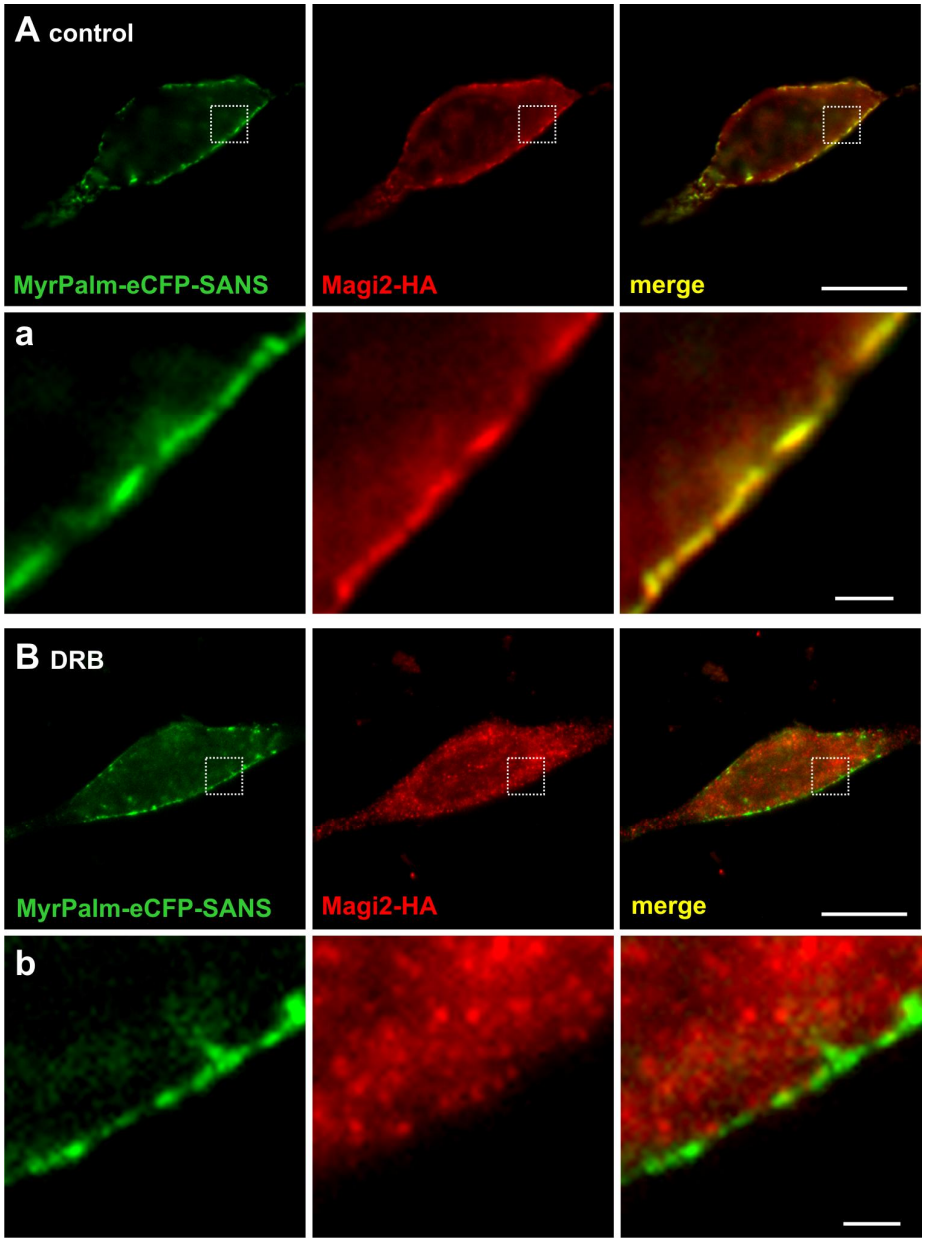

Figure 3: Phosphorylation dependency of SANS-Magi2 interaction in IMCD3 cells: (A) Cells were co-transfected with MyrPalm-eCFP-SANS and Magi2-HA and incubated either with DMSO as control or with D-ribofuranosyl-benzimidazole (DRB). **(A, a)** Immunocytochemistry of DMSO treated IMCD3 cells co-transfected with MyrPalm-eCFP-SANS (green) and Magi2-HA (red) revealed the recruitment of Magi2 towards the cell membrane. In the high magnification the co-localization of Magi2-HA with MyrPalm-eCFP-SANS at the membrane was demonstrated (yellow). **(B, b)** In co-transfected cells incubated with DRB no altered localization of Magi2-HA could be detected. High magnification image showed no co-localization of Magi2-HA with MyrPalm-eCFP-SANS at the cell membrane. Scale bars, 10/1 µm.

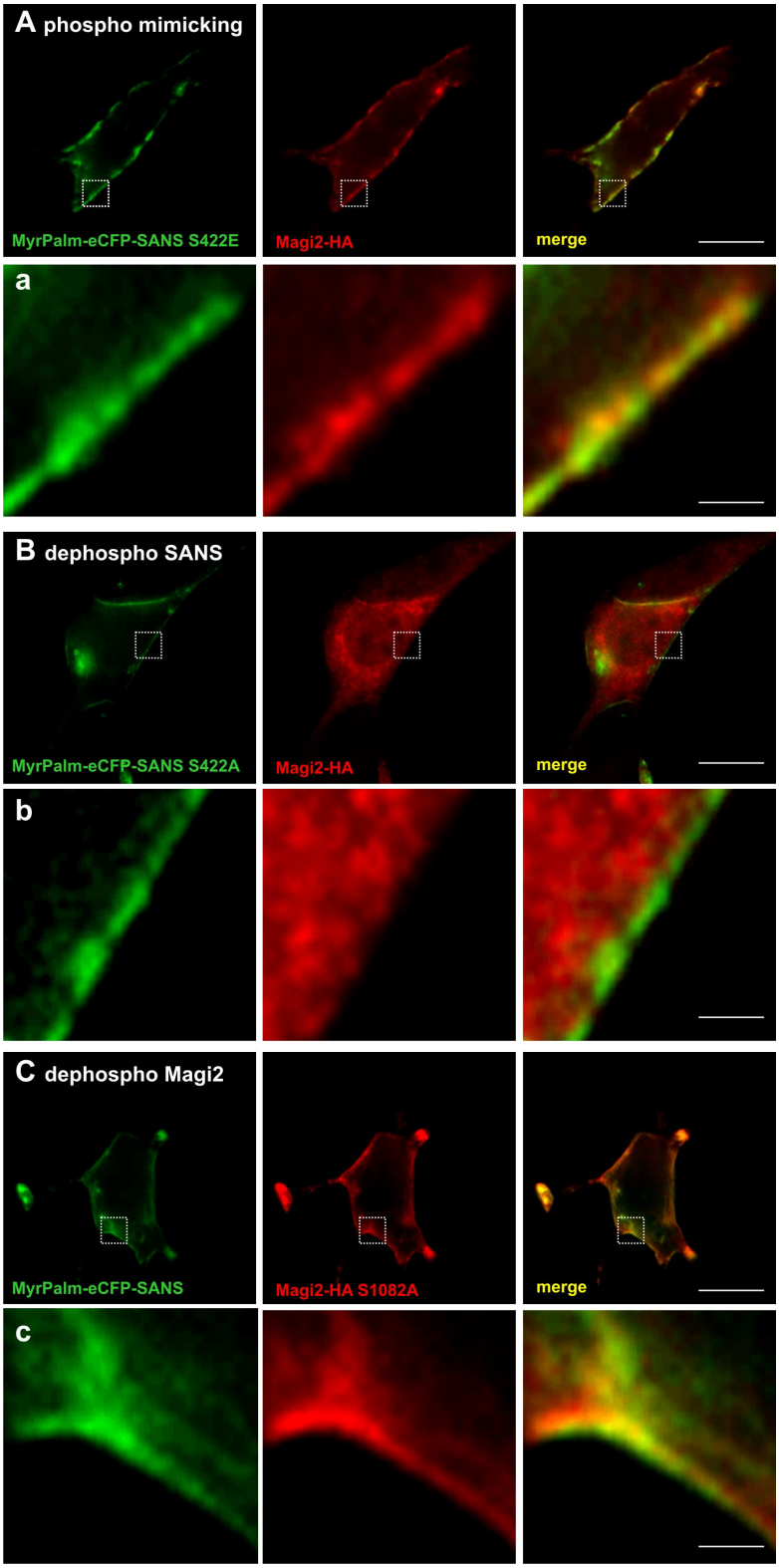

Figure 4: Phosphorylation dependency of SANS-Magi2 interaction in cells transfected with phospho-/dephospho constructs: (A) IMCD3 cells were co-transfected with a phospho-mimicking (serine mutated to glutamic acid) SANS construct (MyrPalm-eCFP-SANS S422E, green) and wild-type Magi2-HA (red). **(a)** High magnification revealed recruitment of Magi2 to the plasma membrane (yellow). **(B)** Cells were co-transfected with the dephospho (serine mutated to alanine) SANS construct MyrPalm-eCFP-SANS S422A (green) and wild-type Magi2-HA (red). **(b)** High magnification demonstrated that Magi2 was no longer recruited to the membrane. **(C)** Cells were co-transfected with wild-type SANS (MyrPalm-eCFP-SANS, green) and a dephospho Magi2 construct (Magi2-HA S1082A, red, serine mutated to alanine). **(c)** High magnification demonstrates that Magi2 was still recruited towards SANS at the membrane (yellow). Scale bars, 10/1 µm.

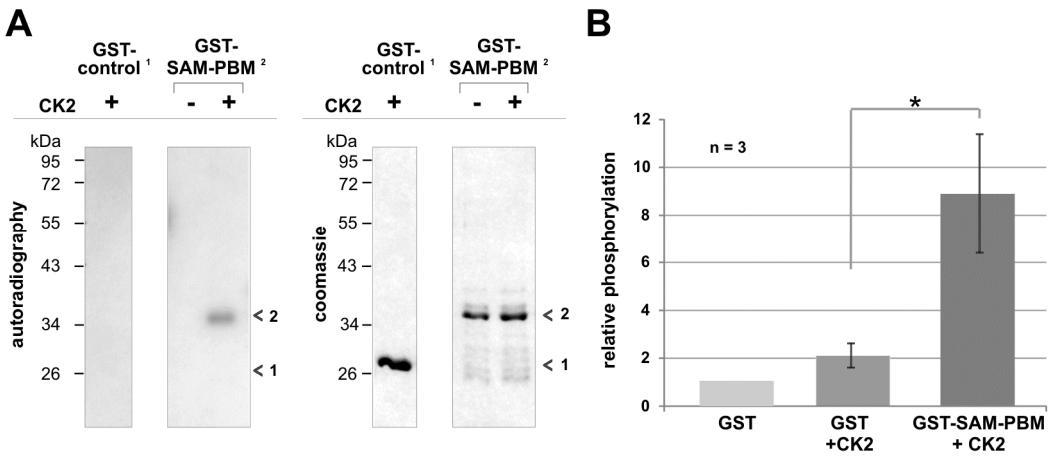

Figure 5: SANS´ C-terminus is phosphorylated by protein kinase CK2: (A) Purified recombinant GST (1) as control or GST-tagged SAM-PBM of SANS (2) were incubated with active CK2 and [γ^{32}P]-ATP. Kinase reaction mixtures were analyzed by SDS-PAGE and autoradiography. Input was determined by coomassie staining (A, left panels). **(B)** Quantification of the radioactivity incorporation using a scintillation counter demonstrated a significant about 4-fold increase in phosphorylation of GST-SAM-PBM compared to GST alone (SD ±2.49, n=3, p-value 0.027).

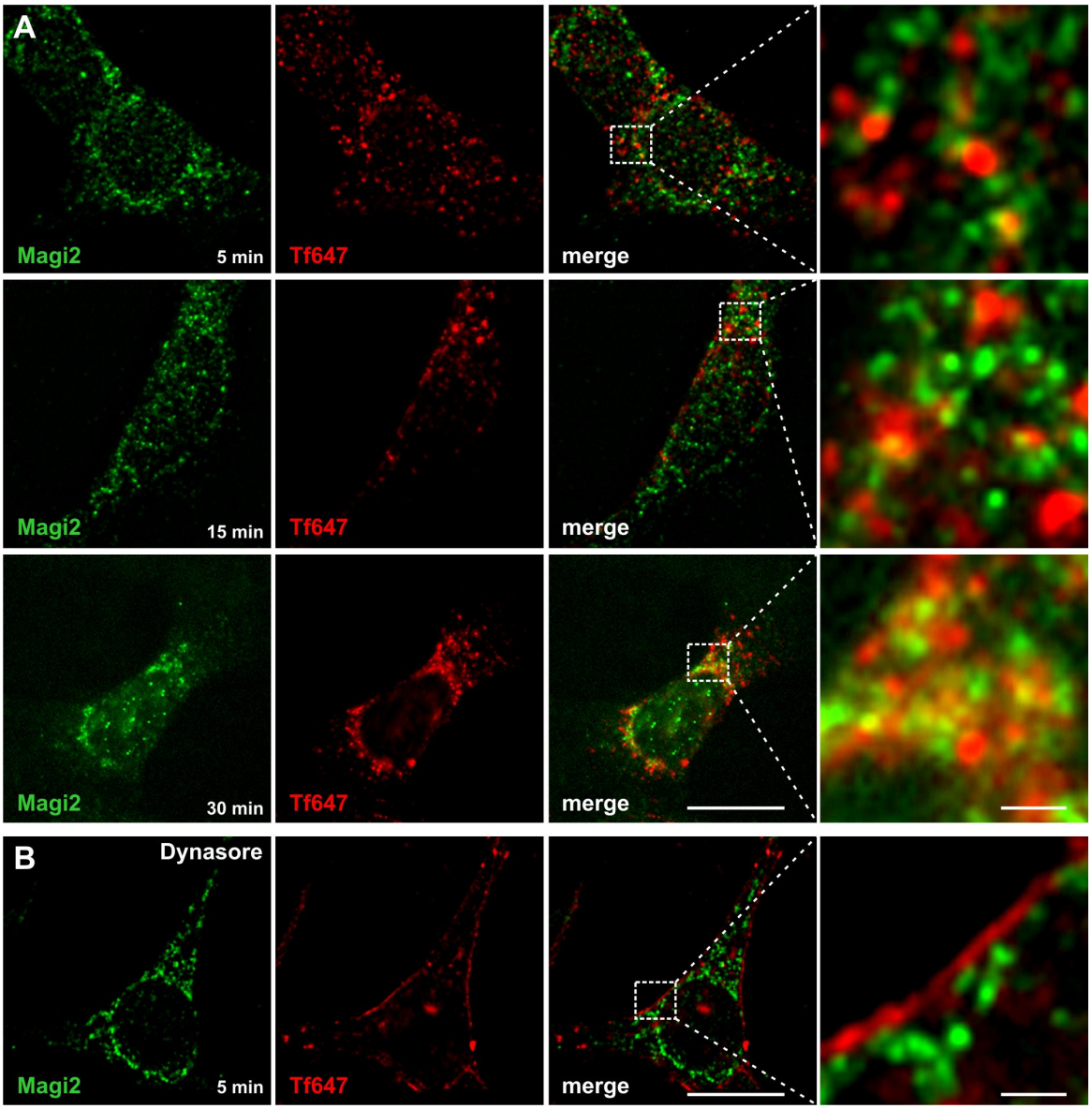

Figure 6: Association of Magi2 with transferrin positive vesicles in IMCD3 cells: (A) Uptake of Alexa647 labelled transferrin (Tf647, red) by IMCD3 cells was fluorescent microscopically monitored during a time course of 5, 15 and 30 min, counterstained with anti-Magi2 (green). Magi2 was associated with Tf647 vesicles after 5 min of endocytotic uptake and accumulates with Tf647 within 30 min in the perinuclear cytoplasm. **(B)** In cells treated with the GTPase inhibitor dynasore uptake of Tf647 was inhibited. Tf647 remained at the plasma membrane and Magi2 was localised in the cytoplasm. Scale bars, 10/1 µm.

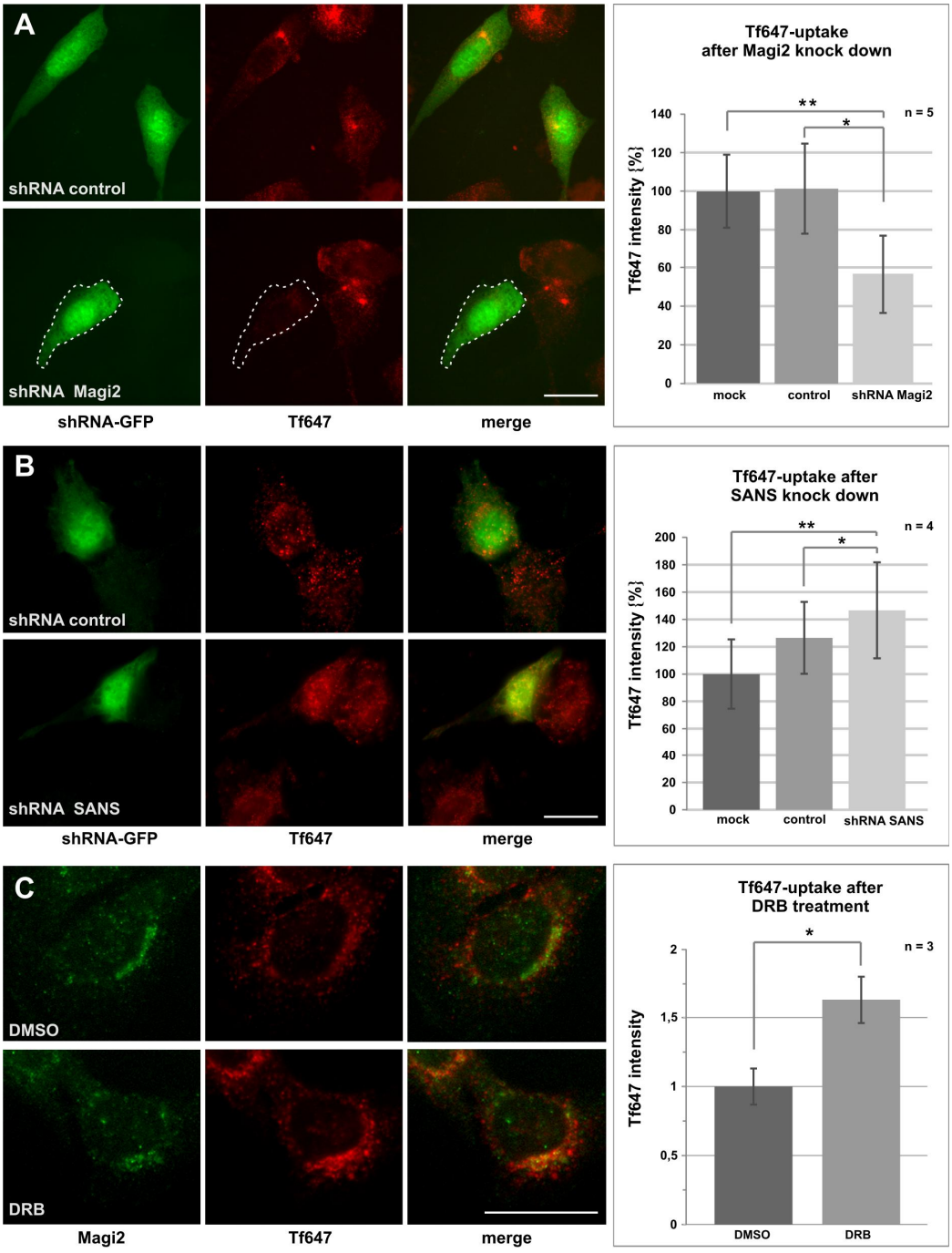

Figure 7: Endocytosis of transferrin is facilitated by Magi2, but decreased by SANS and phosphorylation: **(A)** Tf647 uptake (red) was monitored in IMCD3 cells transfected with scrambled shRNA control (green, upper panel) or shRNA against Magi2 (green, lower panel). Knock down of Magi2 diminished endocytosis of Tf647. Quantification of the mean fluorescence intensity of Tf647, normalized to mock transfected cells revealed significant ~57% decrease of endocytosis (SD ±20.23%, n=5, p-value 0.001) in cells transfected with shRNA-Magi2 compared to cells transfected with scrambled shRNA (101%, SD ±23.35%, p-value 0.032). **(B)** Tf647 uptake was monitored in cells transfected with scrambled shRNA control or shRNA against SANS. Knock down of SANS increased endocytosis of Tf647. Cytochemistry of Tf647 uptake in shRNA-transfected IMCD3 cells shows SANS-dependent endocytosis. Quantification of the mean fluorescence intensity of Tf647, normalized to mock transfected cells revealed a significant ~46% increase of endocytosis (SD ±35.10%, n=4, p-value 0.01) in cells transfected with shRNA-SANS compared to cells transfected with control shRNA (126%, SD ±26.26%, p-value 0.043). **(C)** Tf647 uptake was monitored in IMCD3 cells treated with kinase inhibitor DRB revealing phosphorylation-dependent decrease of endocytosis. Magi2 staining (green) illustrated the association with Tf647. Quantification of the mean fluorescence intensity of Tf647, normalized to control revealed significant 1.63-fold increase of endocytosis (SD ±0.1310, n=3, p-value 0.012) in cells treated with DRB compared to cells treated with DMSO (SD ±0.171). Scale bar, 10 µm.

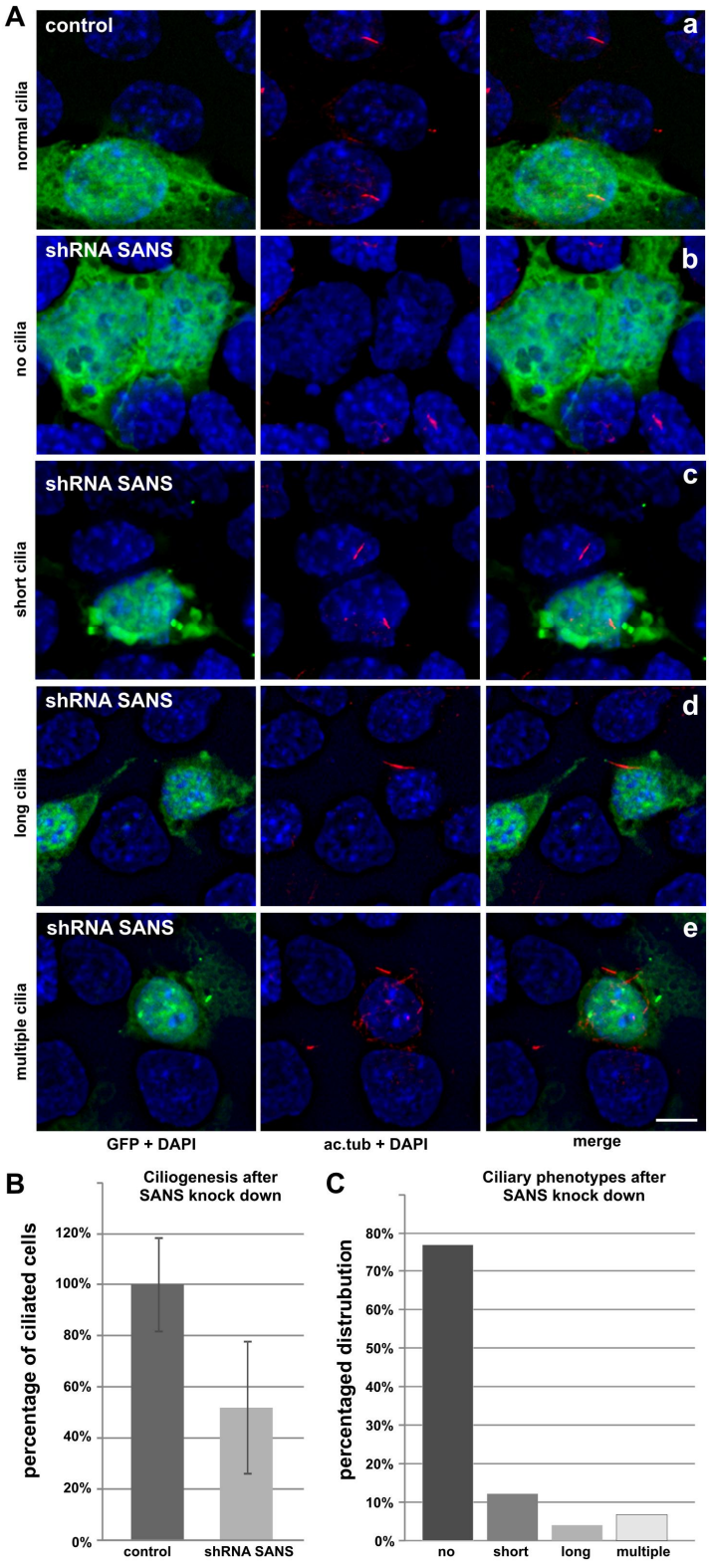

Figure 8: Ciliogenesis is affected by knock down of SANS: (A) Immunocytochemical staining of cilia by antibodies against acetylated tubulin (ac.tub, red) of starved IMCD3 cells transfected with empty shRNA (**a** control, green) or shRNA against SANS (**b-e**, green). Knock down of SANS led to diverse phenotypes: no cilia (**b**), short **(c)**, long **(d)** or multiple cilia **(e)**. **(B)** Quantification of ciliated cells revealed that knock down of SANS diminished number of cells with a primary cilium to 52% normalized to control. **(C)** Quantification of ciliary phenotypes after knock down of SANS revealed that most of the transfected cells (77%) assembled no cilia. The few emerging cilia (23%) showed a ciliary phenotype: 12.2% respectively 4.1% of transfected cells assembled a short (1.15 µm; SD ±0.31) or long cilium (3.60 µm; SD± 1.12) compared to control (1.88 µm; SD ±0.41). 6.8% of the transfected cells had multiple cilia. Scale bars, 5 µm.

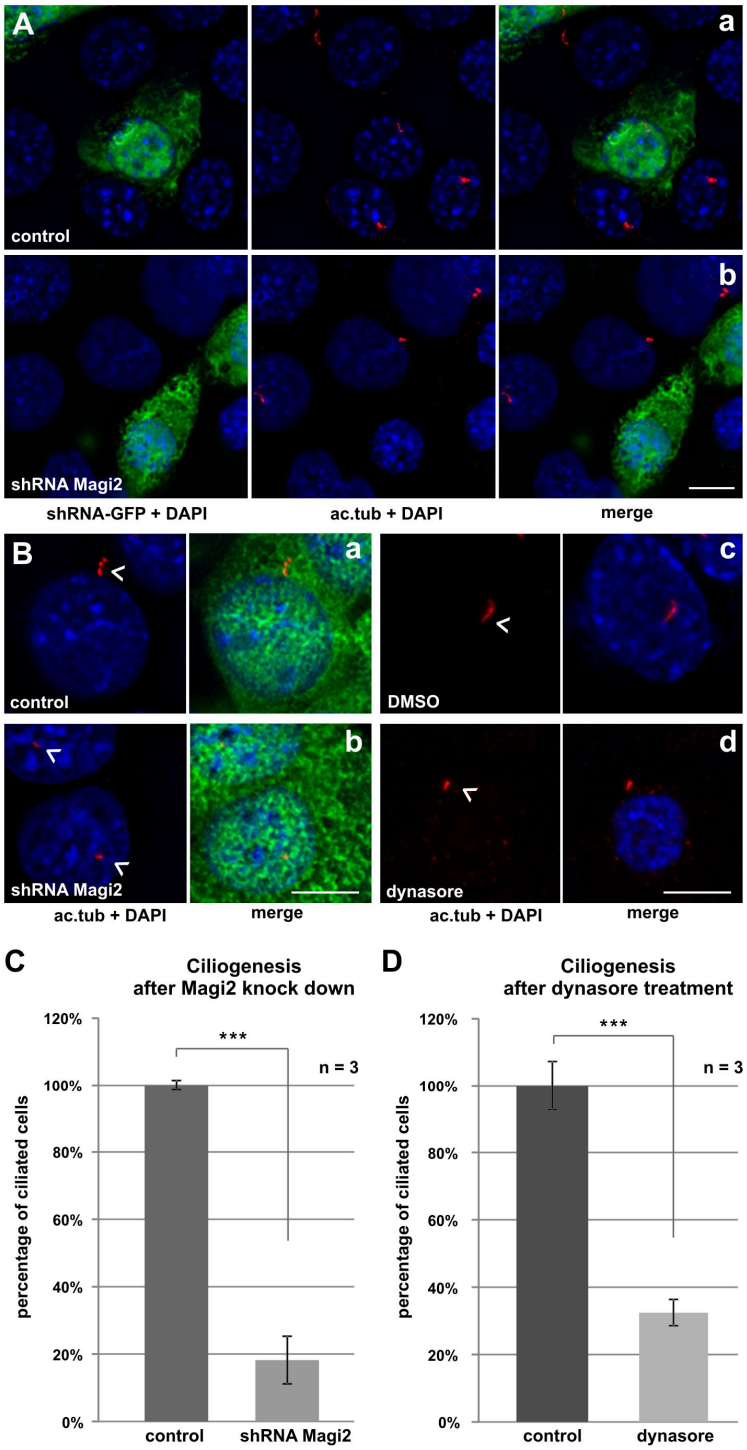

Figure 9: Ciliogenesis is influenced by Magi2 and depends on endocytosis: (A) Immunocytochemical staining of cilia by antibodies against acetylated tubulin (ac.tub, red) of starved IMCD3 cells transfected with empty scrambled shRNA (control, green, upper panel) or shRNA against Magi2 (green, lower panel). Knock down of Magi2 diminished number of cells with a primary cilium. **(B)** Analysis of the ciliary shape of starved IMCD3 cells transfected with shRNA **(b)** or treated with the dynamin-inhibitor dynasore **(d)** revealed that the few emerging primary cilia in shRNA Magi2-transfected as well as in dynasore-treated cells are shortened (0.73 µm, SD ±0.04/0.76 µm, SD ±0.07) compared to controls (1.28 µm, SD ±0.24/1.73 µm, SD ±0.40). **(C)** Quantification of the total number of primary cilia in three independent experiments revealed the highly significant decrease of ciliogensis down to 18% (SD ±7.09%, n=3, p-value 0,000001) in cells transfected with shRNA Magi2, normalized to control transfected cells with scrambled shRNA (100%, SD ±1.47%). **(D)** Quantification of the total number of primary cilia in three independent experiments revealed the highly significant decrease of ciliogensis down to 32% (SD ±3.9%, n=3, p-value 0,0003) in cells treated with dynasore compared to DMSO treated controls (100%, SD ±7.27%). Scale bars, 5 µm.

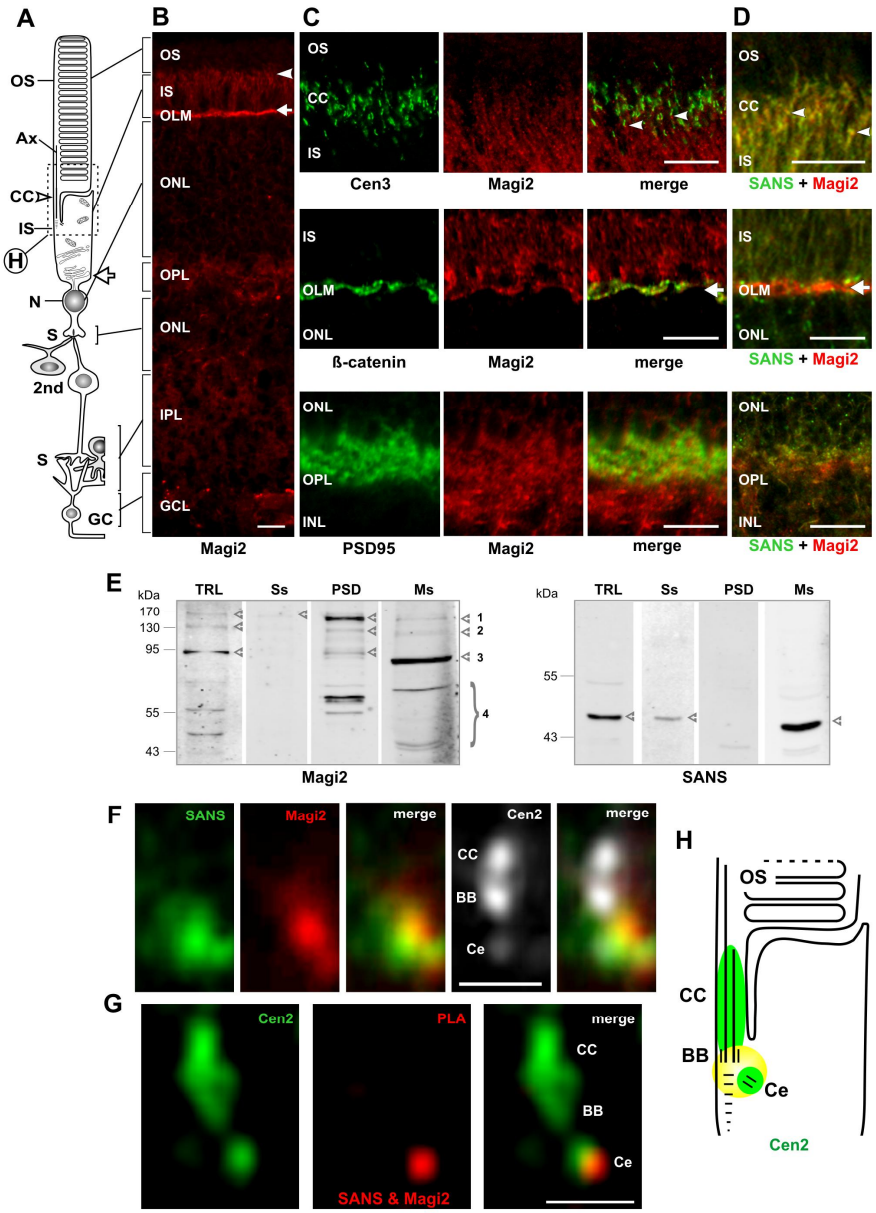

Figure 10: *In situ* localization of Magi2 and SANS-Magi2 in photoreceptor cells of murine retina: (A) Schematic representation of a rod photoreceptor cell. Ax: axoneme, CC: connecting cilium (*arrow head*), IS: inner segment, N: nucleus, OS: outer segment, S: synapses, 2nd: secondary neurons. **(B) Indirect immunofluorescence** demonstrated Magi2 (red) localization in the IS, at the outer limiting membrane (OLM, *arrow*), at synapses (S) of outer and inner plexiform layer (OPL/IPL) and in the ganglion cell layer (GCL) of mouse retina. **(C) Double-labelling** of Magi2 and compartmental marker proteins. Merged image with centrin (Cen3, green) revealed overlapping staining at the CC base. Merged image with the cell adhesion marker β-catenin showed little overlap in the OLM. Merged image with PSD-95 as pre-synaptic marker in the retina revealed little double staining in the OPL. **(D) Double-labelling** of Magi2 (red) and SANS (green) in retinal sub-compartments. Magi2 and SANS were localised in the IS predominantly at the base of the CC (*arrowhead*). **(E) Western blot analyses** of synaptic fractionation of bovine retinas. Magi2 antibodies detected three bands of about 150, 130 and 95 kDa, corresponding to the 3 Magi2 isoforms (*arrowheads*) previously described in mammals, and several bands of lower molecular weight (4, brace) in total retinal lysate (TRL), the post-synaptic density (PSD) and the micorosome fraction (Ms). In PSD variant 1 was most abundant isoform. In the synaptosomal fraction (Ss) only faint bands of high molecular variants were detected. In Ms, isoform 3 is the most abundant. Antibodies detected SANS with a molecular weight of about 50 kDa in TRL, Ss and Ms, but not in PSD. **(F) Triple-labelling** of SANS, Magi2 and centrin-2 (Cen2) revealed the localization of SANS and Magi2 at the base of the CC. **(G)** Proximity ligation assay (PLA) demonstrated the SANS-Magi2 complex at the ciliary base *in situ*; **(H) Schematic illustration of SANS-Magi2 complex localization** in the ciliary region of a rod photoreceptor cell (yellow). BB, basal body; Ce, adjacent centriole. Scale bars, B 10 µm; C/D 5 µm; F/G 1 µm.

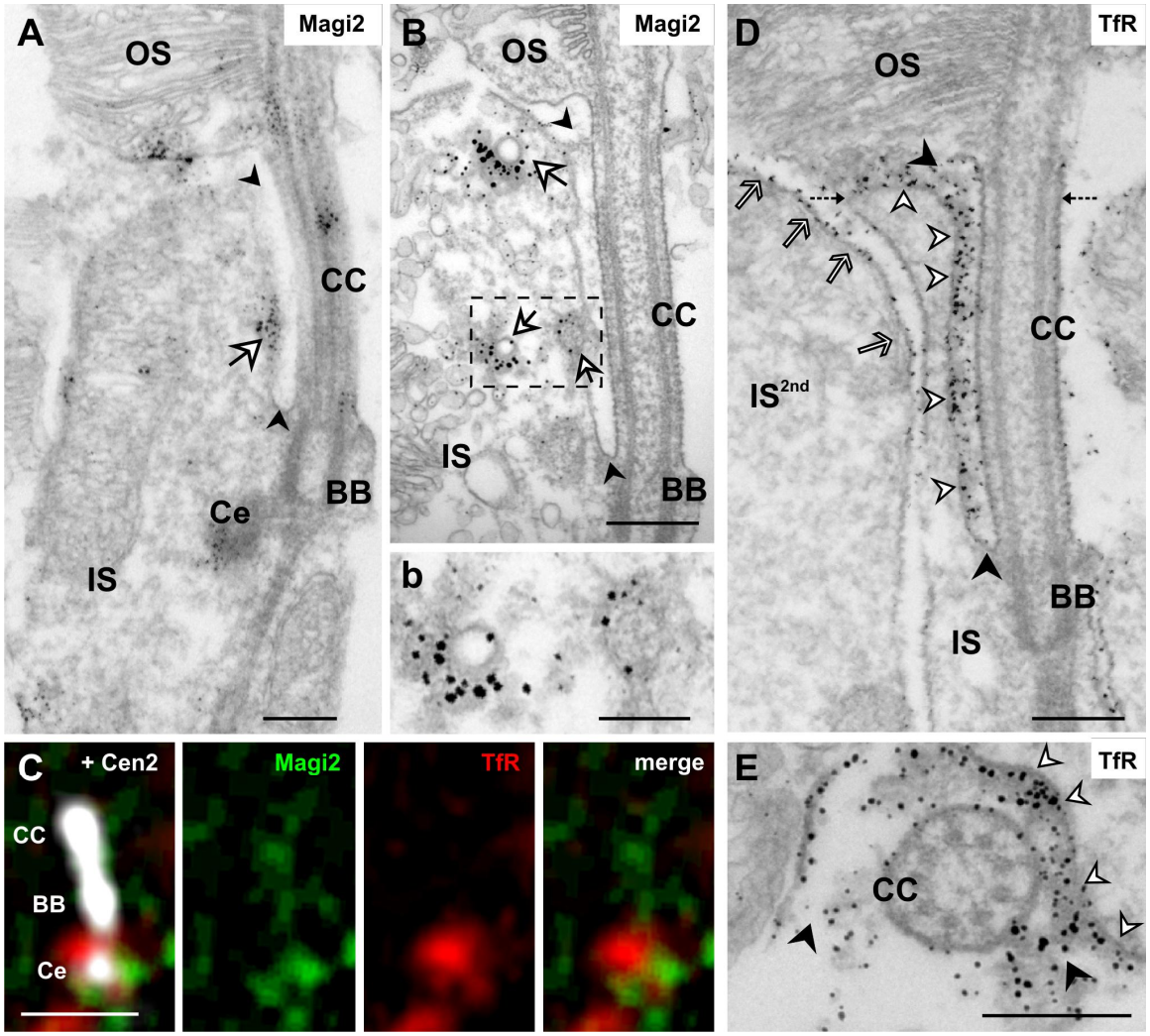

Figure 11: Subcellular localization of Magi2 and transferrin receptor (TfR) in mouse photoreceptor cells: (A, B) Immunoelectron analysis of Magi2 localization on longitudinal sections through parts of mouse rod photoreceptor cells. Magi2 was detected at the outer segment (OS) base, in the connecting cilium (CC), the adjacent centriole (Ce) and the inner segment (IS). **(B) Electron micrograph** demonstrating the association of Magi2 with vesicles in the periciliary compartment of the apical IS (*white arrows*). **(b)** Higher magnification of Magi2-labelling associated with vesicles. **(C) Triple-labelling** of Magi2, TfR and centrin-2 (Cen2) showed localization of Magi2 and TfR at the base of the CC. **(D) Immunoelectron microscopy** analyses of TfR localization in a longitudinal section through the periciliary region of a mouse photoreceptor cell demonstrated TfR decoration at membranes of the apical inner segment (*arrows*) and the membrane (*white arrowheads*) of the ciliary pocket indicated by *black arrowheads*. **(E) Immunoelectron microscopy** of the cross section through the CC showed accumulation of TfR labelling in the ciliary pocket. Scale bars, A/B/D/E 0.25 µm; C 1 µm.

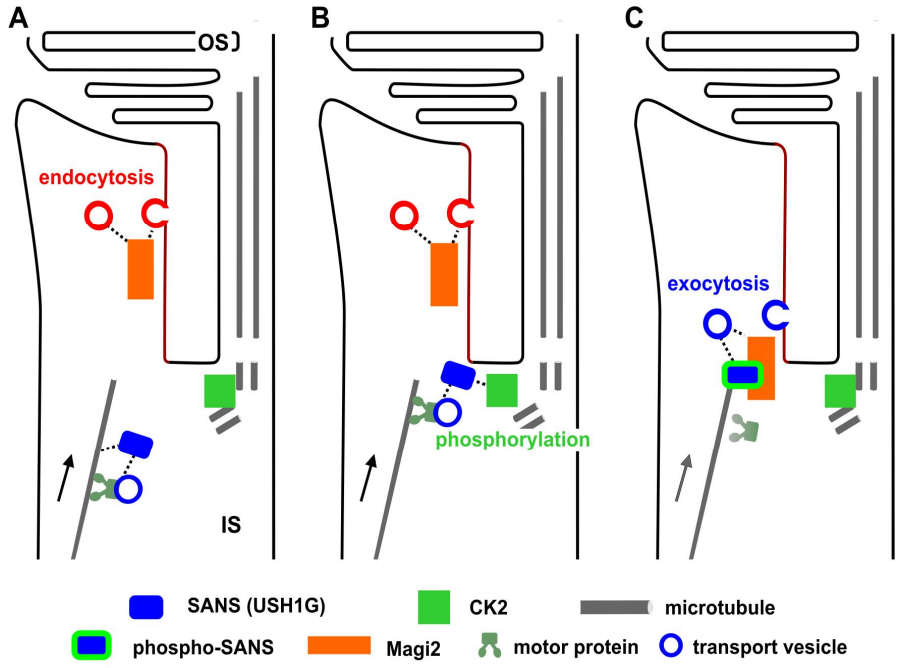

Figure 12: Model for the SANS-Magi2 complex function in the periciliary region of photoreceptor cells: (A) Magi2 molecules mediate **endocytosis** from the ciliary pocket. SANS is associated with vesicular cargo transport through the cytoplasm of the inner segment (IS) towards the ciliary base. **(B)** In the periciliary region, SANS is **phosphorylated** by protein kinase CK2 increasing its affinity to Magi2. **(C)** Phosphorylated SANS recruits Magi2 from the endocytosis module of the ciliary pocket and facilitates cargo vesicle targeting to the periciliary membrane and thereby **exocytosis**. OS, outer segment.

Species	NCBI No.	Alignment of SAM domain sequences
H.sapiens	NP_775748	LEPETSPLETFLASLHMEDFAALLRQEKIDLEALMLC**SDLDL**RSISVPLGPRKKILGAVRRRRQA
P.troglodytes	XP_523715	LEPETSPLETFLASLHMEDFAALLRQEKIDLEALMLC**SDLDL**RSISVPLGPRKKILGAVRRRRQA
P.abelii	XP_002827857	LEPETSPLETFLASLHMEDFAALLRQEKIDLEALMLC**SDLDL**RSISVPLGPRKKILGAVRRRRQA
M.mulatta	XP_002800714	LEPETGPLETFLASLHMEDFAALLRQEKIDLEALMLC**SDLDL**RSISVPLGPRKKILGAVRRRRQA
B.taurus	NP_001179631	LEPETSPLETFLASLHMEDFTSLLRQEKIDLEALMLC**SDLDL**RSISVPLGPRKKILGAVRRRRQA
E.caballus	XP_001496907	LEPETSPLDTFLASLHMEDFASLLRQEKIDLEALMLC**SDLDL**RSISVPLGPRKKILGAVRRRRQA
S.scrofa	XP_003131267	LEPETSPLETFLASLHMEDFTPLLRQEKIDLEALMLC**SDLDL**RSISVPLGPRKKIMGAVRRRRQT
C.familiaris	XP_852112	LEPETSPLETFLASLHMEDFTSLLRQEKIDLEALMLC**SDLDL**RSISVPLGPRKKILGAVRRRRQA
F.catus	XP_003997185	LEPETSPLDTFLASLHMDDFASLLRQEKIDLEALMLC**SDLDL**RSISVPLGPRKKILGAVRRRRQA
M.musculus	NP_789817	LEPETSPLETFLASLHMEDFASLLRHEKIDLEALMLC**SDLDL**RSISVPLGPRKKILGAVRRRRQA
R.norvegicus	NP_001099320	LEPETSPLETFLASLHMEDFASLLRHEKIDLEALMLC**SDLDL**RSISVPLGPRKKILGAVRRRRQA
C.cristata	XP_004693537	LEPETSPLETFLASLHMEDFASLLRQEKIDLEALMLC**SDLDL**RSISVPLGPRKKIMGAVRRRRQA
C.porcellus	XP_003464875	LEPETSPLETFLASLHMEDFASLLRQEKIDLEALMLC**SDLDL**RSISVPLGPRKKILGAVRRRRQA
M.domestica	XP_001369718	LEPETSPLETFLASLHMDDFVALLRQEKIDLDALMLC**SELDL**HSISIPLGPRKKILGAIKRRRLV
X.tropicalis	XP_002939606 XP_004918531 XP_004918532	EEPDTSPLESFLASLQMGDLVTVLQDEKIDLAALTLC**SDHDL**KSIGIPLGPRKKILDGIQRRRQA
D.rerio	XP_002661315	DEPDTSPLEVFLATQSMNEFIPILKREKIDLDALLLC**SDNDL**KGIHIPLGPRKKIMDACMRRLET
G.gallus	XP_426242	DEPDSSPLETFLASLHMFEFISILKKEKIDLEALMLC**SDNDL**KSINIPLGPRKKIVDAIQRRRQT
M.undulates	XP_005144305	DEPDTSPLETFLASLHMFEFISILKKEKIDLEALMLC**SDNDL**KSINIPLGPRKKIVDAIQRRRQT

Table I: Sequence alignment revealed a conserved internal PDZ-binding motif (yellow) in the SAM domain of SANS from diverse vertebrate species.

Bauß et al., Supplemental Material

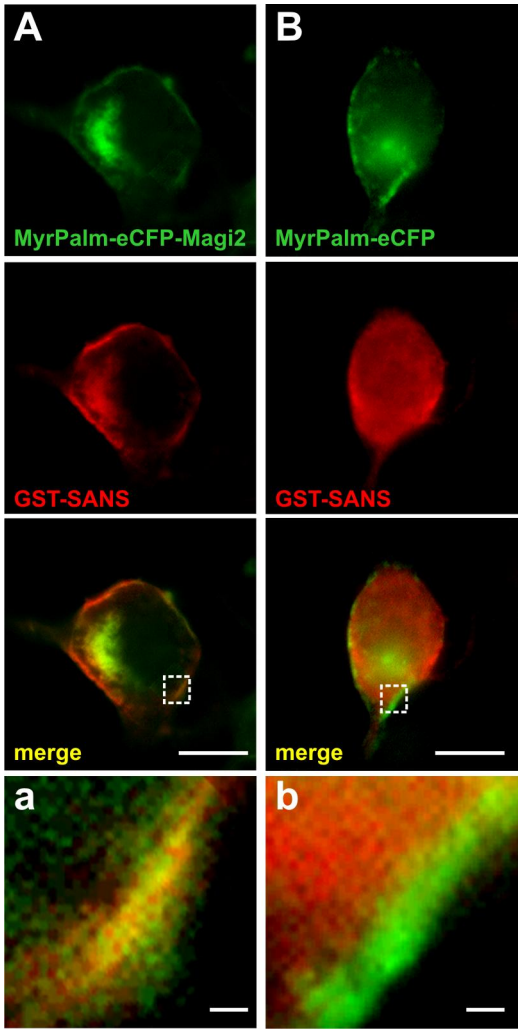

Supplemental Figure 1: Validation of SANS and Magi2 interaction in HEK293 cells by membrane targeting assays. HEK293 cells were double-transfected with plasmids encoding eCFP-tagged Magi2 N-terminally fused with the MyrPalm membrane-anchoring signal (MyrPalm-eCFP-Magi2) or MyrPalm-eCFP as control and GST-SANS. **(A)** In cells double-transfected with MyrPalm-eCFP-Magi2 (green) and GST-SANS (red), SANS is recruited by Magi2 to the cell membrane. **(B)** In cells double-transfected with MyrPalm-eCFP (green) and GST-SANS (red), SANS is not recruited to the membrane. Scale bars, 10/1 µm.

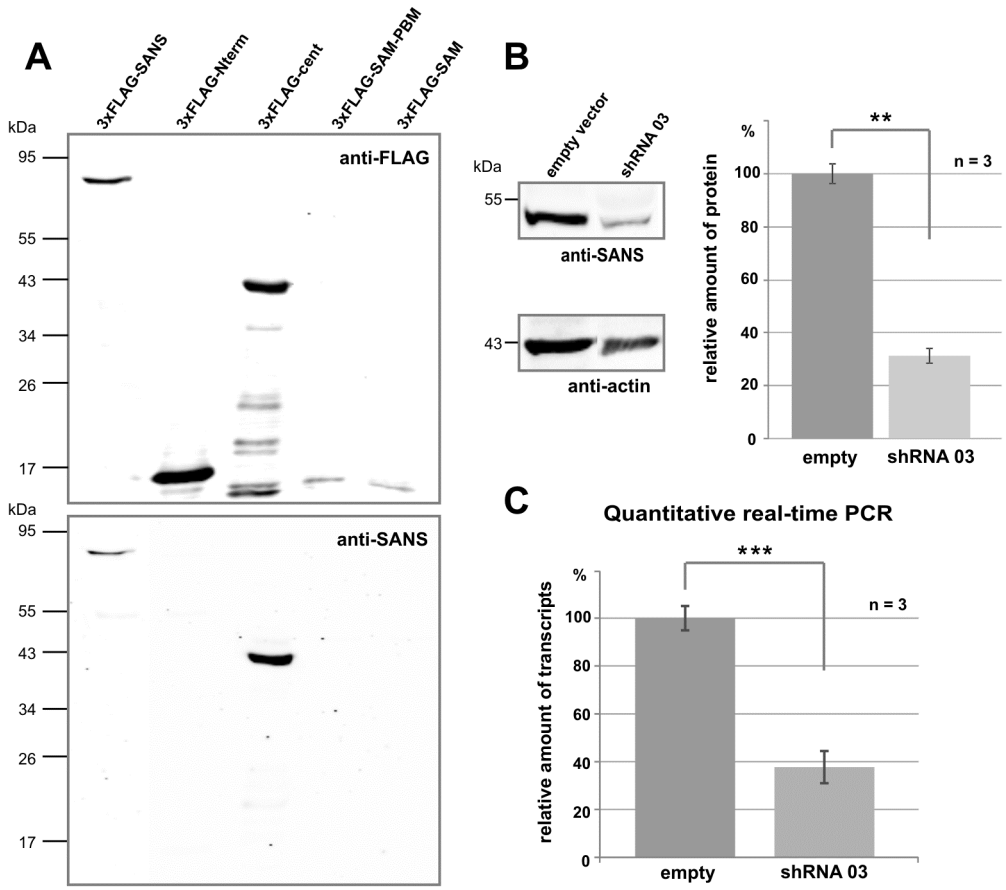

Supplemental Figure 2: **Validation of antibodies and shRNA against SANS.** Antibodies were raised against the C-terminal region of the central domain (aa339-384) of murine SANS in guinea pig. **(A)** Western blots of total cell lysates from HEK293 cells transfected with FLAG-tagged full length or diverse domains of SANS. Lower panel: affinity purified anti-SANS detected only the full length protein and the central domain which was used as antigen. Upper panel: Western blot analysis with anti-FLAG antibodies as loading control. **(B)** Anti-SANS Western blots of IMCD3 cells transfected with shRNA03 against SANS or the empty vector as control. Quantification of SANS knock down by shRNA03 demonstrated ~ 69% decrease of SANS protein expression (SD ±2.80%, n=3, p-value 0.0012) compared to control (SD ±3.68%). Actin was used as loading control. **(C)** Result of quantitative real-time PCR (qPCR) analysis of SANS transcripts revealed ~62% decrease of mRNA expression (SD ±56.70%, n=3, p-value 0.0002) after SANS knock down by shRNA03 compared to control (SD ±5.08%).

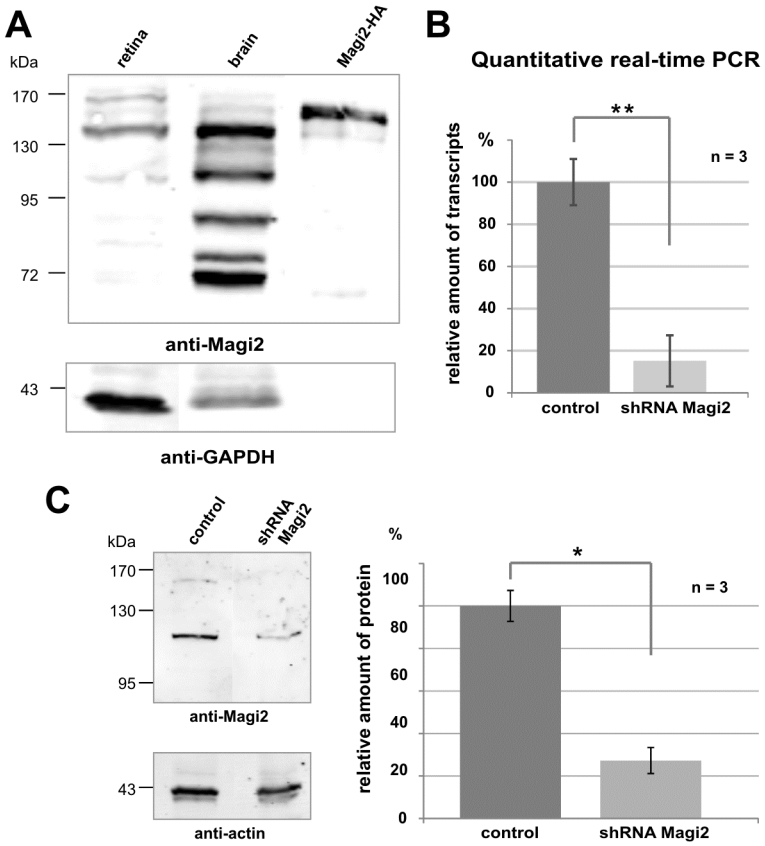

Supplemental Figure 3: Validation of antibodies and shRNA against Magi2. (A) Western blot analysis of total tissue lysates (60 µg) of murine retina and brain and recombinant Magi2-HA applying monoclonal antibody against murine Magi2. Anti-Magi2 detected three distinct bands in the retina lysate corresponding to the 3 previously described murine Magi2 isoforms. In brain lysates there are two prominent bands corresponding to the shorter Magi2 isoforms and different unexpected bands of lower weight. Anti-Magi2 detected recombinant Magi2-HA at the expected molecular weight of about 142 kDa. GAPDH was used as loading control. **(B)** Result of qPCR analysis of Magi2 transcripts revealed ~85% decrease of mRNA expression (SD ±12.13%, n=3, p-value 0.0102) Magi2 knock down by shRNA compared to control (SD ±10.95). **(C)** Anti-Magi2 Western blots of IMCD3 cells transfected with shRNA against Magi2 or the empty vector as control. Quantification of SANS knock down by shRNA demonstrated 73% decrease of Magi2 protein expression (SD ±6.13%, n=3, p- value 0.0173) compared to the scrambled shRNA control (SD ±7.27%). Actin was used as loading control.

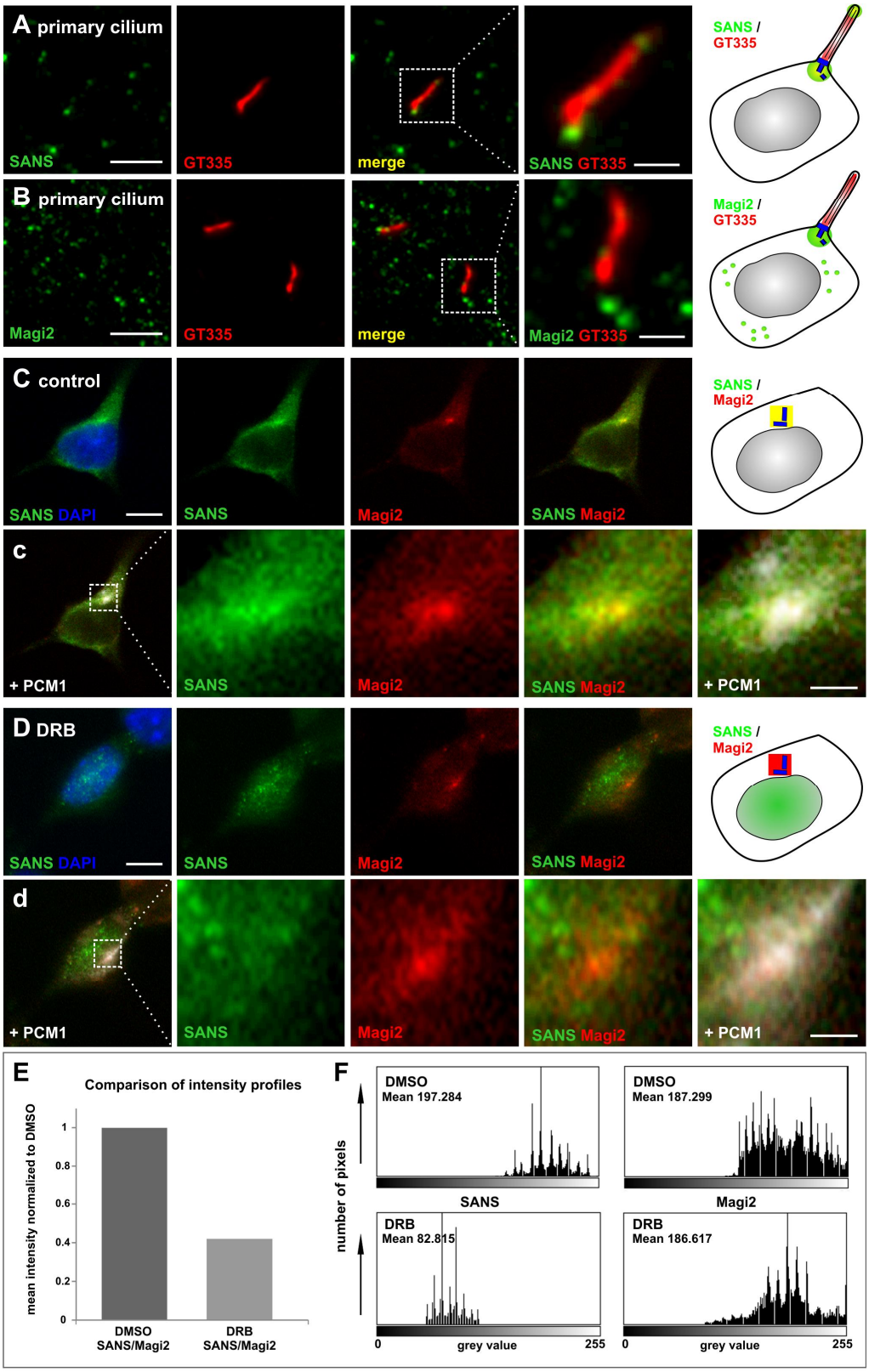

Supplemental Figure 4: Intrinsic phosphorylation dependency of SANS-Magi2 interaction. (A) Double-immunolabelling of SANS (green) and acetylated tubulin (GT335, red) as marker for the primary cilium demonstrated SANS localization at the base and tip of the primary cilium in IMCD3 cells. **(B)** Double-immunolabelling of Magi2 (green) and GT335 (red) demonstrated Magi2 localization at the base of the primary cilium. **(C, D)** SANS and Magi2 localization n after DRB treatment. **(C, c)** In control (DMSO), SANS (green) was localized in the perinuclear cytoplasm while Magi2 (red) was present in a perinuclear spot. Merged images

with the pericentriolar matrix marker PCM1 (white) indicated co-localization (yellow) of SANS and Magi2 in the pericentriolar matrix. (**D, d)** In DRB-treated cells, SANS changed to a more cytoplasmic and nuclear localization. In contrast, Magi2 was still co-localized with PCM1. **(E)** Intensity profile of SANS/Magi2 staining of DRB-treated cells normalized to control demonstrated the decrease of co-expression in the region of interest (ROI) indicated in c and d by *squares*. **(F)** The histograms of SANS and Magi2 grey scales after DMSO and DRB treatment (gained with Image J)**.** The translocation of SANS from the ROI to the nucleus after DRB treatment was depicted by the number of pixels decreasing from 197.284 (DMSO) to 82.815 (DRB) mean pixels, whereas Magi2 histogram did not change. Scale bars, A/B/c/d 0.5 µm; C/D 5 µm.

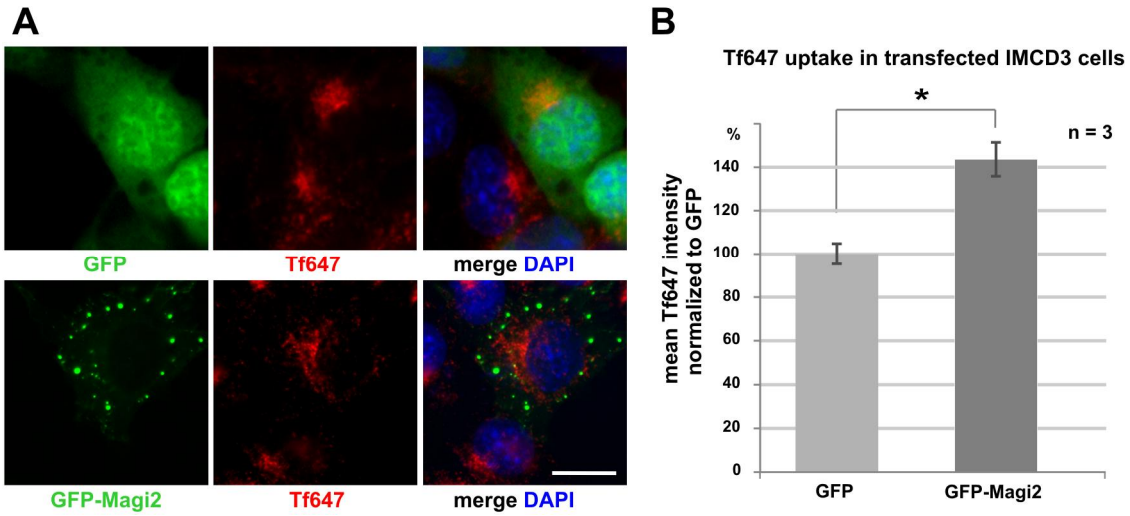

Supplemental Figure 5: Magi2 overexpression increases Tf647 uptake. (A) Tf647 uptake (red) was fluorescent microscopically monitored in IMCD3 cells transiently transfected with GFP-Magi2 or GFP as control. GFP alone (green) did not affect Tf647 uptake (red) (upper panel). In contrast, overexpression of GFP-Magi2 (green) increased endocytotic uptake of Tf647 in transfected cells. **(B)** Quantification of the mean fluorescence intensity of Tf647 normalized to GFP transfected cells revealed ~43% increase of endocytosis (SD ± 7.7, n=3, p-value 0.0362) in cells transfected with GFP-Magi2 compared to cells transfected with GFP alone (100%, SD ± 4.7). Scale bar, 5 µm.

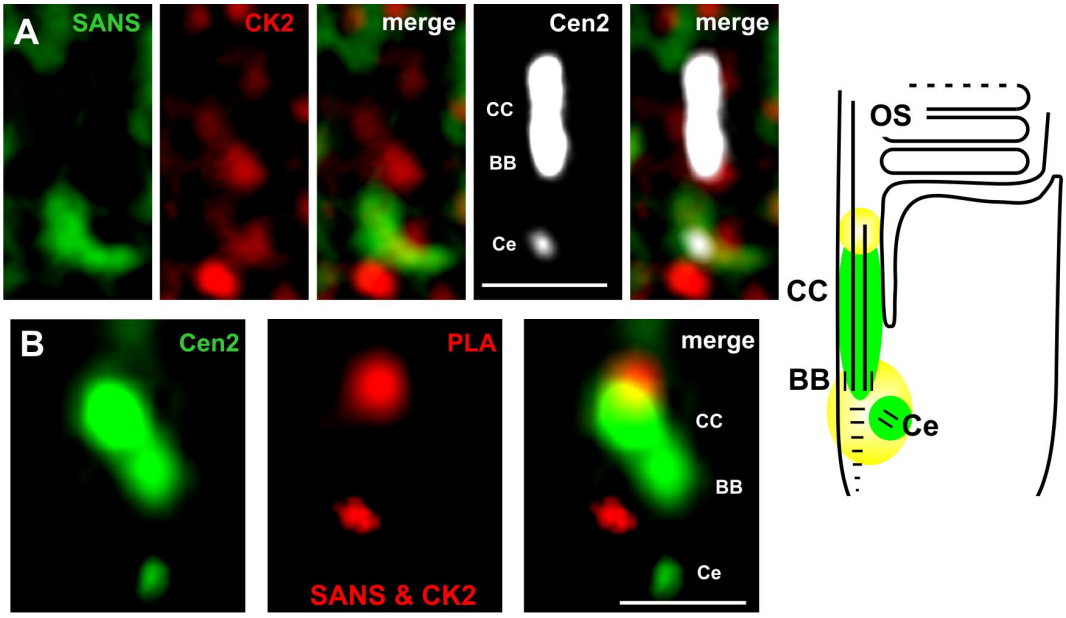

Supplemental Figure 6: *In situ* localization of the SANS-CK2 complexes in the periciliary region of photoreceptor cells of the murine retina. (A) Triple-labelling of SANS (green), CK2 (red), and Cen2 in the ciliary region of photoreceptor cells demonstrated localization of SANS and CK2 at the base of the connecting cilium (CC). **(B)** Proximity ligation assay **(**PLA) of SANS and CK2 (red), counterstained with anti-centrin-2 (green), demonstrated *in situ* localization of SANS-CK2 complexes at the base and at the tip of the CC. **(C)** Schematic illustration of SANS-CK2 complex localization in the ciliary region a rod photoreceptor cell (yellow). BB, basal body; Ce, adjacent daughter centriole. Scale bars: 1 µm.

	SANS	**Magi2**
qPCR primer	ACTCTCTGGGCTGCCTACC TGTTTCCCCAGATGTCACAC	ATGCCTCACGCTGACATTG GGGCTCTGTTTCTCTGAACTG
shRNA oligos		**Oligo 1 bp 602–623** GCGGGACCTATGAAGACAACT
		Oligo 2 bp 2180–2201 GCAGTCCACAAACAAGTTTAT
		Oligo 3 bp 3469–3490 GGAGCCAAAGGATTTGGATTC
		scrambled GAGAGACGTATCCCGCTAGAA
phospho-construct primer	**S422A** GCTTTGATGCTGTGCGCCGACCTCGACCTCCGC GCGGAGGTCGAGGTCGGCGCACAGCATCAAAGC	**S1082A** GAAAAGTGACAAGCATGGGGCCCCATATTTCTACTTACT AGTAAGTAGAAATATGGGGCCCCATGCTTGTCACTTTTC
	S422E AGGCTTTGATGCTGTGCGAAGACCTCGACCTCCGCAG CTGCGGAGGTCGAGGTCTTCGCACAGCATCAAAGCCT	

Supplemental Table 1: Primers and oligonucleotides used in this study

3. Zusammenfassung der Ergebnisse und Diskussion

Die bisherigen Analysen durch uns und andere Arbeitsgruppen haben gezeigt, dass in das USH-Interaktom weit mehr Proteine integriert sind, als nur die USH-Proteine (zusammengefasst in: Wolfrum 2011) (siehe Abb. 1). USH-Proteine stehen über ihre Interaktionsdomänen mit anderen Proteinen und dadurch mit der Funktion anderer Proteinnetzwerke in direkter Verbindung (Gosens *et al,* 2007; Roepman and Wolfrum 2007; van Wijk *et al,* 2009; Wolfrum 2011). Die detaillierte Analyse ciliärer Netzwerke wurde in Publikation I behandelt und verdeutlicht die Verbindung von USH mit anderen Ciliopathien. Zum Verständnis der molekularen Grundlagen von USH ist neben den Analysen zur Funktion des Protein-Netzwerkes auch die Kenntnis über die Funktion der einzelnen Komponenten essentiell. Eine Möglichkeit, die Funktion eines Proteins aufzuklären, ist die Identifizierung und Charakterisierung seiner Interaktionspartner. Die Suche nach potentiellen Interaktoren dient dabei aber nicht nur der Analyse molekularer Wirkmechanismen. Zum einen stellen neue Interaktionspartner potentielle USH-Kandidaten dar, zum anderen können potentielle Interaktoren auch als genetische *modifier* für USH-Gene agieren (Gusella and MacDonald 2009; Schneider *et al,* 2009*; Yan *et al,* 2010). Im Rahmen dieser Arbeit wurden die identifizierten potentiellen SANS-Interaktionspartner Ush2a, Magi2 und TRAK2 analysiert. Die Interaktion zwischen SANS und Ush2a wurde validiert und die Ergebnisse werden aktuell für Publikation II aufbereitet. In Publikation III wird die Funktion der Interaktion zwischen SANS und Magi2 dargestellt. Im letzten Abschnitt der vorliegenden Arbeit wird die Interaktion zwischen SANS und TRAK2 diskutiert. Sie wurde durch unabhängige Assays validiert, eine funktionelle Analyse steht allerdings bisher noch aus.

3.1 Die Bedeutung der USH Proteinnetzwerke für die Photorezeptorzelle

Die USH1- und USH2-Proteine werden über die Gerüstproteine Harmonin, SANS und Whirlin zu funktionellen Einheiten, den USH-Proteinnetzwerken, organisiert, deren Zusammensetzung sich je nach Lokalisation und Funktion unterscheidet (Yang *et al,* 2010; Wolfrum 2011). Für den periciliären Bereich in Photorezeptorzellen wird eine Beteiligung von USH-Proteinen für die Entwicklung und Aufrechterhaltung des Ciliums (Außensegment, siehe Einleitung) diskutiert (Maerker *et al,* 2008; Kersten *et al,* 2012*). In Publikation I haben wir die Komposition des periciliären USH-Proteinnetzwerkes auf seine Zusammensetzung und mögliche Funktion für die Ciliogenese auf Basis der aktuellen Daten analysiert (Publikation I, Abb. 1). Allen syndromischen und nicht-syndromischen Ciliopathien ist der Phänotyp der retinalen Degeneration gemein (zusammengefasst in: Rachel *et al,* 2012). Durch

die bisher identifizierten Cilien-assoziierten Interaktionspartner von USH-Proteinen wird das USH-Interaktom mit den Proteinnetzwerken verschiedener Ciliopathien verknüpft. Eine dieser molekularen Verbindungen zwischen USH und Ciliopathien stellt die direkte Interaktion zwischen dem USH1G-Protein SANS und dem Cilien-assoziierten Molekül CEP290 (*centrosomal protein* 290 kDa) dar (Sorusch *et al,* in prep.*). CEP290 verbindet das USH-Interaktom direkt mit unterschiedlichen Ciliopathie-Netzwerken (Publikation I, Abb. 2) durch die Interaktion mit Cilien-assoziierten Proteinen wie Lebercilin, Nlp (*ninein-like protein*) und BBS6 (Bardet-Biedl-Syndrom-Protein 6) (Coppieters *et al,* 2010). Mutationen in CEP290 führen zu einer Reihe syndromischer und nicht-syndromischer Ciliopathien wie Lebersche Kongenitale Amaurose (LCA), BBS oder das letale Meckel-Gruber-Syndrom (MKS) (Sayer *et al,* 2006; Valente *et al,* 2006; Baala *et al,* 2007; Leitch *et al,* 2008). Die molekulare Vernetzung verschiedener Ciliopathien durch CEP290 zeigt auf, dass dieser SANS-Interaktionspartner ein bedeutendes Protein für die Funktion von Primärcilien ist und bildet damit die Grundlage für weiterführende Analysen zur Funktion von SANS in Cilien-assoziierten Netzwerken.

Die beschriebenen Querverbindungen zu Molekülen anderer Proteinnetzwerke, deren Rolle bei der Entstehung ciliärer Erkrankungen bereits beschrieben wurde, geben uns Hinweise darauf, welche Funktion USH-Proteine im periciliären Komplex (PCC, *periciliary membrane complex*, Abb. 3) der Photorezeptorzelle spielen können. Die Parallelen zu anderen ciliären Interaktomen machen deutlich, dass das USH-Interaktom für die Funktion des Außensegmentes, sprich das sensorische Cilium der Photorezeptorzelle, essentiell ist (Publikation I, Abb. 2). Im periciliären Komplex der Photorezeptorzellen könnten die USH-Proteine die Funktion der Proteinnetzwerke prototypischer Cilien für Aufbau und Funktion der Photorezeptorzelle übernehmen bzw. in ihrer Funktion ergänzen. Kongruente Funktionen der ciliären Proteinnetzwerke in Primärcilien auf der einen und Photorezeptoren auf der anderen Seite liefern möglicherweise eine Erklärung, warum bei USH primär die sensorischen Zellen der Retina und des Innenohres betroffen sind, während bei anderen Ciliopathien verschiedene Zelltypen bzw. Organe betroffen sind. Es gibt allerdings bereits eine Reihe von Hinweisen, dass USH-Patienten neben den klassischen Symptomen Taub- bzw. Schwerhörigkeit und Verlust des Sichtfeldes weitere klinische Symptome zeigen, die ebenfalls auf ciliäre Defekte zurückzuführen sind, wie der Verlust des Geruchssinnes und eine Beeinträchtigung der Spermienmotilität (Hunter *et al,* 1986; Zrada *et al,* 1996).

Die USH-Proteine sind direkt oder indirekt über ihre Interaktionspartner an der Funktion des Verbindungsciliums/Außensegmentes beteiligt. Mutationen in USH-Genen, die zum

Ausfall eines dieser Proteine im Netzwerk führen, könnten zur Desorganisation oder gar zum kompletten Zusammenbruch des periciliären Komplexes und damit zur retinalen Degeneration von USH führen. Die Entwicklung eines ciliären Defektes, der zu einem retinalen Phänotyp führt, ist bereits für eine Reihe von anderen ciliären Proteinnetzwerken belegt, wie z.B. für das BBSome. Mutationen einzelner Komplexpartner führen zu BBS, dessen klinische Definition neben Adipositas und Polydaktylie über den Phänotyp *Retinitis pigmentosa* bestimmt wird (Chang *et al,* 2006; Zaghloul and Katsanis 2009). Die Aufdeckung der Gemeinsamkeiten unterschiedlicher Ciliopathien bildet die Basis für die Entwicklung übergreifender Therapiestrategien zur Behandlung betroffener Patienten.

Wie von Adam und Kollegen schon 2007 postuliert, konnte durch die Zusammenstellung von Primärdaten unserer und anderer Arbeitsgruppen verdeutlicht werden, dass USH als Ciliopathie bezeichnet werden kann, bei der die ciliären Zellen des Innenohrs (Haarsinneszellen) und die Photorezeptorzellen betroffen sind (Adams *et al,* 2007). Wie auch bei anderen Ciliopathien spielen dabei ciliäre / periciliäre Transportprozesse, die durch Mutationen in den Genen der beteiligten Proteine möglicherweise fehlerhaft ablaufen, eine entscheidende Rolle (Ocbina *et al,* 2011; Sang *et al,* 2011; Reiter *et al,* 2012). Die Analyse dieser Transportprozesse bzw. das Zusammenspiel der beteiligten Proteine war ebenfalls Teil der vorliegenden Arbeit und wird in den folgenden Abschnitten diskutiert.

3.2 SANS und Ush2a vernetzen das periciliäre USH-Proteinnetzwerk

Im periciliären Bereich des Innensegmentes von Photorezeptorzellen sind sowohl USH1- als auch USH2-Proteine im periciliären Komplex über die direkte Interaktion zwischen den Gerüstproteinen SANS und Whirlin organisiert (van Wijk *et al,* 2006; Maerker *et al,* 2008; Yang *et al,* 2010).

Um die Komposition eingehender zu analysieren und damit auf die Funktion dieses USH-Proteinnetzwerkes rückschließen zu können, wurden weitere Interaktionen zwischen USH1- und USH2-Proteinen überprüft. Ich konnte im Rahmen dieser Dissertation zeigen, dass die zentrale Domäne von SANS mit dem C-Terminus - der intrazellulären Domäne von Ush2a - interagiert. Ush2a spielt bei der Entwicklung und Funktion sowohl der Haarsinneszellen des Innenohres als auch der Photorezeptorzellen der Retina eine wichtige Rolle (Bhattacharya *et al,* 2002; Liu *et al,* 2007). Wie für die meisten USH-Proteine wurden auch für Ush2a verschiedene Isoformen beschrieben, wobei in der Retina die Isoform b, auch als Usherin bezeichnet, die kanonische Isoform ist (Publikation II, Abb. 1; van Wijk *et al,* 2004; van Wijk *et al,* 2006).

Da BLAST-Analysen für die Aminosäuresequenz von SANS, besonders innerhalb der zentralen Domäne, eine Reihe potentieller Phosphorylierungsstellen aufzeigen, überprüften wir eine möglicherweise phosphorylierungsabhängige Interaktion zwischen SANS und Ush2a. Interaktionsstudien unter Verwendung von Kinase-Inhibitoren belegen die phosphorylierungsabhängige Interaktion zwischen SANS und Ush2a sowohl *in vitro* als auch *in situ* (Publikation II, Abb. 2). Dies ist der erste Hinweis auf die Regulation eines USH-Proteins durch post-translationale Modifikation.

Die Lokalisation des Transmembranproteins Ush2a sowie des Gerüstproteins SANS in der Retina der Maus wurde bereits von uns und anderen dokumentiert (van Wijk *et al,* 2006; Maerker *et al,* 2008; Kersten *et al,* 2012*). Durch die Herstellung eines neuen SANS-Antikörpers konnten wir diese Analysen um den direkten Nachweis der Co-Lokalisation von SANS und Ush2a an der Basis des Verbindungsciliums ergänzen (Publikation II, Abb. 3, 4).

Die Interaktion zwischen SANS und Ush2a ist eine weitere direkte Verknüpfung zwischen den USH1- und USH2-Netzwerken und verdeutlicht erneut die enge molekulare Verbindung zwischen USH1- und USH2-Proteinen in der Photorezeptorzelle. Dies bietet auch eine Erklärung für überlappende Phänotypen zwischen den USH1- und USH2-Subtypen.

Der Vergleich der subzellulären Verteilung der Interaktionspartner lokalisiert beide Proteine im für die Funktion der Photorezeptorzelle wichtigen periciliären Komplex. In diesem Kompartiment ist auch der Interaktionspartner des C-Terminus von SANS, das USH2D-Protein Whirlin lokalisiert, das als Hauptorganisator des periciliären USH-Netzwerkes gilt und ebenfalls mit Ush2a interagiert (van Wijk *et al,* 2006; Maerker *et al,* 2008; Kersten *et al,* 2010; Wang *et al,* 2012). Durch den Nachweis eines ternären Komplexes aus SANS, Ush2a und Whirlin konnten wir zeigen, dass diese Interaktionen nicht unabhängig, sondern simultan stattfinden können (Publikation II, Abb. 5). Zudem nimmt die Interaktion von SANS und Ush2a auf die Bindung zwischen SANS und Whirlin Einfluss. In vorherigen Arbeiten wurde das C-terminale PDZ-Bindemotiv (PBM) in SANS als essentielle Bindedomäne für die Interaktion zwischen SANS und Whirlin nachgewiesen (Maerker *et al,* 2008). Die Interaktion zwischen Whirlin und Ush2a wird ebenfalls von dem PBM in Ush2a vermittelt. In Publikation II konnten wir zeigen, dass dieses für die Interaktion mit SANS nicht maßgeblich ist. Weitere Analysen zur genauen Zusammensetzung dieses Komplexes sind notwendig. Dabei werden Experimente zur post-translationalen Modifikation wichtige Erkenntnisse zur Regulation des USH-Interaktoms liefern, da die Phosphorylierung von SANS die Bildung von Proteinkomplexen und damit die Komposition von Proteinnetzwerke entscheidend beeinflussen kann.

Die Funktion des periciliären USH-Netzwerkes für die Photorezeptorzelle bei der Beteiligung an Transportprozessen im periciliären Komplex wurde in Publikation I diskutiert. Zudem ist die Membran des apikalen Innensegmentes als Zielmembran für Opsin-Transportvesikel beschrieben worden (Papermaster 2002). Das USH1-USH2-Netzwerk als Teil des periciliären Komplexes scheint beim Umladen der Fracht vom Innensegment-Transport in Richtung Außensegment eine wichtige Rolle zu spielen (Roepman and Wolfrum 2007; Maerker *et al,* 2008; Overlack *et al,* 2011b*). Die Interaktion zwischen SANS, Ush2a und Whirlin in der periciliären Region könnte damit zum einen der Integrität der Zielmembran dienen, aber auch direkt am *cargo handover* auf den ciliären Transport beteiligt sein. Zum anderen könnte SANS durch die Assoziation mit Mikrotubuli am Transport von Ush2a selbst und zusammen mit Whirlin an dessen Integration in die periciliäre Membran beteiligt sein (Publikation II, Abb. 6)

3.3 SANS und Magi2 modulieren die Endocytose in Photorezeptorzellen

Um weitere Erkenntnisse über die Funktion von SANS als USH-Schlüsselprotein zu erlangen, wurden zur Identifizierung neuer Interaktionspartner Hefe-2-Hybrid (Y2H, *yeast-2-hybrid*) - Screens durchgeführt. Mit dem C-Terminus von SANS wurde neben dem USH2D-Protein Whirlin (Maerker *et al,* 2008) ein weiteres PDZ-Domänen-Protein identifiziert, das Gerüstprotein Magi2 (*membrane associated guanylate kinase inverted-2*). Magi2 gehört zur Familie der MAGUK-Proteine (*membrane associated guanylate kinases*), Membran-assoziierte Gerüstproteine mit einer Reihe von Interaktionsdomänen zur Bindung an das Aktincytoskelett, an Cytoskelett-assoziierte Proteine und zur Interaktion mit Molekülen, die an zellulären Signalwegen beteiligt sind (Anderson 1996; Dimitratos *et al,* 1999). Magi2 wurde als neuronale Isoform dieser Gerüstproteine mit invertierter Domänenstruktur beschrieben (Hirao *et al,* 1998) (Publikation III, Abb. 1). Für seine Interaktionsdomänen wurden bereits eine Reihe von Interaktionspartnern identifiziert, die zusammen mit Magi2 mit der Funktion von Synapsen assoziiert sind (Iida *et al,* 2004; Deng *et al,* 2006; Fukaya *et al,* 2011). In diesem Zusammenhang wird eine Beteiligung von Magi2 bei neuronalen Prozessen des Lernens und Erinnerns diskutiert (Danielson *et al,* 2012; Koide *et al,* 2012).

Im Rahmen dieser Arbeit konnten wir für die Interaktion zwischen SANS und Magi2 nachweisen, dass die SAM-Domäne von SANS allein ausreichend für die Bindung an die PDZ5-Domäne von Magi2 ist (Publikation III, Abb. 1C, D). Diese Art von Interaktion ist ungewöhnlich, da SANS über ein sogenanntes PDZ-Bindemotiv (PBM) verfügt, an das PDZ-Domänen Proteine allgemein binden (Songyang *et al,* 1997; Bezprozvanny and Maximov

2001; Harris and Lim 2001). Durch das PBM von SANS scheint die Affinität zur PDZ-Domäne von Magi2 dagegen reduziert zu werden. Mittels des Online-Tools POW (http://webservice.baderlab.org/domains/POW/) konnten wir die Interaktionssequenz in SANS zur PDZ5-Domäne von Magi2 bestimmen. Es handelt sich um ein innerhalb der Vertebraten hochkonserviertes internes PDZ-Bindemotiv innerhalb der SAM-Domäne bestehend aus den Aminosäuren Serin, Asparaginsäure, Leucin, Asparaginsäure, Leucin (SDLDL) (Tabelle 2).

Species	NCBI No.	Alignment of SAM domain sequences
H.sapiens	NP_775748	LEPETSPLETFLASLHMEDFAALLRQEKIDLEALMLC**SDLDL**RSISVPLGPRKKILGAVRRRRQA
P.troglodytes	XP_523715	LEPETSPLETFLASLHMEDFAALLRQEKIDLEALMLC**SDLDL**RSISVPLGPRKKILGAVRRRRQA
P.abelii	XP_002827857	LEPETSPLETFLASLHMEDFAALLRQEKIDLEALMLC**SDLDL**RSISVPLGPRKKILGAVRRRRQA
M.mulatta	XP_002800714	LEPETGPLETFLASLHMEDFAALLRQEKIDLEALMLC**SDLDL**RSISVPLGPRKKILGAVRRRRQA
B.taurus	NP_001179631	LEPETSPLETFLASLHMEDFTSLLRQEKIDLEALMLC**SDLDL**RSISVPLGPRKKILGAVRRRRQA
E.caballus	XP_001496907	LEPETSPLDTFLASLHMEDFASLLRQEKIDLEALMLC**SDLDL**RSISVPLGPRKKILGAVRRRRQA
S.scrofa	XP_003131267	LEPETSPLETFLASLHMEDFTPLLRQEKIDLEALMLC**SDLDL**RSISVPLGPRKKIMGAVRRRRQT
C.familiaris	XP_852112	LEPETSPLETFLASLHMEDFTSLLRQEKIDLEALMLC**SDLDL**RSISVPLGPRKKILGAVRRRRQA
F.catus	XP_003997185	LEPETSPLDTFLASLHMDDFASLLRQEKIDLEALMLC**SDLDL**RSISVPLGPRKKILGAVRRRRQA
M.musculus	NP_789817	LEPETSPLETFLASLHMEDFASLLRHEKIDLEALMLC**SDLDL**RSISVPLGPRKKILGAVRRRRQA
R.norvegicus	NP_001099320	LEPETSPLETFLASLHMEDFASLLRHEKIDLEALMLC**SDLDL**RSISVPLGPRKKILGAVRRRRQA
C.cristata	XP_004693537	LEPETSPLETFLASLHMEDFASLLRQEKIDLEALMLC**SDLDL**RSISVPLGPRKKIMGAVRRRRQA
C.porcellus	XP_003464875	LEPETSPLETFLASLHMEDFASLLRQEKIDLEALMLC**SDLDL**RSISVPLGPRKKILGAVRRRRQA
M.domestica	XP_001369718	LEPETSPLETFLASLHMDDFVALLRQEKIDLDALMLC**SELDL**HSISIPLGPRKKILGAIKRRRLV
X.tropicalis	XP_002939606 XP_004918531 XP_004918532	EEPDTSPLESFLASLQMGDLVTVLQDEKIDLAALTLC**SDHDL**KSIGIPLGPRKKILDGIQRRRQA
D.rerio	XP_002661315	DEPDTSPLEVFLATQSMNEFIPILKREKIDLDALLLC**SDNDL**KGIHIPLGPRKKIMDACMRRLET
G.gallus	XP_426242	DEPDSSPLETFLASLHMFEFISILKKEKIDLEALMLC**SDNDL**KSINIPLGPRKKIVDAIQRRRQT

polar/acidic polar/basic polar/neutral

Tabelle 2: Konservierung des internen Bindemotives in der SAM-Domäne von SANS. Es sind die lateinischen Bezeichnungen der Spezies, ihre Protein-Identifikationsnummer aus der NCBI-Datenbank sowie der Abgleich der Aminosäuresequenzen, bezogen auf die Sequenz der SAM-Domäne des humanen USH1G-Proteins aufgelistet. Veränderungen innerhalb des internen Bindemotives sind farbig gekennzeichnet.

Der Grad der Homologie nimmt mit zunehmender stammesgeschichtlicher Entfernung vom Menschen ab. Der erste Aminosäureaustausch innerhalb des Bindemotives findet beim Übergang von Säugetieren zu Beuteltieren statt (*Monodelphis domestica*). Interessanterweise erhöht der Austausch der nichtpolaren, neutralen Aminosäure Leucin (L) mit den polaren Aminosäuren Histidin (H) bzw. Asparagin (N) bei den Modellorganismen Zebrafisch und Krallenfrosch, sowie bei Vögeln, die errechnete Interaktionswahrscheinlichkeit zwischen dem Bindemotiv in SANS und der PDZ5-Domäne von Magi2. Das könnte auf unterschiedliche Funktionen dieser Interaktion zwischen den Spezies hindeuten, evolutionäre Analysen standen allerdings nicht im Fokus der vorliegenden Arbeit.

Bei der Interaktion zwischen SANS und Magi2 konnten wir erstmalig eine direkte Interaktion zwischen der in Vertebraten konservierten SAM-Domäne zu einer PDZ-Domäne nachweisen (Schultz *et al,* 1997; Qiao and Bowie 2005). Die Interaktion zwischen SANS und Magi2 lässt damit, ähnlich wie bei der Interaktion zwischen SANS und Ush2a, eine simultane Bindung an den zweiten im Screen identifizierten Interaktionspartner, das USH2D Protein Whirlin, zu, für dessen Interaktion das PBM von SANS essentiell ist (Maerker *et al,* 2008). Die SANS-Interaktoren können demnach in einem funktionellen Komplex assoziiert vorliegen.

Darüber hinaus haben unsere Analysen gezeigt, dass die Interaktion zwischen SANS und Magi2 von der Phosphorylierung von SANS abhängt. Ich konnte mittels Phospho-Mutanten von SANS belegen, dass das Serin an Position 422 (S422) für die Bindung an Magi2 phosphoryliert werden muss (Publikation III, Abb. 4). Diese Phosphorylierungsstelle ist die erste Aminosäure innerhalb des oben beschriebenen internen Bindemotives und stellt ein Substrat der Casein-Kinase CK2 dar, deren Lokalisation in der Mausretina im periciliären Bereich bereits von uns dokumentiert wurde (Trojan *et al,* 2008). Wir konnten *in vitro* nachweisen, dass der C-Terminus von SANS durch die CK2 phosphoryliert werden kann (Publikation III, Abb. 5).

Diese Ergebnisse bestätigen, dass eines der zentralen USH-Proteine durch post-translationale Modifikation reguliert wird. Die Experimente bilden damit die Grundlage zur Überprüfung der Interaktion zwischen SANS und Ush2a (Publikation II). Der Nachweis phosphorylierungsabhängiger Interaktionen macht deutlich, wie wichtig die Analyse post-translationaler Modifikationen einzelner Proteine für die Analyse von Proteinnetzwerken ist, die zur Regulation ganzer Proteinnetzwerken und damit deren Funktion beitragen können.

Für Magi2 ist bereits bekannt, dass es in Synapsen das *clustern* von Rezeptoren und den Transport von Vesikeln vermittelt (Lehtonen *et al,* 2005; Deng *et al,* 2006). Magi2 wird deshalb eine Funktion für die Endocytose in Synapsen zugesprochen (Xu *et al,* 2001; Kawata *et al,* 2006). Mittels RNAi-Studien überprüften wir den Einfluss der beiden Interaktionspartner SANS und Magi2 auf die Endocytose in Kulturzellen. Die Ergebnisse der vorliegenden Arbeit demonstrieren das komplexe Zusammenspiel von SANS und Magi2 und belegen, dass Magi2 direkten Anteil an der Endocytose hat, während SANS dabei als negativer Regulator durch die phosphorylierungs-abhängige Interaktion zu Magi2 Einfluss nimmt (Publikation III, Abb. 6 und 7).

Da das Außensegment der Photorezeptorzelle als sensorisches Cilium ein modifiziertes Primärcilium darstellt, überprüften wir mittels RNAi den Einfluss von SANS und Magi2 auf

die Ciliogenese in Kulturzellen (Publikation III, Abb. 8 und 9). Wir konnten zeigen, dass Magi2 ein positiver Modulator für die Ausbildung eines Primärciliums ist. In Magi2-defizienten Zellen bilden sich keine oder nur sehr kurze Cilien aus, ein Phänotyp, der in RNAi-Studien für andere ciliäre Proteine bereits gezeigt wurde (Ghosh *et al,* 2010; Patzke *et al,* 2010). Magi2 als neuer SANS-Interaktionspartner ermöglicht die Ausbildung des Primärciliums möglicherweise über seine Beteiligung bei der Endocytose. Kim und Kollegen haben in einem funktionellen Screen eine Reihe von Molekülen identifiziert, die die Ausbildung von Primärcilien und ihre Länge beeinflussen. Dabei wurden auch Proteine als positive Modulatoren der Ciliogenese identifiziert, denen eine Funktion für endocytotisches Recycling zugesprochen wird (Kim *et al,* 2010). Darüber hinaus wird von Nachury und Mitarbeitern dem BBSome eine Funktion bei der Ciliogenese zugesprochen, indem die BBS-Moleküle einen Komplex ähnlich Clathrin ausbilden, durch den Membranproteine das Primärcilium erreichen und aufbauen können (Nachury *et al,* 2007; Jin *et al,* 2010).

Diese Hypothese konnte ich durch Applikation des Dynamin-Inhibitors Dynasore bekräftigen. Durch die Inhibierung der Clathrin-vermittelten Endocytose zeigen die Primärcilien einen vergleichbaren Phänotyp zu den Magi2-defizienten Zellen. Es werden nur sehr wenige Cilien ausgebildet, die, im Vergleich zu den Kontrollen, ähnlich kurz wie in den RNAi-Studien zu Magi2 sind (Publikation III, Abb. 9B). Für SANS als negativen Regulator der Funktion von Magi2 haben wir den gegenteiligen Effekt, nämlich eine Verlängerung der Primärcilien nach SANS *knock down* erwartet, durch die fehlende Regulation der Funktion von Magi2 bei der Endocytose. SANS sollte demnach als negativer Modulator der Ciliogenese charakterisiert werden. Die RNAi-Experimente konnten diese Hypothese nicht eindeutig bestätigen. Wir finden in SANS-defizienten Zellen verschiedene Cilien-Phänotypen, von Zellen, die kein Primärcilium, bis hin zu Zellen, die mehrere Cilien ausbilden (Publikation II, Abb. 8). Diese phänotypische Varianz lässt sich durch die vielfältigen Interaktionspartner von SANS erklären. SANS kann neben der Regulation von Magi2 bei der Ausbildung des Primärciliums mit seinen verschiedenen (Transport-assoziierten) Interaktoren auch eine Rolle bei anderen Prozessen innerhalb der Ciliogenese spielen. Das Protein CP110, ein Interaktionspartner des SANS-Interaktors CEP290, ist ein Beispiel dafür, wie die Interaktionspartner eines Proteins in verschiedenen Netzwerken organisiert sind, deren Zusammenspiel bei der Ciliogenese unter anderem durch Phosphorylierung reguliert wird (zusammengefasst in: Tsang and Dynlacht 2013).

In der Retina der Maus konnten wir *in situ* die Ausbildung von SANS-Magi2-Komplexen dokumentieren, besonders in der periciliären Region. An der Basis des Verbindungsciliums

sind ebenfalls die Kinase CK2 und ihr Substrat SANS lokalisiert. Immunelektronische Analysen zeigen die Assoziation von Magi2 mit vesikulären Strukturen in diesem Kompartiment im Bereich der *ciliary pocket*, die membranständig von elektronendichtem Material umgeben sind (Publikation III, Abb. 10 und 11). Die Gitterstruktur ist typisch für das aus Clathrin-Untereinheiten aufgebaute Netzwerk um Membranvesikel (Harrison and Kirchhausen 1983; Cheng *et al,* 2007). Dies lieferte uns den Hinweis auf eine Beteiligung des SANS-Interaktionspartners Magi2 an Clathrin-abhängiger Endocytose in den Photorezeptorzellen der Retina. In Kulturzellen konnten wir die direkte Beteiligung von Magi2 an der Aufnahme von Transferrin mittels Rezeptor-vermittelter Endocytose nachweisen. Die Co-Lokalisation von Magi2 mit dem Transferrin-Rezeptor im apikalen Innensegment an der Basis des Verbindungsciliums bestärkt die Hypothese um eine Beteiligung des periciliären USH-Interaktoms an der Endocytose von Molekülen, reguliert durch SANS. Die Lokalisation des Transferrin-Rezeptors in der *ciliary pocket* kann der Aufnahme von Eisen aus der extrazellulären Matrix dienen und damit die Versorgung der Zelle mit diesem essentiellen Baustein sicher stellen (zusammengefasst in: Gnana-Prakasam *et al,* 2010). Diese Ergebnisse assoziieren den SANS-Magi2-Komplex mit der Homöostase von Eisen und anderen essentiellen Nährstoffen oder Ionen für die Photorezeptorzelle. Es ist bekannt, dass die ausreichende, aber streng regulierte Versorgung mit Eisen sehr wichtig für die Funktion der Retina ist. Paracelsus hat mit seiner Aussage *sola dosis facit venenum* (Paracelsus 1493-1541) festgestellt, dass für die Definition von Gift die Dosis entscheidend ist. Beides, ein Zuviel und ein Zuwenig an Eisen, wurde bereits als schädigend für die Retina dokumentiert (Wang *et al,* 1998; Kurz *et al,* 2009; Picard *et al,* 2011).

Die kontrollierte Aufnahme von Stoffen aus der extrazellulären Matrix ist an der Engstelle des Verbindungscilium am Übergang zwischen Außen- und Innensegment einfacher zu regulieren, als über die gesamte Oberfläche der Photorezeptorzelle. Durch die Interaktion von Magi2 als Endocytose-vermittelndes Protein mit dem USH1G-Protein SANS wird das periciliäre USH-Proteinnetzwerk demnach mit dem Prozess der Endocytose in diesem Kompartiment verknüpft. Aktuelle Analysen von Kaplan und Kollegen stellen den Einfluss Endocytose-vermittelnder Proteine auf die sensorischen Cilien des Nematoden *C. elegans* dar. Sie demonstrieren in ihrer Arbeit die Wichtigkeit der Balance zwischen Exocytose und Endocytose für Entwicklung und Aufrechterhaltung der Funktion dieser Cilien (Kaplan *et al,* 2012). SANS könnte als Regulator für die Funktion von Magi2 in Endocytose-Prozessen der Photorezeptorzelle diese Balance sicherstellen, in dem es, reguliert durch Phosphorylierung,

ein Gleichgewicht zwischen Aufnahme und Abgabe von Membranen bzw. Membran-assoziierten Molekülen und Transportvesikeln herstellt.

Während der Vorbereitung der Publikation III wurde mit dem C-Terminus von VLGR1/GPR98 ein Y2H-Screen durchgeführt, um neue Erkenntnisse zur Funktion des USH2C-Proteins zu erlangen. Die Sequenzierung einiger Klone hat ebenfalls die PDZ5-Domäne von Magi2 als potentielle Interaktionssequenz zu VLGR1 ergeben. VLGR1 ist durch die Interaktion mit Whirlin in das periciliäre USH1-USH2-Interaktom integriert (van Wijk *et al,* 2006; Yang *et al,* 2010). Demnach ist in diesem Bereich der Photorezeptorzelle die Bildung eines ternären Komplexes zwischen Magi2 und den beiden USH-Proteinen SANS und VLGR1 möglich. Erste Experimente in Kulturzellen weisen allerdings auf unterschiedlich starke Bindungsaffinitäten zwischen SANS und VLGR1 zu Magi2 hin (Knapp *et al*, in prep*). Der Nachweis dieser unterschiedlichen Bindungsaffinitäten würde unsere Hypothese um die Funktion von Magi2 bei endocytotischen Prozessen in der periciliären Region weiter stützen. VLGR1 als Transmembranprotein könnte Magi2 mit der Membran des apikalen Innensegmentes assoziieren und damit seine Beteiligung an der Endocytose gewährleisten. Die Phosphorylierung von SANS durch die CK2 an der Basis des Ciliums erhöht die Affinität von SANS zu Magi2, vermittelt die phosphorylierungsabhängige Interaktion und nimmt darüber negativ Einfluss auf die Endocytose in der *ciliary pocket*. Dadurch könnte als Gegengewicht zur Endocytose eine positive Regulation des Prozesses der Exocytose für den Transfer von Fracht in Richtung Außensegment ermöglicht werden (vergleiche dazu Abb. 12 in Publikation III). Bisher steht die Visualisierung der Endocytose in der Retina, insbesondere in den Photorezeptorzellen, noch aus. Dennoch stellen die vorgelegten Ergebnisse dar, dass die bisher identifizierten, pathogenen Mutationen im *USH1G*-Gen, die zu dem Verlust eines funktionellen SANS-Proteins und damit zur fehlenden Interaktion mit Magi2 führen, die Feinregulation der Endocytose stören und damit zum retinalen Phänotyp bei USH1 führen können (zusammengestellt in Publikation III, Abb. 2).

Eine weiteres Indiz für eine Rolle des SANS-Magi2-Komplexes bei der Endocytose als wichtigen Prozess für die Funktion der Photorezeptorzelle ist die Co-Lokalisation des *interphotoreceptor retinal binding protein* (IRBP) mit Magi2 an Basis des Verbindungsciliums. Mittels hochauflösender Immunfluoreszenz- und Elektronenmikroskopie konnten wir zeigen, dass IRBP im periciliären Bereich lokalisiert ist (Abb. 4). Die Lokalisation von IRBP in der extrazellulären Matrix, insbesondere im Bereich der *ciliary pocket*, spricht dafür, dass im apikalen Innensegment der Photorezeptorzellen das Recycling von Retinal stattfindet. Retinal als Licht-absorbierender Grundbaustein des Sehpurpurs

Rhodopsin wird vom retinalen Pigmentepithel bei der Phagozytose der Disks recycelt und über IRBP den Photorezeptorzellen wieder zur Verfügung gestellt (Liou *et al,* 1982; Saari *et al,* 1985). SANS als Mikrotubuli-assoziiertes Protein könnte den Transport der Opsin-Vesikel durch das Innensegment vermitteln und die Komposition des kovalenten Komplexes aus neu synthetisiertem Opsin und recyceltem Retinal könnte an der Basis des Verbindungsciliums stattfinden. Am *cargo handover* von Transportvesikeln auf die ciliären Transportprozesse ins Außensegment der Photorezeptorzelle wurde eine Beteiligung der USH-Proteine im periciliären Komplex bereits diskutiert (Publikation I und II; Maerker *et al,* 2008; Overlack *et al,* 2011b).

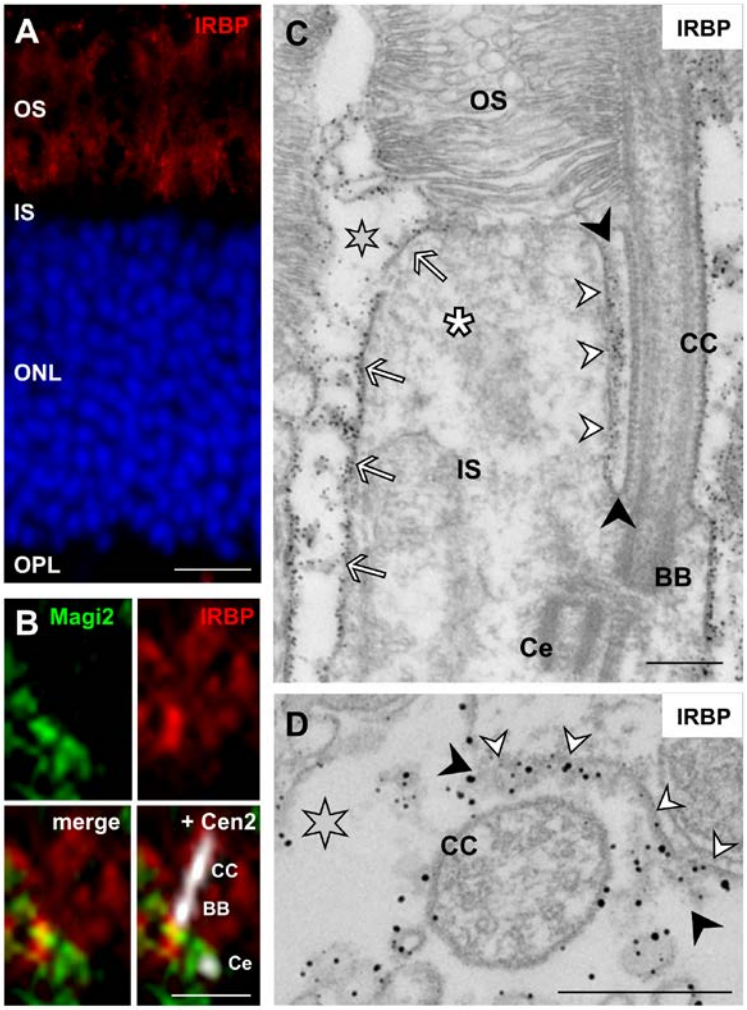

Abbildung 4: Die Lokalisation des *interphotoreceptor retinal binding protein* IRBP in der Mausretina.
(A) Die indirekte Immunfluoreszenzanalyse im Längsschnitte dokumentiert die Lokalisation von IRBP zwischen Außen- und Innensegment (OS, IS) der Photorezeptorzelle in der ciliären Region und am retinalen Pigmentepithel (RPE). **(B)** Die Dreifachmarkierung von Magi2, IRBP und Centrin2 als Marker für das Verbindungscilium (CC) zeigt die Lokalisation von Magi2 und IRBP an der Basis des CC zwischen Basalkörper (BB) und Centriol (Ce). **(C)** Die immunelektronenmikroskopische Analyse eines Längsschnittes demonstriert die Dekoration der Membranen des IS (weiße Pfeile, weiße Pfeilköpfe) und der *ciliary pocket* (schwarze Pfeilköpfe) durch IRBP auf. IRBP ist ebenfalls in der extrazellulären Matrix (Stern) lokalisiert. **(D)** Der Querschnitt zeigt die Akkumulation der IRBP-Markierung in der *ciliary pocket* (weiße Pfeilköpfe) und der umgebenden extrazellulären Matrix. Zellkerne gefärbt mit DAPI, Größenbalken: A 10 µm, B 1 µm, C/D 0.25 µm.

Zusammenfassend lässt sich für das USH-Protein SANS und damit für das periciliäre USH-Proteinnetzwerk feststellen, dass das komplexe Zusammenspiel der einzelnen Interaktionspartner bei Endocytose und Exocytose eine Grundlage für die Funktion der Photorezeptorzelle bildet. Die Regulation dieser Interaktionen durch Phosphorylierung ermöglicht das geforderte Gleichgewicht zwischen Auf- und Abbauprozessen und stellt damit die Aufrechterhaltung der Funktion der Photorezeptorzelle und damit die Integrität der Retina sicher. Die Analysen der vorliegenden Arbeit leisten damit einen wichtigen Beitrag für das Verständnis der pathophysiologischen Prozesse, die zur Degeneration der Photorezeptorzellen und damit zum retinalen Phänotyp in USH-Patienten führen.

3.4 Die Interaktion zwischen SANS und dem Transport-assoziierten Protein TRAK2

Vorangegangene Arbeiten aus unserer Arbeitsgruppe assoziieren SANS mit Mikrotubuli-abhängigen Transportprozessen in der Retina (Maerker *et al,* 2008; Overlack *et al,* 2008). Für die zentrale Domäne von SANS wurden 50 neue, potentielle Interaktoren identifiziert, von denen einige diese Funktion von SANS bestätigen. Die interessantesten Interaktionspartner sind in Tabelle 3 aufgelistet.

Protein	#	Funktion	Expression	Referenz
Myomegalin	58	Rekrutierung von Komponenten cAMP-abhängiger Signalwege	Testis, Herz, Retina Skelettmuskulatur	Verde *et al,* 2001; Overlack *et al,* 2011b*
TRAK2	26	Transport, Signaltransduktion, Endosomendynamik, Makropinocytose	Neuronales Gewebe, Leber	Hadano *et al,* 2001; Beck *et al,* 2002
CEP290	6	Regulation von Transkriptionsfaktoren, ciliärer Transport	Gehirn, Retina, Niere	Chang *et al,* 2006; Sayer *et al,* 2006;
AKAP450	5	Komplexorganisation am Centrosom und Golgi-Apparat, Transport, Signaltransduktion	Gehirn, Pankreas, Muskel	Keryer *et al,* 2003; Kim *et al,* 2007;
Dynaktin-1 (p150^{Glued})	3	Dynein-vermittelter Vesikeltransport, Positionierung des Zellkerns in Photorezeptorzellen	Gehirn, Retina	Tsujikawa *et al,* 2007; Chevalier-Larsen *et al,* 2008
Optineurin	2	Zellmorphogenese, Membran- und Vesikeltransport, Transkriptionsaktivierung	Neuronales Gewebe	Meng *et al,* 2012; Ito *et al,* 2011
KIF2a	1	Motorprotein (plus-Ende), notwendig für Mitose (Spindelaktivität) und Gehirnentwicklung	ubiquitär	Ganem and Compton 2004; Jang *et al,* 2009

Tabelle 3: Liste ausgewählter, mittels Y2H identifizierter Interaktionspartner der zentralen Domäne von SANS gelistet nach ihrer Häufigkeit im Screen (# Anzahl der positiven Klone). Das Protein TRAK2 ist blau hervorgehoben.

Die Validierung der Interaktion mit Proteinen, die direkt oder indirekt am Transport beteiligt sind, bildet die Grundlage für die Analyse der Funktion des USH-Interaktoms in intra- und interzellulären Transportwegen der Retina. Die Interaktion zu Myomegalin wurde

bereits publiziert, sie verdeutlicht die molekulare Verbindung eines USH-Proteins mit intrazellulären Transportwegen in den Photorezeptorzellen von Maus und Mensch (Overlack *et al,* 2011b*).

Im Rahmen der vorliegenden Arbeit haben wir uns auf die Interaktion zwischen SANS und den positiven Klonen aus dem Y2H fokussiert, deren Sequenzierung eine Teilsequenz von TRAK2 (*trafficking protein, kinesin binding 2*) als potentielle Interaktionssequenz zu SANS ergeben hat.

TRAK2 ist ein Kandidatengen für Amyotrophe Lateralsklerose (ALS), eine degenerative Erkrankung des motorischen Nervensystems mit progressivem Verlauf (Hadano *et al,* 2001; Swarup and Julien 2011). Das Protein gehört zur TRAK-Familie von *coiled-coil* Proteinen, für die eine Funktion im Transport von Vesikeln und Mitochondrien diskutiert wird (Brickley *et al,* 2005; Smith *et al,* 2006). Die strukturelle Ähnlichkeit mit Proteinen, die an Vesikel- und Organelldynamik beteiligt sind, und die Bindung an Kinesin als Adapterprotein lassen eine Funktion im anterograden Transport membranöser Partikel vermuten (Smith *et al,* 2006; Brickley *et al,* 2011). Dafür spricht auch die Homologie im N-Terminus von TRAK2 zu HAP-1 (*huntingtin-associated protein* 1), das beim Transport von Vesikeln und Organellen in Neuronen eine Rolle spielt (Li *et al,* 1995; Grishin *et al,* 2006). Die Expression von TRAK2 ist nach bisherigen Erkenntnissen auf neuronales Gewebe beschränkt, die Genomanalyse zeigt eine Expression von TRAK2 in der Mausretina (Blackshaw *et al,* 2001; Iyer *et al,* 2003). Als Interaktionspartner sind bisher GABA-A-Rezeptoren, die Rho-GTPasen Miro-1 und -2 sowie die *O*-GlcNAc Transferase bekannt (Beck *et al,* 2002; Iyer *et al,* 2003; Brickley *et al,* 2005). In *Drosophila* wird das Protein Milton als Homolog von TRAK2 beschrieben (Misko *et al,* 2010). Milton ist als Kinesin-Adapterprotein am axonalen Transport von Mitochondrien beteiligt und sein Fehlen in Photorezeptorzellen von *Drosophila* führt zu einer Veränderung der Lokalisation von Mitochondrien und des MTOC (*microtubule organization center*) (Stowers *et al,* 2002; Gorska-Andrzejak *et al,* 2003; Glater *et al,* 2006).

TRAK2 als neuer, potentieller Interaktionspartner assoziiert das USH1G-Protein SANS damit direkt mit Transportprozessen in der Retina.

Zunächst wurde die Interaktion zwischen SANS und TRAK2 durch unabhängige Assays validiert. Als Beispiel zum Nachweis der Interaktion ist hier der Western Blot einer Co-Präzipitation dargestellt (Trap®) (Abb. 5).

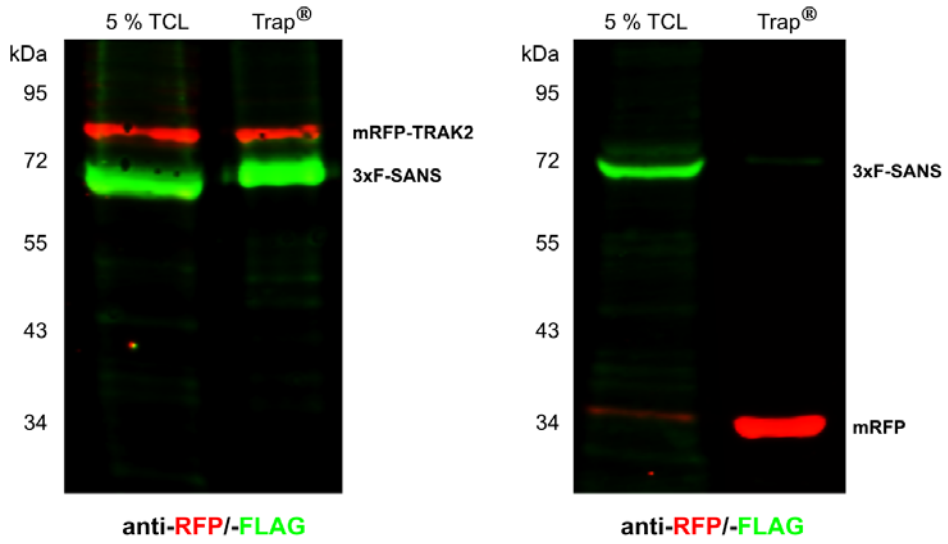

Abbildung 5: Validierung der direkten Interaktion zwischen SANS und TRAK2 mittels Co-Präzipitation. HEK293T Zellen wurden mit FLAG-markiertem SANS (3xF-SANS, ~70 kDa) und mRFP-markiertem TRAK2 (mRFP-TRAK2, ~80 kDa) oder mRFP (~34 kDa, Negativkontrolle) co-transfiziert. Die Zell-Lysate wurden mit RFP-Beads® inkubiert und die direkte Interaktion mittels Antikörper gegen FLAG (grün) und RFP (rot) im Western Blot nachgewiesen. TRAK2 (rot) co-präzipitiert SANS (grün) (linker Blot, 2. Spur), während mRFP alleine (rot) SANS nicht co-präzipitiert (rechter Blot, 2. Spur). Die ersten beiden Spuren zeigen jeweils 5 % des eingesetzten Zellysates (TCL – *total cell lysate*).

Eine Grundvoraussetzung für die Ausbildung eines funktionellen Komplexes *in vivo* ist die Expression beider Moleküle im gleichen Kompartiment einer Zelle. Mittels Antikörpern gegen SANS und TRAK2 (freundlicherweise zur Verfügung gestellt von Prof. Anne Stephenson, School of Pharmacy, University of London) wurden im Rahmen dieser Dissertation Lokalisationsstudien von SANS und TRAK2 an Längsschnitten von Maus- und humaner Retina durchgeführt. Als Beispiel ist hier die Lokalisation von SANS und TRAK2 in der humanen Retina dargestellt (Abb. 6).

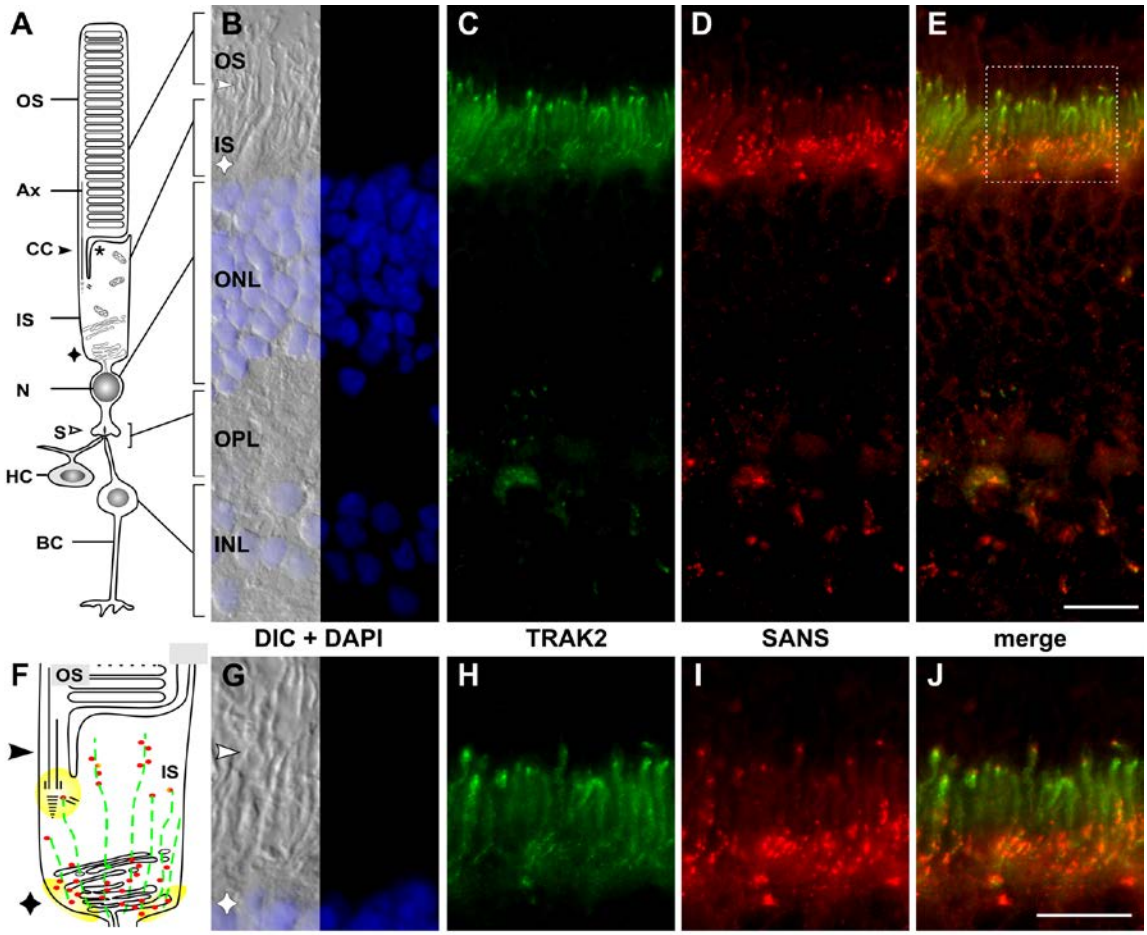

Abbildung 6: Co-Lokalisation von SANS und TRAK2 in der humanen Retina. (A) Schematische Darstellung einer Photorezeptorzelle. **(B)** Durchlichtbild des Retinaschnittes (Differentieller Interferenzkontrast – DIC) und der Kernfärbung mittels DAPI. **(C)** TRAK2 (grün) ist im Innensegment (IS) im Bereich des Verbindungsciliums (CC, Pfeilkopf) und an den Synapsen (S) in der äußeren plexiformen Schicht (OPL) lokalisiert. **(D)** SANS (rot) ist an der Basis des CC, im IS, an der äußeren limitierenden Membran (OLM, Sternchen) und in der OPL lokalisiert. **(E)** Die Übereinanderlagerung (merge) zeigt eine partielle Co-Lokalisation von TRAK2 und SANS im Bereich des CC der humanen Retina. **(G-J)** Der Ausschnitt aus **(E)** in der höheren Vergrößerung zeigt die Co-Lokalisation von TRAK2 und SANS im IS im Bereich von CC und der OLM, schematisch dargestellt in **(F)** durch die gelben Markierungen. Ax: Axonem, BC: Bipolarzelle, HC: Horizontalzelle, INL: inner nuclear layer, N: Nukleus, ONL: outer nuclear layer; OS: Außensegment, Größenbalken: 10 µm.

Die Analyse der Lokalisation von TRAK2 und SANS in der humanen Retina zeigt, dass beide potentiellen Interaktionspartner im funktionell wichtigen periciliären Komplex lokalisiert sind. In diesem Kompartiment könnte TRAK2 zusammen mit SANS den Transport von Vesikel vermitteln, an deren Endocytose zuvor Magi2 beteiligt war (Publikation III). Diese Vesikel können durch ein Adapterprotein wie TRAK2 mittels des molekularen Motors Kinesin anterograd entlang von Mikrotubuli zu ihrem Bestimmungsort transportiert werden. An der Beladung auf den Innensegment-Transport ist möglicherweise das Mikrotubuli-

assoziierte SANS beteiligt, dessen direkte Interaktion mit TRAK2 im Rahmen dieser Arbeit bestätigt werden konnte.

TRAK2 wird eine Funktion in der Positionierung von Mitochondrien zugeschrieben, die Eisen benötigen, für die Bereitstellung von Energie in Form von ATP (Adenosin-Tri-Phosphat) durch die Bildung wichtiger Co-Faktoren wie des Eisen-Sulfur Komplexes (Sheftel and Lill 2009; Shvartsman and Ioav 2012; Stehling and Lill 2013). Neuere Analysen zeigen, dass TRAK2 mit einem weiteren, potentiellen SANS-Interaktor, der Dynaktin-Untereinheit $p150^{Glued}$ (Dynaktin-1) interagiert und für den Dynein-vermittelten retrograden Transport von Mitochondrien verantwortlich ist (van Spronsen *et al,* 2013). Die Photorezeptorzelle benötigt in hohem Ausmaß Energie und elektronenmikroskopische Aufnahmen zeigen, dass sehr viele Mitochondrien im apikalen Innensegment vorliegen (Niven and Laughlin 2008; Okawa *et al,* 2008). Möglicherweise bringt TRAK2 gemeinsam mit seinen Interaktionspartnern SANS und $p150^{Glued}$ die Mitochondrien zu dem Kompartiment im Innensegment der Photorezeptorzellen, an der das zur Energiegewinnung notwendige Eisen aufgenommen wird – in die periciliäre Region.

Der Nachweis der direkten Interaktion zwischen TRAK2 und dem USH1G-Protein ist damit ein weiterer Hinweis auf die Beteiligung von SANS an gerichteten Transportprozessen in der Photorezeptorzelle und bekräftigt unsere Arbeitshypothese zur Funktion der USH-Proteinnetzwerke in der Retina (Publikation I, II & III; Maerker *et al,* 2008; Overlack *et al,* 2011b*).

Die in der vorgelegten Dissertation zusammengestellten Informationen erweitern das Wissen über die zelluläre Funktion der an USH beteiligten Proteine und ihrer Interaktionspartner. Diese Arbeit leistet damit einen wichtigen Beitrag zum Verständnis der pathogenen Mechanismen von USH. Dies bildet die Grundlage für die Entwicklung von Therapiestrategien für USH-Patienten.

4. Ausblick

Grundlagenforschung liefert die Basis, durch die komplexe Zusammenhänge, die zu einer Erkrankung wie dem humanen Usher-Syndrom (USH) führen, verstanden werden können. Dadurch wird es möglich, Erkenntnisse über allgemeine molekulare Mechanismen in Zellen zu gewinnen und sie bildet somit die Voraussetzung für die Entwicklung wirksamer Therapien. Im folgenden Abschnitt werden weiterführende Analysen auf Grundlage der Ergebnisse der vorgelegten Arbeit diskutiert.

Die Interaktion zwischen SANS und Harmonin (USH1C) erfolgt über den C-Terminus von SANS, im Gegensatz zur Interaktion mit Magi2 verstärkt das PBM hierbei allerdings die Bindung. Für diese Interaktion steht eine Überprüfung der Phosphorylierungsabhängigkeit aus. Die 50 durch den Y2H identifizierten Interaktionspartner der zentralen Domäne von SANS können offensichtlich nicht gleichzeitig binden, sie stehen möglicherweise sogar in direkter Konkurrenz zueinander. Diese Interaktionen können ebenfalls durch die De-, bzw. Phosphorylierung von SANS reguliert und damit räumlich und / oder zeitlich voneinander getrennt werden. Um dies zu belegen, ist es notwendig, den Netzwerkpartnern die von der Zelle genutzten Regulationsmechanismen zuzuordnen. Durch die Analyse von post-translationalen Modifikationen wie z.B. Glykosylierung und Phosphorylierung ergeben sich neue Einblicke in die *pathways*, die in jeder Zelle geschaltet sind. Die Betrachtung eines Proteinnetzwerkes, wie das des USH-Interaktoms, kann dabei aufzeigen, wie die Proteine eines Signalweges – die Aneinanderreihung verschiedener Proteine in einer Zelle hin zu einem bestimmten Resultat – verschaltet sind (Pereira-Leal *et al,* 2004; Ideker 2004; Lee *et al,* 2008).

Die Analyse der Bindungsaffinitäten verschiedener Proteine zum gleichen Interaktionspartner ist eine weitere Möglichkeit, Proteinnetzwerke zu analysieren. Die Stärke der Bindung kann mittels Plasmonresonanz-Experimenten (SPR, *surface plasmon resonance*) oder thermophoretischer Analysen bestimmt werden (Cullen *et al,* 1987; Pollard-Knight *et al,* 1990; Wienken *et al,* 2010; Jerabek-Willemsen *et al,* 2011). Durch die Zugabe spezifischer Inhibitoren oder bestimmter Kinasen bzw. Phosphatasen lässt sich auch in diesen Experimenten überprüfen, wie zelleigene Regulationsmechanismen die Zusammensetzung eines Proteinnetzwerkes verändern können. Für SANS und die anderen USH-Proteine kann dabei geklärt werden, wie post-translationale Modifikationen die Interaktion mit den zahlreichen identifizierten Interaktionspartnern beeinflussen und unter welchen Bedingungen sich die Komposition eines Proteinnetzwerkes ändert und damit zu seiner Funktion für die Zelle beiträgt. Diese Experimente bilden die Grundlage zur Analyse der Zusammensetzung

des ternären USH-Komplexes aus SANS, Ush2a und Whirlin, außerdem lässt sich überprüfen, ob Magi2 und VLGR1 ebenfalls in diesem Komplex vorliegen. Des Weiteren können wir nachweisen, ob eine Komplexbildung zwischen SANS, Magi2 und VLGR1 möglich ist oder ob es sich um die favorisierte, kompetitive Interaktion von SANS und VLGR1 zu Magi2 handelt. Die Analyse der Bindungsaffinitäten zur Analyse der Interaktionen innerhalb von Netzwerken erweitern die Experimente im artifiziellen System von Zellkulturexperimenten, dessen Möglichkeiten der gleichzeitigen Analyse mehrerer Interaktionspartner begrenzt sind. Diese Studien werden aufzeigen, ob die Regulation der Interaktion zwischen SANS und Magi2 bzw. Ush2a durch Phosphorylierung eine Sonderstellung oder einen generellen Mechanismus innerhalb des USH-Interaktoms darstellt.

Die von uns und anderen Arbeitsgruppen aufgestellten Hypothesen um eine Beteiligung des USH-Interaktoms an Transportprozessen stützen sich auf bereits identifizierte Interaktionspartner (van Wijk *et al,* 2009; Lopes *et al,* 2011; Overlack *et al,* 2011b*). Die im Rahmen dieser Arbeit validierten Interaktionen zwischen SANS und Magi2 bzw. TRAK2 bekräftigen diese Beteiligung von USH-Proteinen an Transportprozessen in Photorezeptorzellen. Eine Möglichkeit, die Funktion eines Proteins für die Zelle zu überprüfen, ist der *knock down* der Proteinexpression mittels RNAi. Die Klonierung der shRNA gegen TRAK2 ist bereits im Rahmen dieser Dissertation erfolgt, die Validierung und funktionelle Überprüfung stehen allerdings noch aus. Weiterführende Analysen zur Funktion der Interaktion zwischen SANS und TRAK2 werden dazu beitragen, die molekularen Mechanismen des anterograden Transports in Photorezeptorzellen zu verstehen. Die Einbeziehung des SANS- und TRAK2-Interaktionspartners $p150^{Glued}$ (Dynaktin-1) in diese Analysen wird aufzeigen, wie SANS am retrograden Transport entlang von Mikrotubuli beteiligt ist

In Publikation I konnten wir durch die detaillierte Analyse des USH-Interaktoms und deiner Verbindung zu anderen Cilien-assoziierten Netzwerken USH zum einen als Ciliopathie definieren. Zum anderen verdeutlicht der Übersichtsartikel die Beteiligung von USH-Proteinen an gerichteten Transportprozessen. In Publikation II und III stellen wir dar, dass für die Funktion des sensorischen Primärciliums der Photorezeptorzelle das periciliäre USH-Proteinnetzwerk und die damit verknüpften Transportprozesse essentiell sind. Weiterführende Analysen, besonders die Studien zur Ciliogenese, werden dazu beitragen zu erfassen, welche Funktion die einzelnen Proteine des USH-Interaktoms haben und wie sie durch ihre Interaktion mit anderen Komponenten zur Aufrechterhaltung der Funktion der Photorezeptorzelle beitragen. Dabei spielt die Lokalisation der USH-Proteine und ihrer

Interaktionspartner mittels hochauflösender Fluoreszenz- und Elektronenmikroskopie eine wichtige Rolle. RNAi-Analysen werden dabei weitere Erkenntnisse liefern, welche USH-Proteine direkt oder über ihre Interaktionspartner als positive oder negative Modulatoren auf die Ausbildung von Cilien bzw. bei der Aufrechterhaltung ihrer Funktion z.B. durch die Beteiligung an Transportprozessen Einfluss nehmen.

Die negative Regulation der Funktion von Magi2 durch die Phosphorylierung von SANS deutet auf eine Rolle des USH-Interaktoms bei der Endocytose in Photorezeptorzellen hin. Die USH-Proteine können in den zelleigenen Kontrollmechanismen damit sowohl bei der Exocytose als auch bei der Endocytose eine regulatorische Funktion übernehmen. Der Ausfall von SANS, wie es bei Mutationen, die zu USH1 führen, der Fall ist, würde diese feinregulierten Mechanismen zum Erliegen bringen und könnte durch eine Über- oder Unterversorgung der Photorezeptorzellen zum Zelltod und damit zum retinalen Phänotyp von USH führen.

Die Analyse des retinalen USH-Phänotyps wird durch das Fehlen von Mausmodellen, die einen retinalen Phänotyp vergleichbar dem des Menschen ausbilden, erschwert. Eine Strategie wäre die Generierung von Zebrafischen, die für die einzelnen USH-Proteine und ihre Interaktionspartner defizient sind. Damit lassen sich die Pathomechanismen, die auf ciliäre Defekte zurückzuführen sind, *in vivo* nachvollziehen. Die Studien in SANS-defizienten Zebrafischen können Aufschluss geben, ob die beobachtete Heterogenität der Ciliogenese in den RNAi-Studien auf das artifizielle Zellkultursystem zurückzuführen ist oder ob es sich um eine phänotypische Varianz durch die Deletion von SANS handelt. In diesem etablierten Tiermodell lässt sich der Einfluss von SANS auf verschiedene Prozesse innerhalb der Ciliogenese nachweisen. In *rescue*-Experimenten kann mittels Einbringen einzelner Domänen von SANS auch die Funktion der verschiedenen von SANS organisierten Proteinnetzwerke verglichen werden. Außerdem kann die Funktion des SANS-Magi2-Komplexes auf die Entwicklung der Larve und damit auf die Ciliogenese durch Doppel-Mutanten überprüft werden. Die vergleichenden Analysen zwischen SANS/Magi2-Mutanten und Mutanten, deren Gene in ihrer Funktion charakterisiert sind, werden aufklären, welche Funktion die von Magi2 vermittelte und durch SANS regulierte Endocytose für die Photorezeptorzelle hat. Spielt Endocytose eine Rolle für Entwicklung und Funktion des sensorischen Ciliums der Photorezeptorzellen oder dient sie der Versorgung der Photorezeptorzellen mit Nährstoffen? Diese Experimente werden Aufschluss über die Zusammenhänge zwischen diesen scheinbar unabhängigen Prozessen geben.

Um die Zusammenhänge zwischen USH und Transportprozessen zu verifizieren, sind weitere, unabhängige Analysen notwendig. Bioinformatisch gestützte Analysen, wie sie von unseren Kooperationspartnern in Nijmegen (Niederlanden) und am EMBL (Heidelberg) durchgeführt werden, können dabei durch die gesammelten Informationen über das USH-Interaktom und seine Vernetzung mit anderen Proteinkomplexen zu einem übergreifenden, systembiologischen Verständnis führen. Außerdem können diese Analysen zur Identifizierung weiterer USH-Proteine beitragen. Ein Beispiel hierfür ist die Arbeit von Sang und Kollegen, die durch die Proteom-Analyse von drei ciliären Proteinnetzwerken neue krankheitsassoziierte Gene identifizieren und so die Gemeinsamkeiten zwischen verschiedenen Ciliopathien aufzeigen konnte (Sang *et al,* 2011). Die ganzheitliche Betrachtung von krankheitsassoziierten Interaktomen bildet damit einen Grundstein für die Entwicklung übergreifender Therapiestrategien, die der Behandlung von Erkrankungen innerhalb solcher Signalwege dienen.

Die Ergebnisse dieser Experimente lassen sich auf die USH-Proteinnetzwerke in den anderen funktionell wichtigen Kompartimenten (*hot spots*), z.B. auf die Synapsen der Photorezeptorzellen, übertragen. Die Kombination der dargestellten molekular-biologischen, protein-biochemischen und systembiologischen Analysen zusammen mit den Studien in USH-defizienten Tiermodellen wird dazu beitragen, die Funktion des USH-Interaktoms für die Retina in seiner Gesamtheit zu erfassen.

5. Zusammenfassung - deutsch

Die vorliegende kumulative Arbeit umfasst Analysen zur Aufklärung der molekularen Grundlagen des humanen Usher-Syndroms (USH), der häufigsten Ursache kombinierter vererblicher Taub-Blindheit. Ziel dieser Arbeit war es, neue Erkenntnisse zur Funktion der USH-Proteine und den von ihnen organisierten Protein-Netzwerken in der Photorezeptorzelle zu erhalten. Dadurch sollten weitere Einsichten in die molekularen Ursachen des retinalen Phänotyps von USH gewonnen werden. Die Ergebnisse dieser Analysen wurden in einem Übersichtsartikel (I) und zwei Originalarbeiten (II, III) zusammengestellt.

Im Übersichtsartikel (I) wurden die vorliegenden Hinweise zusammengefasst, die USH auf Grundlage der molekularen Verbindungen ebenfalls als Ciliopathien definiert. Zudem wird die Bedeutung des periciliären USH-Proteinnetzwerkes für das sensorische Cilium (Außensegment) der Photorezeptorzelle herausgestellt.

In Publikation II wurde der Aufbau des USH1-USH2-Proteinnetzwerkes als Teil des periciliären Komplexes analysiert, der beim *cargo handover* von vesikulärer Fracht vom Innensegment- auf den ciliären Transport für die Photorezeptorzelle essentiell ist. Experimentell wurde Ush2a als neuer SANS-Interaktionspartner validiert. Des Weiteren wurde ein ternärer Komplex aus den USH-Proteinen SANS, Ush2a und Whirlin identifiziert, dessen Zusammensetzung durch die phosphorylierungsabhängige Interaktion zwischen SANS und Ush2a reguliert werden könnte. Dieser ternäre Komplex kann sowohl der Integrität der Zielmembran dienen als auch am Transfer von Molekülen ins Außensegment beteiligt sein.

In Publikation III wurde das MAGUK-Protein Magi2 als neuer Interaktionspartner von SANS identifiziert und die Interaktion durch komplementäre Interaktionsassays validiert. Dabei wurde ein internes PDZ-Binde-Motiv in der SAM-Domäne von SANS identifiziert, das die Interaktion zur PDZ5-Domäne von Magi2 phosphorylierungsabhängig vermittelt. Dadurch wurde bestätigt, dass SANS durch post-translationale Modifizierung reguliert wird. Weiterführende Experimente zur Funktion des Magi2-SANS-Komplexes zeigen, dass Magi2 an Prozess der Rezeptor-vermittelten Endocytose beteiligt ist. Die Phosphorylierung von SANS durch die Kinase CK2 spielt bei der Endocytose ebenfalls eine wichtige Rolle. Der Phosphorylierungsstatus von SANS moduliert die Interaktion zu Magi2 und reguliert dadurch negativ den Prozess der Endocytose. In RNAi-Studien wurde die durch Magi2-vermittelte Endocytose darüber hinaus mit dem Prozess der Ciliogenese verknüpft. Die Analyse der subzellulären Verteilung der Interaktionspartner lokalisieren Magi2 im periciliären Komplex und assoziieren das periciliäre USH-Proteinnetzwerk dadurch mit dem Prozess der Endocytose in der *ciliary pocket*. Der SANS-Magi2-Komplex sollte demnach für Aufbau und Funktion des sensorischen Ciliums der Photorezeptorzelle eine wichtige Rolle spielen.

Die Gesamtheit an Informationen, die aus den Publikationen dieser Dissertation und aus den Kooperationsprojekten (*) resultieren, haben die Kenntnisse zur zellulären Funktion der USH-Proteine und ihrer Interaktionspartner und damit über die pathogenen Mechanismen von USH erweitert. Dies bildet die Basis, um fundierte Therapiestrategien zu entwickeln.

6. Zusammenfassung - englisch

The present cumulative thesis deals with analyses to elucidate the molecular base of the human Usher syndrome (USH), the most common form of combined hereditary deaf-blindness. Aim of the project was to gather novel insights into the function of USH proteins and associated protein networks in photoreceptor cells. Thereby, a deeper understanding of the molecular cause of the retinal USH-phenotype should be gained. The results of these analyses were assembled in one review article (publication I) and two papers (publication II and III).

The review article summarized the existing references defining USH as a ciliopathy based on the molecular links. Furthermore, the importance of the periciliary USH protein network for the sensory cilium (outer segment) of the photoreceptor cells was featured.

In publication II the composition of the periciliary USH1-USH2 protein network was analyzed. As part of the periciliary complex this network is essential for cargo handover of load vesicles from the inner segment transport to the ciliary transport system. In assays we identified Ush2a as new SANS interaction partner and validated a ternary complex composed of the USH proteins SANS, Ush2a and whirlin. The complex assembly might be regulated by the phosphorylation dependent interaction between SANS and Ush2a and could be involved in maintaining the integrity of the cargo target membrane as well as transporting molecules into the outer segment.

In publication III the MAGUK protein Magi2 was identified as new SANS´ interaction partner and the direct interaction was validated by complementary binding assays. Thereby, an internal binding motif in the SAMS domain of SANS was identified, which regulates the interaction to the PDZ5 domain of Magi2 phosphorylation dependent. This confirmed the regulation of SANS by post-translational modifications Further experiments to analyze the function of the SANS-Magi2 complex demonstrated the involvement of Magi2 in receptor-dependent endocytosis. This process is regulated by the phosphorylation of SANS by the kinase CK2. The phosphorylation state of SANS modulates the interaction to Magi2 and regulates thereby negatively the endocytosis. In RNAi studies, the Magi2-mediated endocytosis could be associated with the process of ciliogenesis. Analyses of the subcellular distribution of SANS and Magi2 localize Magi2 in the periciliary complex and associate the periciliary USH protein network with the process of endocytosis in the ciliary pocket. The SANS-Magi2 complex might play an important role in development and maintenance of the sensory cilium of the photoreceptor cell.

The information resulting from the publication of this thesis and from cooperation projects (*) extended the knowledge of the cellular function of USH proteins and their interaction partners and with it the pathogenic mechanisms leading to USH. This is the base to develop substantiated therapeutic strategies.

6. Referenzen

Adams NA, Awadein A, Toma HS (2007). The retinal ciliopathies. *Ophthalmic Genet.*, **28:**113-125.

Adato A, Lefevre G, Delprat B, Michel V, Michalski N, Chardenoux S, Weil D, El Amraoui A, Petit C (2005). Usherin, the defective protein in Usher syndrome type IIA, is likely to be a component of interstereocilia ankle links in the inner ear sensory cells. *Hum. Mol. Genet.*, **14:**3921-3932.

Adato A, Vreugde S, Joensuu T, Avidan N, Hamalainen R, Belenkiy O, Olender T, Bonne-Tamir B, Ben Asher E, Espinos C, et al (2002). USH3A transcripts encode clarin-1, a four-transmembrane-domain protein with a possible role in sensory synapses. *Eur. J. Hum. Genet.*, **10:**339-350.

Ahmed ZM, Riazuddin S, Bernstein SL, Ahmed Z, Khan S, Griffith AJ, Morell RJ, Friedman TB, Riazuddin S, Wilcox ER (2001). Mutations of the protocadherin gene PCDH15 cause Usher syndrome type 1F. *Am. J. Hum. Genet.*, **69:**25-34.

Ahmed ZM, Riazuddin S, Khan SN, Friedman PL, Riazuddin S, Friedman TB (2009). USH1H, a novel locus for type I Usher syndrome, maps to chromosome 15q22-23. *Clin. Genet.*, **75:**86-91.

Alagramam KN, Yuan H, Kuehn MH, Murcia CL, Wayne S, Srisailpathy CR, Lowry RB, Knaus R, Van Laer L, Bernier FP, et al (2001). Mutations in the novel protocadherin PCDH15 cause Usher syndrome type 1F. *Hum. Mol. Genet.*, **10:**1709-1718.

Anderson JM (1996). Cell signalling: MAGUK magic. *Curr. Biol.*, **6:**382-384.

Astuto LM, Weston MD, Carney CA, Hoover DM, Cremers CW, Wagenaar M, Moller C, Smith RJ, Pieke-Dahl S, Greenberg J, et al (2000). Genetic heterogeneity of Usher syndrome: analysis of 151 families with Usher type I. *Am. J. Hum. Genet.*, **67:**1569-1574.

Baala L, Audollent S, Martinovic J, Ozilou C, Babron MC, Sivanandamoorthy S, Saunier S, Salomon R, Gonzales M, Rattenberry E, et al (2007). Pleiotropic effects of CEP290 (NPHP6). mutations extend to Meckel syndrome. *Am. J. Hum. Genet.*, **81:**170-179.

Badano JL, Katsanis N (2006). Life without centrioles: cilia in the spotlight. *Cell*, **125:**1228-1230.

Beck M, Brickley K, Wilkinson HL, Sharma S, Smith M, Chazot PL, Pollard S, Stephenson FA (2002). Identification, molecular cloning, and characterization of a novel GABAA receptor-associated protein, GRIF-1. *J. Biol. Chem.*, **277:**30079-30090.

Benmerah A (2013). The ciliary pocket. *Curr. Opin. in Cell Biol.*, **25:**78–84

Berbari NF, O'Connor AK, Haycraft CJ, Yoder BK (2009). The primary cilium as a complex signaling center. *Curr. Biol.*, **19:**526-535.

Besnard T, Vache C, Baux D, Larrieu L, Abadie C, Blanchet C, Odent S, Blanchet P, Calvas P, Hamel C, et al (2012). Non-USH2A mutations in USH2 patients. *Hum. Mutat.* **33:** 504-510.

Bezprozvanny I, Maximov A (2001). PDZ domains: More than just a glue. *Proc.Natl.Acad.Sci. USA*, **98:** 787-789.

Bhattacharya G, Miller C, Kimberling WJ, Jablonski MM, Cosgrove D (2002). Localization and expression of usherin: a novel basement membrane protein defective in people with Usher's syndrome type IIa. *Hear. Res.*, **163:**1-11.

Bisgrove BW, Yost HJ (2006). The roles of cilia in developmental disorders and disease. *Development*, **133:** 4131-4143.

Bitner-Glindzicz M, Lindley KJ, Rutland P, Blaydon D, Smith VV, Milla PJ, Hussain K, Furth-Lavi J, Cosgrove KE, Shepherd RM, et al (2000). A recessive contiguous gene deletion causing infantile hyperinsulinism, enteropathy and deafness identifies the Usher type 1C gene. *Nat. Genet.*, **26:**56-60.

Blackshaw S, Fraioli RE, Furukawa T, Cepko CL (2001). Comprehensive analysis of photoreceptor gene expression and the identification of candidate retinal disease genes. *Cell*, **107:**579-589.

Bolz H, Ebermann I, Gal A (2005). Protocadherin-21 (PCDH21), a candidate gene for human retinal dystrophies. *Mol. Vis.*, **11:**929-933.

Bolz H, von Brederlow B, Ramirez A, Bryda EC, Kutsche K, Nothwang HG, Seeliger M, Salcedo Cabrera Md, Caballero Vila M, Pelaez Molina O, Gal A, Kubisch C (2001). Mutation of *CDH23*, encoding a new member of the cadherin gene family, causes Usher syndrome type 1D. *Nat. Genet*, **27:**108-112.

Bonnet C, El Amraoui A (2012). Usher syndrome (sensorineural deafness and retinitis pigmentosa): pathogenesis, molecular diagnosis and therapeutic approaches. *Curr. Opin. Neurol.*, **25:**42-49.

Bonnet C, Grati M, Marlin S, Levilliers J, Hardelin JP, Parodi M, Niasme-Grare M, Zelenika D, Delepine M, Feldmann D, et al (2011). Complete exon sequencing of all known Usher syndrome genes greatly improves molecular diagnosis. *Orphanet. J. Rare Dis.*, **6:**21.

Bork JM, Peters LM, Riazuddin S, Bernstein SL, Ahmed ZM, Ness SL, Polomeno R, Ramesh A, Schloss M, Srikumari CRS, et al (2001). Usher syndrome 1D and nonsyndromic autosomal recessive deafness DFNB12 are caused by allelic mutations of the novel cadherin-like gene *CDH23*. *Am. J. Hum. Genet*, **68:** 26-37.

Brickley K, Pozo K, Stephenson FA (2011). N-acetylglucosamine transferase is an integral component of a kinesin-directed mitochondrial trafficking complex. *Biochem. Biophys. Acta*, **1813:**269-281.

Brickley K, Smith MJ, Beck M, Stephenson FA (2005). GRIF-1 and OIP106, members of a novel gene family of coiled-coil domain proteins: association in vivo and in vitro with kinesin. *J. Biol. Chem.*, **280:**14723-14732.

Caberlotto E, Michel V, Foucher I, Bahloul A, Goodyear RJ, Pepermans E, Michalski N, Perfettini I, Alegria-Prevot O, Chardenoux S, et al (2011). Usher type 1G protein sans is a critical component of the tip-link complex, a structure controlling actin polymerization in stereocilia. *Proc. Natl. Acad. Sci. USA*, **108:** 5825-5830.

Chaib H, Kaplan J, Gerber S, Vincent C, Ayadi H, Slim R, Munnich A, Weissenbach J, Petit C (1997). A newly identified locus for Usher syndrome type I, USH1E, maps to chromosome 21q21. *Hum. Mol. Genet.*, **6:**27-31.

Chang B, Khanna H, Hawes N, Jimeno D, He S, Lillo C, Parapuram SK, Cheng H, Scott A, Hurd RE, et al (2006). In-frame deletion in a novel centrosomal/ciliary protein CEP290/NPHP6 perturbs its interaction with RPGR and results in early-onset retinal degeneration in the rd16 mouse. *Hum. Mol. Genet.*, **15:**1847-1857.

Cheng Y, Boll W, Kirchhausen T, Harrison SC, Walz T (2007). Cryo-electron tomography of clathrin-coated vesicles: structural implications for coat assembly. *J. Mol. Biol.*, **365:**892-899.

Chevalier-Larsen ES, Wallace KE, Pennise CR, Holzbaur EL (2008). Lysosomal proliferation and distal degeneration in motor neurons expressing the G59S mutation in the p150Glued subunit of dynactin. *Hum. Mol. Genet.*, **17:** 1946-1955.

Coppieters F, Lefever S, Leroy BP, De Baere E (2010). CEP290, a gene with many faces: mutation overview and presentation of CEP290 base. *Hum. Mutat.*, **31:**1097-1108.

Cullen DC, Brown RG, Lowe CR (1987). Detection of immuno-complex formation via surface plasmon resonance on gold-coated diffraction gratings. *Biosensors*, **3:**211-225.

D'Angelo A, Franco B (2009). The dynamic cilium in human diseases. *Pathogenetics*, **2:**3.

Danielson E, Zhang N, Metallo J, Kaleka K, Shin SM, Gerges N, Lee SH (2012). S-SCAM/MAGI-2 is an essential synaptic scaffolding molecule for the GluA2-containing maintenance pool of AMPA receptors. *J. Neurosci.*, **32:**6967-6980.

Davenport JR, Yoder BK (2005). An incredible decade for the primary cilium: a look at a once-forgotten organelle. *Am. J. Physiol. Renal Physiol.*, **289:**1159-1169.

Davenport SLH, Omenn GS. The heterogeneity of Usher syndrome. Vth Int.Conf. Birth Defects, Montreal. 1977.

Deng F, Price MG, Davis CF, Mori M, Burgess DL (2006). Stargazin and other transmembrane AMPA receptor regulating proteins interact with synaptic scaffolding protein MAGI-2 in brain. *J. Neurosci.*, **26:**7875-7884.

Deretic D (1998). Post-Golgi trafficking of rhodopsin in retinal photoreceptors. *Eye (Lond)*, **12:**526-530.

Dimitratos SD, Woods DF, Stathakis DG, Bryant PJ (1999). Signaling pathways are focused at specialized regions of the plasma membrane by scaffolding proteins of the MAGUK family. *Bioessays*, **21:**912-921.

Ebermann I, Phillips JB, Liebau MC, Koenekoop RK, Schermer B, Lopez I, Schafer E, Roux AF, Dafinger C, Bernd A, et al (2010). PDZD7 is a modifier of retinal disease and a contributor to digenic Usher syndrome. *J. Clin. Invest.*, **120:**1812-1823.

Ebermann I, Wilke R, Lauhoff T, Lubben D, Zrenner E, Bolz HJ (2007). Two truncating USH3A mutations, including one novel, in a German family with Usher syndrome. *Mol. Vis.*, **13:**1539-1547.

El Amraoui A, Petit C (2005). Usher I syndrome: unravelling the mechanisms that underlie the cohesion of the growing hair bundle in inner ear sensory cells. *J. Cell Sci.*, **118:**4593-4603.

Eudy JD, Yao S, Weston MD, Ma-Edmonds M, Talmadge CB, Cheng JJ, Kimberling WJ, Sumegi J (1998). Isolation of a gene encoding a novel member of the nuclear receptor superfamily from the critical region of Usher syndrome type IIa at 1q41. *Genomics*, **50:**382-384.

Fukaya M, Kamata A, Hara Y, Tamaki H, Katsumata O, Ito N, Takeda S, Hata Y, Suzuki T, Watanabe M, et al (2011). SynArfGEF is a guanine nucleotide exchange factor for Arf6 and localizes preferentially at post-synaptic specializations of inhibitory synapses. *J. Neurochem.*, **116:**1122-1137.

Ganem NJ, Compton DA (2004). The KinI kinesin Kif2a is required for bipolar spindle assembly through a functional relationship with MCAK. *J. Cell Biol.*, **166:**473-478.

Ghosh AK, Murga-Zamalloa CA, Chan L, Hitchcock PF, Swaroop A, Khanna H (2010). Human retinopathy-associated ciliary protein retinitis pigmentosa GTPase regulator mediates cilia-dependent vertebrate development. *Hum. Mol. Genet.*, **19:**90-98.

Ghossoub R, Molla-Herman A, Bastin P, Benmerah A (2011). The ciliary pocket: a once-forgotten membrane domain at the base of cilia. *Biol. Cell*, **103:**131-144.

Glater EE, Megeath LJ, Stowers RS, Schwarz TL (2006). Axonal transport of mitochondria requires milton to recruit kinesin heavy chain and is light chain independent. *J. Cell Biol.*, **173:**545-557.

Gnana-Prakasam JP, Martin PM, Smith SB, Ganapathy V (2010). Expression and function of iron-regulatory proteins in retina. *IUBMB. Life*, **62:**363-370.

Goldmann T, Rebibo-Sabbah A, Overlack N, Nudelman I, Belakhov V, Baasov T, Ben Yosef T, Wolfrum U, Nagel-Wolfrum K (2010). Beneficial read-through of a USH1C nonsense mutation by designed aminoglycoside NB30 in the retina. *Invest. Ophthalmol. Vis. Sci.*, **51:**6671-6680.

Gorska-Andrzejak J, Stowers RS, Borycz J, Kostyleva R, Schwarz TL, Meinertzhagen IA (2003). Mitochondria are redistributed in Drosophila photoreceptors lacking milton, a kinesin-associated protein. *J. Comp. Neurol.*, **463:**372-388.

Gosens I, van Wijk E, Kersten FF, Krieger E, van der Zwaag B, Maerker T, Letteboer SJ, Dusseljee S, Peters T, Spierenburg HA, et al (2007). MPP1 links the Usher protein network and the Crumbs protein complex in the retina. *Hum. Mol. Genet.*, **16:**1993-2003.

Grati M, Kachar B (2011). Myosin VIIa and sans localization at stereocilia upper tip-link density implicates these Usher syndrome proteins in mechanotransduction. *Proc. Natl. Acad. Sci. USA*, **108:** 11476-11481.

Grati M, Shin JB, Weston MD, Green J, Bhat MA, Gillespie PG, Kachar B (2012). Localization of PDZD7 to the stereocilia ankle-link associates this scaffolding protein with the Usher syndrome protein network. *J. Neurosci.*, **32:**14288-14293.

Grishin A, Li H, Levitan ES, Zaks-Makhina E (2006). Identification of gamma-aminobutyric acid receptor-interacting factor 1 (TRAK2) as a trafficking factor for the K+ channel Kir2.1. *J. Biol. Chem.*, **281:**30104-30111.

Gusella JF, MacDonald ME (2009). Huntington's disease: the case for genetic modifiers. *Genome Med.*, **1:**80.

Hadano S, Yanagisawa Y, Skaug J, Fichter K, Nasir J, Martindale D, Koop BF, Scherer SW, Nicholson DW, Rouleau GA, et al (2001). Cloning and characterization of three novel genes, ALS2CR1, ALS2CR2, and ALS2CR3, in the juvenile amyotrophic lateral sclerosis (ALS2) critical region at chromosome 2q33-q34: candidate genes for ALS2. *Genomics*, **71:**200-213.

Harris BZ, Lim WA (2001). Mechanism and role of PDZ domains in signaling complex assembly. *J. Cell Sci.*, **114:**3219-3231.

Harrison SC, Kirchhausen T (1983). Clathrin, cages, and coated vesicles. *Cell*, **33:**650-652.

Hartwell LH, Hopfield JJ, Leibler S, Murray AW (1999). From molecular to modular cell biology. *Nature*, **402:** C47-C52.

Hirao K, Hata Y, Ide N, Takeuchi M, Irie M, Yao I, Deguchi M, Toyoda A, Sudhof TC, Takai Y (1998). A novel multiple PDZ domain-containing molecule interacting with N-methyl-D-aspartate receptors and neuronal cell adhesion proteins. *J. Biol. Chem.*, **273:**21105-21110.

Horst CJ, Johnson LV, Besharse JC (1990). Transmembrane assemblage of the photoreceptor connecting cilium and motile cilium transition zone contain a common immunologic epitope. *Cell Motil. Cytoskeleton,* **17:**329-44.

Hunter DG, Fishman GA, Mehta RS, Kretzer FL (1986). Abnormal sperm and photoreceptor axonemes in Usher's syndrome. *Arch. Ophthalmol.*, **104:**385-389.

Ideker T (2004). A systems approach to discovering signaling and regulatory pathways-or, how to digest large interaction networks into relevant pieces. *Adv. Exp. Med. Biol.*, **547:**21-30.

Iida J, Hirabayashi S, Sato Y, Hata Y (2004). Synaptic scaffolding molecule is involved in the synaptic clustering of neuroligin. *Mol. Cell Neurosci.*, **27:**497-508.

Ito H, Fujita K, Nakamura M, Wate R, Kaneko S, Sasaki S, Yamane K, Suzuki N, Aoki M, Shibata N, et al (2011). Optineurin is co-localized with FUS in basophilic inclusions of ALS with FUS mutation and in basophilic inclusion body disease. *Acta Neuropathol.*, **121:**555-557.

Iyer SP, Akimoto Y, Hart GW (2003). Identification and cloning of a novel family of coiled-coil domain proteins that interact with O-GlcNAc transferase. *J. Biol. Chem.*, **278:**5399-5409.

Jang CY, Coppinger JA, Seki A, Yates JR, III, Fang G (2009). Plk1 and Aurora A regulate the depolymerase activity and the cellular localization of Kif2a. *J. Cell Sci.*, **122:**1334-1341.

Jerabek-Willemsen M, Wienken CJ, Braun D, Baaske P, Duhr S (2011). Molecular interaction studies using microscale thermophoresis. *Assay Drug Dev. Technol.*, **9:**342-353.

Jin H, White SR, Shida T, Schulz S, Aguiar M, Gygi SP, Bazan JF, Nachury MV (2010). The conserved Bardet-Biedl syndrome proteins assemble a coat that traffics membrane proteins to cilia. *Cell*, **141:**1208-1219.

Joensuu T, Hamalainen R, Yuan B, Johnson C, Tegelberg S, Gasparini P, Zelante L, Pirvola U, Pakarinen L, Lehesjoki AE, de la CA, Sankila EM (2001). Mutations in a novel gene with transmembrane domains underlie Usher syndrome type 3. *Am. J. Hum. Genet.*, **69:**673-684.

Kaplan OI, Doroquez DB, Cevik S, Bowie RV, Clarke L, Sanders AA, Kida K, Rappoport JZ, Sengupta P, Blacque OE (2012). Endocytosis genes facilitate protein and membrane transport in C. elegans sensory cilia. *Curr. Biol.*, **22:**451-460.

Kawata A, Iida J, Ikeda M, Sato Y, Mori H, Kansaku A, Sumita K, Fujiwara N, Rokukawa C, Hamano M, et al (2006). CIN85 is localized at synapses and forms a complex with S-SCAM via dendrin. *J. Biochem.*, **139:** 931-939.

Kazmierczak P, Sakaguchi H, Tokita J, Wilson-Kubalek EM, Milligan RA, Muller U, Kachar B (2007). Cadherin 23 and protocadherin 15 interact to form tip-link filaments in sensory hair cells. *Nature*, **449:**87-91.

Kersten FF, van Wijk E, Hetterschijt L, Bauss K, Peters TA, Aslanyan MG, van der Zwaag B, Wolfrum U, Keunen JE, Roepman R, Kremer H (2012). The mitotic spindle protein SPAG5/Astrin connects to the Usher protein network postmitotically. *Cilia*, **1:**2.

Kersten FF, van Wijk E, van Reeuwijk J, van der Zwaag B, Maerker T, Peters TA, Katsanis N, Wolfrum U, Keunen JE, Roepman R, Kremer H (2010). Association of whirlin with Cav1.3 (alpha1D) channels in photoreceptors, defining a novel member of the usher protein network. *Invest. Ophthalmol. Vis. Sci.*, **51:** 2338-2346.

Keryer G, Witczak O, Delouvee A, Kemmner WA, Rouillard D, Tasken K, Bornens M (2003). Dissociating the centrosomal matrix protein AKAP450 from centrioles impairs centriole duplication and cell cycle progression. *Mol. Biol. Cell*, **14:**2436-2446.

Kikkawa Y, Shitara H, Wakana S, Kohara Y, Takada T, Okamoto M, Taya C, Kamiya K, Yoshikawa Y, Tokano H, et al (2003). Mutations in a new scaffold protein Sans cause deafness in Jackson shaker mice. *Hum. Mol. Genet.*, **12:**453-461.

Kim H, Ling SC, Rogers GC, Kural C, Selvin PR, Rogers SL, Gelfand VI (2007). Microtubule binding by dynactin is required for microtubule organization but not cargo transport. *J. Cell Biol.*, **176:**641-651.

Kim J, Lee JE, Heynen-Genel S, Suyama E, Ono K, Lee K, Ideker T, Aza-Blanc P, Gleeson JG (2010). Functional genomic screen for modulators of ciliogenesis and cilium length. *Nature*, **464:**1048-1051.

Koide T, Banno M, Aleksic B, Yamashita S, Kikuchi T, Kohmura K, Adachi Y, Kawano N, Kushima I, Nakamura Y, et al (2012). Common variants in MAGI2 gene are associated with increased risk for cognitive impairment in schizophrenic patients. *PLoS One*, **7:**e36836.

Kurz T, Karlsson M, Brunk UT, Nilsson SE, Frennesson C (2009). ARPE-19 retinal pigment epithelial cells are highly resistant to oxidative stress and exercise strict control over their lysosomal redox-active iron. *Autophagy*, **5:**494-501.

Lagziel A, Overlack N, Bernstein SL, Morell RJ, Wolfrum U, Friedman TB (2009). Expression of cadherin 23 isoforms is not conserved: implications for a mouse model of Usher syndrome type 1D. *Mol. Vis.*, **15:** 1843-1857.

Lee E, Chuang HY, Kim JW, Ideker T, Lee D (2008). Inferring pathway activity toward precise disease classification. *PLoS Comput. Biol.*, **4:**e1000217.

Lehtonen S, Ryan JJ, Kudlicka K, Iino N, Zhou H, Farquhar MG (2005). Cell junction-associated proteins IQGAP1, MAGI-2, CASK, spectrins, and alpha-actinin are components of the nephrin multiprotein complex. *Proc. Natl. Acad. Sci. USA*, **102:**9814-9819.

Leitch CC, Zaghloul NA, Davis EE, Stoetzel C, Diaz-Font A, Rix S, Alfadhel M, Lewis RA, Eyaid W, Banin E, et al (2008). Hypomorphic mutations in syndromic encephalocele genes are associated with Bardet-Biedl syndrome. *Nat. Genet.*, **40:**443-448.

Li XJ, Li SH, Sharp AH, Nucifora FC Jr, Schilling G, Lanahan A, Worley P, Snyder SH, Ross CA (1995). A huntingtin-associated protein enriched in brain with implications for pathology. *Nature*, **378:**398-402.

Liou GI, Bridges CD, Fong SL, Alvarez RA, Gonzalez-Fernandez F (1982). Vitamin A transport between retina and pigment epithelium-an interstitial protein carrying endogenous retinol (interstitial retinol-binding protein). *Vision Res.*, **22:** 1457-1467.

Liu X, Bulgakov OV, Darrow KN, Pawlyk B, Adamian M, Liberman MC, Li T (2007). Usherin is required for maintenance of retinal photoreceptors and normal development of cochlear hair cells. *Proc. Natl. Acad. Sci. USA*, **104:**4413-4418.

Lopes VS, Gibbs D, Libby RT, Aleman TS, Welch DL, Lillo C, Jacobson SG, Radu RA, Steel KP, Williams DS (2011). The Usher 1B protein, MYO7A, is required for normal localization and function of the visual retinoid cycle enzyme, RPE65. *Hum. Mol. Gent.*, **20:**2560-70.

Maerker T, van Wijk E, Overlack N, Kersten FF, McGee J, Goldmann T, Sehn E, Roepman R, Walsh EJ, Kremer H, Wolfrum U (2008). A novel Usher protein network at the periciliary reloading point between molecular transport machineries in vertebrate photoreceptor cells. *Hum. Mol. Genet.*, **17:**71-86.

Meng Q, Xiao Z, Yuan H, Xue F, Zhu Y, Zhou X, Yang B, Sun J, Meng B, Sun X, Cheng F (2012). Transgenic mice with overexpression of mutated human optineurin(E50K) in the retina. *Mol. Biol. Rep.*, **39:**1119-1124.

Michalski N, Michel V, Caberlotto E, Lefevre GM, van Aken AF, Tinevez JY, Bizard E, Houbron C, Weil D, Hardelin JP, et al (2009). Harmonin-b, an actin-binding scaffold protein, is involved in the adaptation of mechanoelectrical transduction by sensory hair cells. *Pflugers Arch.*, **459:**115-130.

Misko A, Jiang S, Wegorzewska I, Milbrandt J, Baloh RH (2010). Mitofusin 2 is necessary for transport of axonal mitochondria and interacts with the Miro/Milton complex. *J. Neurosci.*, **30:**4232-4240.

Molla-Herman A, Ghossoub R, Blisnick T, Meunier A, Serres C, Silbermann F, Emmerson C, Romeo K, Bourdoncle P, Schmitt A, et al (2010). The ciliary pocket: an endocytic membrane domain at the base of primary and motile cilia. *J. Cell Sci.*, **123:**1785-1795.

Nachury MV, Loktev AV, Zhang Q, Westlake CJ, Peranen J, Merdes A, Slusarski DC, Scheller RH, Bazan JF, Sheffield VC, Jackson PK (2007). A core complex of BBS proteins cooperates with the GTPase Rab8 to promote ciliary membrane biogenesis. *Cell*, **129:**1201-1213.

Nachury MV, Seeley ES, Jin H (2010). Trafficking to the ciliary membrane: how to get across the periciliary diffusion barrier? *Annu. Rev. Cell Dev. Biol.*, **26:**59-87.

Niven JE, Laughlin SB (2008). Energy limitation as a selective pressure on the evolution of sensory systems. *J. Exp. Biol.*, **211:**1792-1804.

Ocbina PJ, Eggenschwiler JT, Moskowitz I, Anderson KV (2011). Complex interactions between genes controlling trafficking in primary cilia. *Nat. Genet.*, **43:**547-553.

Okawa H, Sampath AP, Laughlin SB, Fain GL (2008). ATP consumption by mammalian rod photoreceptors in darkness and in light. *Curr. Biol.*, **18:**1917-1921.

Overlack N, Kilic D, Bauss K, Maerker T, Kremer H, van Wijk E, Wolfrum U (2011b). Direct interaction of the Usher syndrome 1G protein SANS and myomegalin in the retina. *Biochem. Biophys. Acta*, **10:**1883-92.

Overlack N, Goldmann T, Wolfrum U, Nagel-Wolfrum K (2012). Gene repair of an Usher syndrome causing mutation by zinc-finger nuclease mediated homologous recombination. *Invest. Ophthalmol. Vis. Sci.*, **53:** 4140-4146.

Overlack N, Maerker T, Latz M, Nagel-Wolfrum K, Wolfrum U (2008). SANS (USH1G) expression in developing and mature mammalian retina. *Vision Res.*, **48:**400-412.

Overlack N, Nagel-Wolfrum K, Wolfrum U (2010). 17. The role of cadherins in sensory cell function. In: Yoshida K, *Molecular and Functional Diversities of Cadherin and Protocadherin*. Kerala, India: Research Signpost, 297-311.

Papermaster DS (2002). The birth and death of photoreceptors: the Friedenwald Lecture. *Invest. Ophthalmol. Vis. Sci.*, **43:**1300-1309.

Patzke S, Redick S, Warsame A, Murga-Zamalloa CA, Khanna H, Doxsey S, Stokke T (2010). CSPP is a ciliary protein interacting with Nephrocystin 8 and required for cilia formation. *Mol. Biol. Cell*, **21:**2555-2567.

Pazour GJ, Baker SA, Deane JA, Cole DG, Dickert BL, Rosenbaum JL, Witman GB, Besharse JC (2002). The intraflagellar transport protein, IFT88, is essential for vertebrate photoreceptor assembly and maintenance. *J. Cell Biol.*, **157:**103-113.

Pazour GJ, Witman GB (2003). The vertebrate primary cilium is a sensory organelle. *Curr. Opin. Cell Biol.*, **15:** 105-110.

Pereira-Leal JB, Enright AJ, Ouzounis CA (2004). Detection of functional modules from protein interaction networks. *Proteins*, **54:**49-57.

Picard E, Ranchon-Cole I, Jonet L, Beaumont C, Behar-Cohen F, Courtois Y, Jeanny JC (2011). Light-induced retinal degeneration correlates with changes in iron metabolism gene expression, ferritin level, and aging. *Invest. Ophthalmol. Vis. Sci.*, **52:**1261-1274.

Pollard-Knight D, Hawkins E, Yeung D, Pashby DP, Simpson M, McDougall A, Buckle P, Charles SA (1990). Immunoassays and nucleic acid detection with a biosensor based on surface plasmon resonance. *Ann. Biol. Clin. (Paris)*, **48:**642-646.

Qiao F, Bowie JU (2005). The many faces of SAM. *Sci. STKE.*, **2005:** re7.

Rachel RA, Li T, Swaroop A (2012). Photoreceptor sensory cilia and ciliopathies: focus on CEP290, RPGR and their interacting proteins. *Cilia*, **1:**22.

Reiners J, Nagel-Wolfrum K, Jürgens K, Maerker T, Wolfrum U (2006). Molecular basis of human Usher syndrome: deciphering the meshes of the Usher protein network provides insights into the pathomechanisms of the Usher disease. *Exp. Eye Res.*, **83:**97-119.

Reiners J, van Wijk E, Maerker T, Zimmermann U, Juergens K, te Brinke H, Overlack N, Roepman R, Knipper M, Kremer H, Wolfrum U (2005). Scaffold protein harmonin (USH1C) provides molecular links between Usher syndrome type 1 and type 2. *Hum. Mol. Genet.*, **14:**3933-3943.

Reiter JF, Blacque OE, Leroux MR (2012). The base of the cilium: roles for transition fibres and the transition zone in ciliary formation, maintenance and compartmentalization. *EMBO Rep.*, **13:**608-618.

Riazuddin S, Belyantseva IA, Giese AP, Lee K, Indzhykulian AA, Nandamuri SP, Yousaf R, Sinha GP, Lee S, Terrell D, et al (2012). Alterations of the CIB2 calcium- and integrin-binding protein cause Usher syndrome type 1J and nonsyndromic deafness DFNB48. *Nat. Genet.*, **44:**1265-1271.

Roepman R, Wolfrum U (2007). Protein networks and complexes in photoreceptor cilia. *Subcell. Biochem.*, **43:** 209-235.

Rohlich P (1975). The sensory cilium of retinal rods is analogous to the transitional zone of motile cilia. *Cell Tissue Res.*, **161:**421-430.

Rosenbaum JL, Cole DG, Diener DR (1999). Intraflagellar transport: the eyes have it. *J. Cell Biol.*, **144:**385-388.

Rosenbaum JL, Witman GB (2002). Intraflagellar transport. *Nat. Rev. Mol. Cell Biol.*, **3:**813-825.

Saari JC, Teller DC, Crabb JW, Bredberg L (1985). Properties of an interphotoreceptor retinoid-binding protein from bovine retina. *J. Biol. Chem.*, **260:**195-201.

Saihan Z, Webster AR, Luxon L, Bitner-Glindzicz M (2009). Update on Usher syndrome. *Curr. Opin. Neurol.*, **22:**19-27.

Sang L, Miller JJ, Corbit KC, Giles RH, Brauer MJ, Otto EA, Baye LM, Wen X, Scales SJ, Kwong M, et al (2011). Mapping the NPHP-JBTS-MKS protein network reveals ciliopathy disease genes and pathways. *Cell*, **145:**513-528.

Satir P, Christensen ST (2007). Overview of structure and function of mammalian cilia. *Annu. Rev. Physiol*, **69:** 377-400.

Sayer JA, Otto EA, O'Toole JF, Nurnberg G, Kennedy MA, Becker C, Hennies HC, Helou J, Attanasio M, Fausett BV, et al (2006). The centrosomal protein nephrocystin-6 is mutated in Joubert syndrome and activates transcription factor ATF4. *Nat. Genet.*, **38:**674-681.

Schneider E, Maerker T, Daser A, Frey-Mahn G, Beyer V, Farcas R, Schneider-Ratzke B, Kohlschmidt N, Grossmann B, Bauss K, et al (2009). Homozygous disruption of PDZD7 by reciprocal translocation in a consanguineous family: a new member of the Usher syndrome protein interactome causing congenital hearing impairment. *Hum. Mol. Genet.*, **18:**655-666.

Schultz J, Ponting CP, Hofmann K, Bork P (1997). SAM as a protein interaction domain involved in developmental regulation. *Protein Sci.*, **6:**249-253.

Sedmak T, Wolfrum U (2010). Intraflagellar transport molecules in ciliary and nonciliary cells of the retina. *J. Cell Biol.*, **189:**171-186.

Sheftel AD, Lill R (2009). The power plant of the cell is also a smithy: the emerging role of mitochondria in cellular iron homeostasis. *Ann. Med.*, **41:**82-99.

Shvartsman M, Ioav CZ (2012). Intracellular iron trafficking: role of cytosolic ligands. *Biometals*, **25:** 711-723.

Singla V, Reiter JF (2006). The primary cilium as the cell's antenna: signaling at a sensory organelle. *Science*, **313:**629-633.

Smith MJ, Pozo K, Brickley K, Stephenson FA (2006). Mapping the GRIF-1 binding domain of the kinesin, KIF5C, substantiates a role for GRIF-1 as an adaptor protein in the anterograde trafficking of cargoes. *J. Biol. Chem.*, **281:**27216-27228.

Songyang Z, Fanning AS, Fu C, Xu J, Marfatia SM, Chishti AH, Crompton A, Chan AC, Anderson JM, Cantley LC (1997). Recognition of unique carboxyl-terminal motifs by distinct PDZ domains. *Science*, **275:**73-77.

Spirin V, Mirny LA (2003). Protein complexes and functional modules in molecular networks. *Proc. Natl. Acad. Sci. USA*, **100:**12123-12128.

Stehling O, Lill R (2013). The role of mitochondria in cellular iron-sulfur protein biogenesis: mechanisms, connected processes, and diseases. *Cold Spring Harb. Perspect. Biol.*, **5**.

Stowers RS, Megeath LJ, Gorska-Andrzejak J, Meinertzhagen IA, Schwarz TL (2002). Axonal transport of mitochondria to synapses depends on milton, a novel Drosophila protein. *Neuron*, **36:**1063-1077.

Swarup V, Julien JP (2011). ALS pathogenesis: recent insights from genetics and mouse models. *Prog. Neuropsychopharmacol. Biol. Psychiatry*, **35:**363-369.

Tai AW, Chuang JZ, Bode C, Wolfrum U, Sung CH (1999). Rhodopsin's carboxy-terminal cytoplasmic tail acts as a membrane receptor for cytoplasmic dynein by binding to the dynein light chain Tctex-1. *Cell*, **97**

Trojan P, Rausch S, Giessl A, Klemm C, Krause E, Pulvermuller A, Wolfrum U 2008. Light-dependent CK2-mediated phosphorylation of centrins regulates complex formation with visual G-protein. *Biochem.Biophys.Acta* **1783**:1248-1260.

Tsang WY, Bossard C, Khanna H, Peranen J, Swaroop A, Malhotra V, Dynlacht BD (2008). CP110 suppresses primary cilia formation through its interaction with CEP290, a protein deficient in human ciliary disease. *Dev. Cell*, **15:**187-197.

Tsang WY, Dynlacht BD (2013). CP110 and its network of partners coordinately regulate cilia assembly. *Cilia*, **2:**9.

Tsujikawa M, Omori Y, Biyanwila J, Malicki J (2007). Mechanism of positioning the cell nucleus in vertebrate photoreceptors. *Proc. Natl. Acad. Sci. USA*, **104:**14819-14824.

Valente EM, Silhavy JL, Brancati F, Barrano G, Krishnaswami SR, Castori M, Lancaster MA, Boltshauser E, Boccone L, Al Gazali L, et al (2006). Mutations in CEP290, which encodes a centrosomal protein, cause pleiotropic forms of Joubert syndrome. *Nat. Genet.*, **38:**623-625.

van Spronsen M, Mikhaylova M, Lipka J, Schlager MA, van den Heuvel DJ, Kuijpers M, Wulf PS, Keijzer N, Demmers J, Kapitein LC, et al (2013). TRAK/Milton motor-adaptor proteins steer mitochondrial trafficking to axons and dendrites. *Neuron*, **77:**485-502.

van Wijk E, Kersten FF, Kartono A, Mans DA, Brandwijk K, Letteboer SJ, Peters TA, Maerker T, Yan X, Cremers CW, et al (2009). Usher syndrome and Leber congenital amaurosis are molecularly linked via a novel isoform of the centrosomal ninein-like protein. *Hum. Mol. Genet.*, **18:**51-64.

van Wijk E, Pennings RJ, te Brinken H, Claassen A, Yntema HG, Hoefsloot LH, Cremers FP, Cremers CW, Kremer H (2004). Identification of 51 Novel Exons of the Usher Syndrome Type 2A (USH2A) Gene That Encode Multiple Conserved Functional Domains and That Are Mutated in Patients with Usher Syndrome Type II. *Am. J. Hum. Genet.*, **74:**738-744.

van Wijk E, van der Zwaag B, Peters T, Zimmermann U, te Brinke H, Kersten FF, Maerker T, Aller E, Hoefsloot LH, Cremers CW, et al (2006). The DFNB31 gene product whirlin connects to the Usher protein network in the cochlea and retina by direct association with USH2A and VLGR1. *Hum. Mol. Genet.*, **15:**751-765.

Verde I, Pahlke G, Salanova M, Zhang G, Wang S, Coletti D, Onuffer J, Jin SL, Conti M (2001). Myomegalin is a novel protein of the golgi/centrosome that interacts with a cyclic nucleotide phosphodiesterase. *J. Biol. Chem.*, **276:**11189-11198.

Vernon M (1969). Usher's syndrome-deafness and progressive blindness. Clinical cases, prevention, theory and literature survey. *J. Chronic. Dis.*, **22:**133-151.

Verpy E, Leibovici M, Zwaenepoel I, Liu XZ, Gal A, Salem N, Mansour A, Blanchard S, Kobayashi I, Keats BJ, et al (2000). A defect in harmonin, a PDZ domain-containing protein expressed in the inner ear sensory hair cells, underlies Usher syndrome type 1C. *Nat. Genet.*, **26:**51-55.

Wang L, Zou J, Shen Z, Song E, Yang J (2012). Whirlin interacts with espin and modulates its actin-regulatory function: an insight into the mechanism of Usher syndrome type II. *Hum. Mol. Genet.*, **21:**692-710.

Wang ZJ, Lam KW, Lam TT, Tso MO (1998). Iron-induced apoptosis in the photoreceptor cells of rats. *Invest. Ophthalmol. Vis. Sci.*, **39:**631-633.

Weil D, Blanchard S, Kaplan J, Guilford P, Gibson F, Walsh J, Mburu P, Varela A, Levilliers J, Weston MD, (1995). Defective myosin VIIA gene responsible for Usher syndrome type 1B. *Nature*, **374:**60-61.

Weil D, El Amraoui A, Masmoudi S, Mustapha M, Kikkawa Y, Laine S, Delmaghani S, Adato A, Nadifi S, Zina ZB, et al (2003). Usher syndrome type I G (USH1G) is caused by mutations in the gene encoding SANS, a protein that associates with the USH1C protein, harmonin. *Hum. Mol. Genet.*, **12:**463-471.

Weston MD, Luijendijk MW, Humphrey KD, Moller C, Kimberling WJ (2004). Mutations in the VLGR1 gene implicate G-protein signaling in the pathogenesis of Usher syndrome type II. *Am. J. Hum. Genet.*, **74:**357-366.

Wienken CJ, Baaske P, Rothbauer U, Braun D, Duhr S (2010). Protein-binding assays in biological liquids using microscale thermophoresis. *Nat. Commun.*, **1:**100.

Wolfrum U (2011). Protein networks related to the Usher syndrome gain insights in the molecular basis of the disease. In: Satpal A, *Usher Syndrome: Pathogenesis, Diagnosis and Therapy.* Nova Science Publishers, 51-73.

Wu L, Pan L, Wei Z, Zhang M (2011). Structure of MyTH4-FERM domains in myosin VIIa tail bound to cargo. *Science*, **331:**757-760.

Xu J, Paquet M, Lau AG, Wood JD, Ross CA, Hall RA (2001). beta 1-adrenergic receptor association with the synaptic scaffolding protein membrane-associated guanylate kinase inverted-2 (MAGI-2). Differential regulation of receptor internalization by MAGI-2 and PSD-95. *J. Biol. Chem.*, **276:**41310-41317.

Yagi H, Takamura Y, Yoneda T, Konno D, Akagi Y, Yoshida K, Sato M (2005). Vlgr1 knockout mice show audiogenic seizure susceptibility. *J. Neurochem.*, **92:**191-202.

Yan J, Pan L, Chen X, Wu L, Zhang M (2010). The structure of the harmonin/sans complex reveals an unexpected interaction mode of the two Usher syndrome proteins. *Proc.Natl.Acad.Sci. USA*, **107:**4040-4045.

Yang J, Liu X, Zhao Y, Adamian M, Pawlyk B, Sun X, McMillan DR, Liberman MC, Li T (2010). Ablation of whirlin long isoform disrupts the USH2 protein complex and causes vision and hearing loss. *PLoS Genet.*, **6:**e1000955.

Young RW (1967). The renewal of photoreceptor cell outer segments. *J. Cell Biol.*, **33:**61-72.

Zaghloul NA, Katsanis N (2009). Mechanistic insights into Bardet-Biedl syndrome, a model ciliopathy. *J. Clin. Invest.*, **119:**428-437.

Zallocchi M, Sisson JH, Cosgrove D (2010). Biochemical characterization of native Usher protein complexes from a vesicular subfraction of tracheal epithelial cells. *Biochemistry*, **49:**1236-1247.

Zou J, Luo L, Shen Z, Chiodo VA, Ambati BK, Hauswirth WW, Yang J (2011). Whirlin replacement restores the formation of the USH2 protein complex in whirlin knockout photoreceptors. *Invest. Ophthalmol. Vis. Sci.*, **52:**2343-2351.

Zrada SE, Braat K, Doty RL, Laties AM (1996). Olfactory loss in Usher syndrome: another sensory deficit? *Am. J. Med. Genet.*, **64:**602-603.

7. Anhang

7.1 Abkürzungsverzeichnis

AL	ankle Links (*transiente Verbindungen in Haarsinneszellen*)
Ax	Axonem
BB	Basalkörper
BBS	Bardet-Biedl Syndrom
CC	Verbindungscilium (*connecting cilium*)
Ce	Centriol
CEP290	centrosomal protein 290 kDa
CP	ciliary pocket
DAPI	4,6-Diamidino-2-Phenylindol
DRB	5,6-dichloro-1-β-D-ribofuranosyl-1H-benzimidazole (Kinaseinhibitor)
IFT	intraflagellarer Transport
IS	Innensegment der Photorezeptorzelle
KC	Kinocilium
LCA	Lebersche Kongenitale Amaurose
Magi2	membrane associated guanylate kinase inverted-2
MAGUK	membrane associated guanylate kinases (Proteinfamilie)
MET	mechano-elektrische Signaltransduktion
MTOC	microtubule organization center
N	Nukleus
ONL	äußere Körnerschicht
OPL	äußere plexiforme Schicht
OS	Außensegment der Photorezeptorzelle
PBM	PDZ-Bindemotiv (Interaktionsdomäne)
PCC	periciliary (membrane) complex
PDZ	PSD-95, DLG, ZO-1 (Interaktionsdomäne)
RNAi	RNA interference
RPE	retinales Pigmentepithel
S	Synapse
SAM	sterile alpha motif (Interaktionsdomäne)
SANS	scaffold protein containing ankyrin repeats and SAM domain
SC	Stereocilium
TL	tip Link (*Verbindungen zwischen den Stereocilien in Haarsinneszellen*)
TRAK2	trafficking associated kinesin binding protein 2
TZ	transition zone
USH	humanes Usher Syndrom
Y2H	yeast-2-hybrid

7.2 Zuordnungen der geleisteten Beiträge zu den einzelnen Publikationen

Bei Publikation I, *Sorusch et al, in press*, handelt es sich um einen Übersichtsartikel zum Thema Ciliopathien, der das humane Usher-Syndrom durch seine molekularen Verbindungen zu anderen Netzwerken als Ciliopathie darstellt. Außerdem wird die Funktion des USH-Interaktoms für die Photorezeptorzelle diskutiert. Der konzeptionelle Entwurf wurde von den Co-Autoren Nasrin Sorusch, Kirsten Wunderlich und mir, sowie Prof. Uwe Wolfrum erarbeitet. Die Abbildungen und die schriftliche Ausarbeitung wurden von den Co-Autoren vorbereitet und anschließend mit Prof. Uwe Wolfrum überarbeitet.

In Publikation II, *Bauß et al, in Vorbereitung*, teile ich die Erstautorenschaft mit meiner Kollegin Nasrin Sorusch. Der Pull down zur Identifizierung der zentralen Domäne als Interaktionsdomäne zum C-Terminus von Ush2a war Teil meiner Arbeiten. Die Klonierungsarbeiten zur unabhängigen Validierung der Interaktion, sowie der Nachweis der direkten, phosphorylierungsabhängigen Interaktion mittels Co-Präzipitation und *membrane targeting assay* wurden von mir durchgeführt. Der konzeptionelle Entwurf, sowie die Abbildungen und der Text wurden von Nasrin Sorusch und mir vorbereitet und gemeinsam mit Prof. Wolfrum überarbeitet.

Für Publikation III, *Bauß et al, unter Begutachtung*, wurde in Kooperation mit der AG Kremer der Y2H-Screen mit dem C-Terminus von SANS durchgeführt. Die Validierung der Interaktion mittels 1:1 Y2H, Pull down- und Zellkultur-Assays, sowie der Nachweis der Phosphorylierungsabhängigkeit wurden von mir durchgeführt. Die funktionelle Analyse des SANS-Magi2-Komplexes mittels RNAi und Applikation von Inhibitoren, sowie die Herstellung und Validierung des SANS-Antikörpers wurde von mir mit technischer Unterstützung von Ulrike Maas erarbeitet. Die Analyse der subzellulären Lokalisation der Interaktionspartner SANS und Magi2, sowie der Markerproteine in der Mausretina erfolgte mit technischer Unterstützung von Gabi Stern-Schneider und Elisabeth Sehn. Alle Abbildungen, sowie der Text wurden von mir erstellt und gemeinsam mit Prof. Wolfrum überarbeitet.

Neben den genannten Hauptpublikationen I - III konnte ich weitere Beiträge zu Veröffentlichungen unserer Arbeitsgruppe, sowie zu gemeinsamen Publikationen mit unseren Kooperationspartnern leisten. Bei der Publikation *Schneider et al, 2009* habe ich die Interaktion von SANS und PDZD7 mittels GST-Pull down validiert. An der Publikation *Overlack et al, 2011b* war ich durch die Durchführung des 1:1 Y2H beteiligt. In der Publikation *Kersten et al, 2012* war ich mit technischer Unterstützung von Elisabeth Sehn für die elektronenmikroskopische Analyse der subzellulären Lokalisation von SPAG5 verantwortlich.

7.3 Kongressbeiträge

Wolfrum U, Knapp B, van Wijk E, Roepman R, Kremer H, **Bauß K** (2013) Magi2 links the periciliary Usher syndrome protein network to endocytosis. FASEB Meeting on "The Biology of Cilia and Flagella

Bauß K, Etz V, Knapp B, Maerker T, van Wijk E, Roepman R, Kremer H, Wolfrum U (2013) Magi2 links the periciliary Usher syndrome protein network to endocytosis. Pro Retina Research Colloquium Retinal Degeneration „Accelerating Progress in Research and Translation", Potsdam (**Posterpreis**)

Sorusch N, Overlack N, Kunz A, **Bauß K**, van Wijk E, Maerker T, Roepman R, Kremer H, Wolfrum U (2012) The Usher syndrome 1G protein SANS scaffolds the dynein mediated transport of rhodopsin in photoreceptor cells. 2nd International Symposium on "Protein Trafficking in Health and Disease" (DFG - GRK1459), Hamburg

Sorusch N, **Bauß K**, Overlack N, Kunz A, van Wijk E, Maerker T, Roepman R, Kremer H, Wolfrum U (2012) Usher syndrome 1G protein SANS in ciliary cargo delivery in photoreceptor cells. Rhine-Main Neuroscience Network (rmn²), Oberwesel

Tebbe L, Karam A, Sehn E, **Bauß K**, Maerker T, Trottier Y, van Wijk E, Roepman R, Kremer H, Wolfrum U (2012) Binding of Usher syndrome 1G protein SANS to optineurin links the Usher protein network to the neurodegenerative disorders ALS and Huntington's disease. Rhine-Main Neuroscience Network (rmn²), Oberwesel

Sorusch N, **Bauß K**, Kunz A, van Wijk E, Roepman R, Kremer H, Wolfrum U (2012) The Usher syndrome 1G protein SANS scaffolds ciliary cargoes for dynein mediated transport in photoreceptor cells. 14th Vision Research Conference (2012) - Retina Ciliopathies: From Genes to Mechanisms and Treatment, Fort Lauderdale, USA

Bauß K, Maerker T, van Wijk E, Kersten F, Roepman R, Kremer H, Wolfrum U (2012) Direct binding of Magi2 to the USH1G protein SANS links the periciliary USH protein network to endocytosis. CILIA 2012 - Cilia in Development and Disease, London, UK

Sorusch N, **Bauß K**, Overlack N, Kunz A, van Wijk E, Maerker T, Roepman R, Kremer H, Wolfrum U (2012) The Usher syndrome 1G protein SANS participates in the transport of ciliary cargo in photoreceptor cells. CILIA 2012 - Cilia in Development and Disease, London, UK

Sorusch N, Overlack N, Maerker T, van Wijk E, **Bauß K**, Kersten F, Roepman R, Kremer H, Wolfrum U (2011) The USH1G protein SANS is a microtubule-binding protein and part of the cytoplasmic dynein motor in mammalian photoreceptor cells. 9th Göttingen Meeting of the German Neurosience Society, Göttingen

Bauß K, Maerker T, van Wijk E, Kersten F, Roepman R, Kremer H, Wolfrum U (2011) The USH1G Protein SANS Interacts With The Vesicular Traffic Associated Protein Magi2. ARVO Annual Meeting 2011 – Visionary Genomics, Fort Lauderdale, USA

Bauß K, Maerker T, van Wijk E, Kersten F, Roepman R, Kremer H, Wolfrum U (2011) Vesicular Traffic Associated Protein Magi2 Interacts With The USH1G Protein SANS. Pro Retina Research-Colloquium, Retinal Degeneration: "Vision and Beyond", Potsdam

Bauß K, Maerker T, van Wijk E, Kersten F, Roepman R, Kremer H, Wolfrum U (2011) Magi2 is a novel interaction partner of the USH1G protein SANS. 9th Göttingen Meeting of the German Neurosience Society, Göttingen

Bauß K, Maerker T, van Wijk E, Kersten F, Roepman R, Kremer H, Wolfrum U (2010) Magi2 is a new identified interaction partner of the USH1G protein SANS. Rhine-Main Neuroscience Network (rmn²), Oberwesel

Bauß K, Maerker T, van Wijk E, Kersten F, Roepman R, Kremer H, Wolfrum U (2010) Magi2 is a novel interaction partner of the USH1G protein SANS in murine retina. International Symposium on Usher Syndrome and Related Diseases. Valencia, Spain

Overlack N, Kilic D, Maerker T, **Bauß K**, van Wijk E, Stern-Schneider G, Roepman R, Kremer H, Wolfrum U (2010) USH1G protein SANS interacts with Myomegalin in mammalian photoreceptor cells. ARVO Annual Meeting 2010 – For Sight, Fort Lauderdale, USA

Overlack N, Kilic D, Maerker T, **Bauß K**, van Wijk E, Stern-Schneider G, Roepman R, Kremer H, Wolfrum U (2010) A new member of the USH protein network: USH1G protein SANS interacts with myomegalin in mammalian photoreceptor cells. International Symposium on Usher Syndrome and Related Diseases, Valencia, Spain

Sorusch N, Overlack N, **Bauß K**, Maerker T, van Wijk E, Kersten F, Roepman R, Kremer H, Wolfrum U (2010) The Usher syndrome protein SANS participates in cargo reloading from the post-Golgi transport to the ciliary delivery in photoreceptor cells. FASEB Meeting – Biology of Cilia and Flagella, Vermont, USA

Sorusch N, Overlack N, **Bauß K**, Maerker T, van Wijk E, Kersten F, Roepman R, Kremer H, Wolfrum U (2010) The USH1G protein SANS interacts with the dynein-dynactin motor component p150Glued and the ciliopathy related CEP290. Pro Retina Research-Colloquium, Retinal Degeneration: "10 years into the new century, where do we go from here?" Potsdam

Bauß K, Maerker T, van Wijk E, Kersten F, Roepman R, Kremer H, Wolfrum U (2009) Identification and characterization of direct binding proteins to the USH1G protein SANS. Pro Retina Research-Colloquium, Retinal Degeneration: "Focus on Therapy", Potsdam (**Posterpreis**)

Jores P, Sorusch N, van Wijk E, Maerker T, Kersten F, Boldt K, Overlack N, **Bauß K**, Glöckner CJ, Roepman R, Ueffing M, Kremer H, Wolfrum U (2009) The periciliary Usher syndrome protein network participates in ciliary cargo delivery in vertebrate photoreceptor cells. ERM-Oldenburg

Bauß K, Maerker T, van Wijk E, Kersten F, Roepman R, Kremer H, Wolfrum U (2009) Identification and characterization of Magi2 and Alsin as direct interacting proteins to the USH1G protein SANS. 9th Annual Meeting of the Interdisciplinary Science Network Molecular & Cellular Neurobiology, Mainz

Overlack N, Kilic D, Maerker T, **Bauß K**, van Wijk E, Kremer H, Wolfrum U (2009) Myomegalin interacts with the USH1G protein SANS and is expressed in mammalian retinas. 9th Annual Meeting of the Interdisciplinary Science Network Molecular & Cellular Neurobiology, Mainz

Sorusch N, Overlack N, **Bauß K**, Maerker T, van Wijk E, Kersten F, Roepman R, Kremer H, Wolfrum U (2009) The mircotubule associated proteins $p150^{Glued}$ and CEP290 are novel binding partners of USH1G protein SANS. 9th Annual Meeting of the Interdisciplinary Science Network Molecular & Cellular Neurobiology, Mainz

Wolfrum U, **Bauß K**, Overlack N, van Wijk E, Kersten F, Roepman R, Kremer H and Maerker T (2008) Novel SANS interactors in the periciliary Usher syndrome protein network of photoreceptor cells. Arvo Annual Meeting 2008 – Eyes on innovation, Fort Lauderdale, USA

Overlack N, Maerker T, van Wijk E, **Bauß K**, Kersten K, Roepman K, Kremer H, Wolfrum U (2008) Novel Components in the Periciliary Usher Syndrome Protein Network of Photoreceptor Cells. ISOCB, San Diego, USA

Bauß K, Maerker T, Overlack N, van Wijk E, Kersten F, Goldmann T, Kremer H, Wolfrum U (2007) SANS interactors in the periciliary Usher syndrome protein network in photoreceptor cells. 7th Annual Meeting of the Interdisciplinary Science Network Molecular & Cellular Neurobiology, Mainz

7.4 Lebenslauf

7.5 Danksagung

Danke!

7.6 Eidesstattliche Erklärung

Hiermit erkläre ich an Eides statt, dass ich diese Dissertation selbstständig und nur unter Verwendung der angegebenen Hilfsmittel angefertigt habe.
Ich habe keinen vorherigen Promotionsversuch unternommen.

Mainz, den 12.12.2013

Katharina Bauß